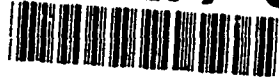


AD-A277 645



2

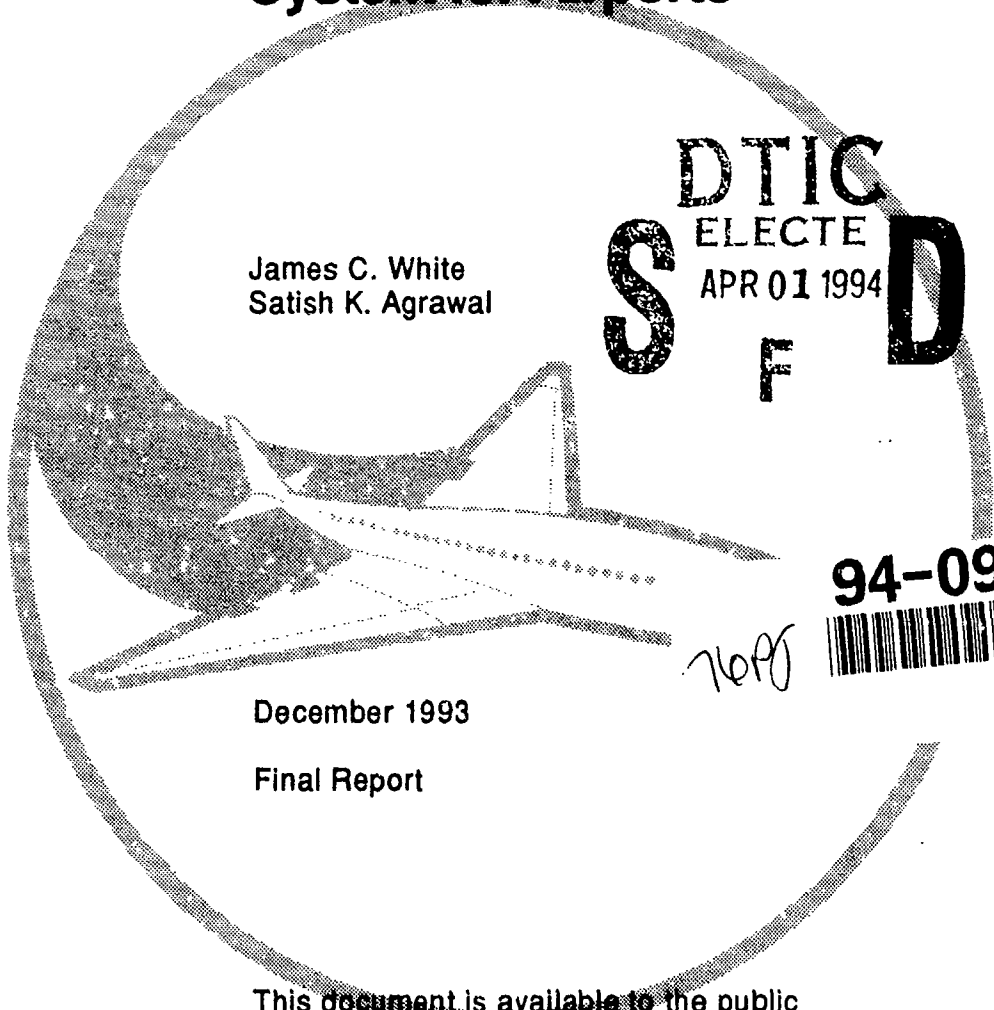
DOT/FAA/CT-93/80

FAA Technical Center  
Atlantic City International Airport,  
N.J. 08405

# Soft Ground Arresting System for Airports

James C. White  
Satish K. Agrawal

DTIC  
ELECTE  
APR 01 1994  
S F D



94-09922  
7690

December 1993

Final Report

This document is available to the public  
through the National Technical Information  
Service, Springfield, Virginia 22161.

This document has been approved  
for public release and sale; its  
distribution is unlimited.



U.S. Department of Transportation  
Federal Aviation Administration

94 3 31 218

## NOTICE

This document is disseminated under the sponsorship of the U. S. Department of Transportation in the interest of information exchange. The United States Government assumes no liability for the contents or use thereof.

The United States Government does not endorse products or manufacturers. Trade or manufacturer's names appear herein solely because they are considered essential to the objective of this report.

1. Report No. DOT/FAA/CT-93/80		2. Government Accession No.		3. Recipient's Catalog No.	
4. Title and Subtitle SOFT GROUND ARRESTING SYSTEM FOR AIRPORTS				5. Report Date December 1993	
				6. Performing Organization Code	
7. Author(s) James C. White* Satish K. Agrawal*				8. Performing Organization Report No. DOT/FAA/CT-93/80	
9. Performing Organization Name and Address Federal Aviation Administration* Technical Center Atlantic City International Airport, NJ 08405				10. Work Unit No. (TRAIS)	
				11. Contract or Grant No.	
12. Sponsoring Agency Name and Address U.S. Department of Transportation Federal Aviation Administration Technical Center Atlantic City International Airport, NJ 08405				13. Type of Report and Period Covered	
				14. Sponsoring Agency Code ACD-110	
15. Supplementary Notes Messrs. Paul H. Jones and Jay Repko provided technical direction during the conduct of the full-scale demonstration of the Soft Ground Arresting System. Previous efforts leading to this demonstration were monitored by Messrs. Rick Marinelli, Larry VanHoy, and Hector Daiutolo.					
16. Abstract  Aircraft can and do overrun the ends of runways, sometimes with disastrous consequences. Safety overrun areas are designed to provide an additional 1,000 feet of length for stopping overrunning aircraft. At many airports, however, the additional 1,000-foot safety area is not available. At these locations, soft ground arresting systems can be employed to decelerate or stop an overrunning aircraft. A mathematical model representing the interface between the aircraft and the soft ground was developed. This model was used to predict aircraft gear loads, deceleration, and stopping distance within the soft ground system. The validity of the mathematical model was confirmed by eight tests with the use of an instrumented Boeing 727 aircraft. A phenolic foam bed 680 feet long by 48 feet wide and 18 inches deep was used to demonstrate the effectiveness of safely stopping a Boeing 727 aircraft entering the bed at 50 knots and 60 knots: at 50 knots the aircraft came to a complete stop in 420 feet and at 60 knots in 540 feet. The aircraft was successfully extracted from the bed, the foam was successfully repaired, and airport rescue and firefighting equipment and personnel were able to maneuver without difficulty on the foam.					
17. Key Words Soft Ground Arresting System, overrun, phenolic foam, safety area, mathematical model			18. Distribution Statement Document is available to the public through the National Technical Information Service, Springfield, VA 22161		
19. Security Classif. (of this report) UNCLASSIFIED		20. Security Classif. (of this page) UNCLASSIFIED		21. No. of Pages 76	22. Price

## ACKNOWLEDGMENTS

The efforts of many individuals and organizations made this report possible. The support provided at the Federal Aviation Administration Technical Center by the Special Projects and Operations Staff, Facility Engineering and Operations Division, and by Flight Test and Aircraft Engineering & Modification Branches was vital to the success of the project. Aircraft instrumentation and data reduction were provided by Messrs. Joe Manning, John Zvanya, and Wayne Marsey. Comrise Technologies, Inc., and their subcontractors are recognized for their contribution towards the installation and repair of the arrestor bed. Special thanks are extended to Ms. Pam Walden of the Port Authority of New York and New Jersey for her continuous support towards the successful completion of this project.

Accession For	
NTIS CRA&I	<input checked="" type="checkbox"/>
DTIC TAB	<input type="checkbox"/>
Unannounced	<input type="checkbox"/>
Justification	
By	
Distribution /	
Availability Codes	
Dist	Avail and/or Special
A-1	

# Table of Contents

	Page
<b>EXECUTIVE SUMMARY</b>	vii
<b>1. INTRODUCTION</b>	1
<b>2. SOFT GROUND ARRESTING SYSTEMS</b>	4
<b>2.1 PREVIOUS RESEARCH</b>	4
2.1.1 Great Britain	4
2.1.2 Military Arrestment Systems	5
2.1.3 Research by Port Authority of New York and New Jersey	5
<b>2.2 FAA RESEARCH</b>	6
2.2.1 Soft Ground Materials	6
2.2.2 Mathematical Model	7
2.2.3 Soft Ground Material Response Prediction	7
2.2.4 Verification of the Mathematical Model	8
<b>3. FULL-SCALE DEMONSTRATION OF SOFT GROUND ARRESTOR</b>	14
3.1 Foam Bed Design	14
3.2 Foam Bed Construction	15
3.3 Aircraft Arrest at 50 Knots	15
3.4 Aircraft Extraction and Foam Bed Repair	17
3.5 Aircraft Arrest at 60 Knots	17
<b>4. CONCLUSIONS</b>	19
<b>5. REFERENCES</b>	20
<b>Appendix A</b>	Mathematical Model Verification Tests
<b>Appendix B</b>	Full-Scale Arresting System Demonstrations
<b>Appendix C</b>	Computer Inputs for Mathematical Model
<b>Appendix D</b>	Aircraft Undershoots into Phenolic Foam Arrestor Bed

## List of Illustrations

	Page
FIGURE 1. Runway Exit Speeds During an Overrun	1
FIGURE 2. Aircraft Overrun Accident Locations Beyond the Runway	2
FIGURE 3. Typical Airport Safety Area	3
FIGURE 4. Soft Ground Arrestor System Installation	4
FIGURE 5. Wheel/Foam Interface Model	7
FIGURE 6. Longitudinal Acceleration Comparison	9
FIGURE 7. Nose Gear Drag and Vertical Loads	10
FIGURE 8. Main Gear Vertical and Drag Loads	11
FIGURE 9. Comparison of Computed and Measured Ground Speed	12
FIGURE 10. Soft Ground Arrestor System Layout	14
FIGURE 11. Nose Gear Travel Distance in Feet - 50-Knot Demonstration	16
FIGURE 12. Overhead View of Arrested Aircraft	17
FIGURE 13. Nose Gear Travel Distance in Feet - 60-Knot Demonstration	18
FIGURE 14. P-19 Airport Rescue / Firefighting Truck Operating in Arrestor Bed	18

## **EXECUTIVE SUMMARY**

Aircraft can and do overrun the ends of runways, sometimes with disastrous results. An overrun, by definition, occurs anytime an aircraft passes beyond the end of a runway during an aborted takeoff or while landing. The majority of such overruns in the past have occurred with aircraft traveling at 80 knots or less. In order to minimize the hazards of overruns, the Federal Aviation Administration (FAA) requires a safety area of 1000 feet in length beyond the end of the runway. Although this safety area is now an FAA standard many runways were constructed prior to its adoption. For those locations where natural obstacles (bodies of water or sharp drop-offs), local development (roads and rail lines), or environmental restraints (wetland encroachment) prohibit the installation of a safety area, a soft ground arresting system has been developed.

Soft ground means any material which will deform readily when an aircraft traverses through it. As the tires crush the material, the drag forces decelerate the aircraft. The FAA research program, leading to the full-scale demonstration of the effectiveness of a soft ground arresting system in stopping a Boeing 727 aircraft, consisted of (a) development of a mathematical model to represent the tire/foam interface, (b) prediction of stopping distance within the bed, and (c) verification of the mathematical model by field testing.

A series of field tests were conducted using an instrumented Boeing 727 aircraft. In these tests, the aircraft taxied through foam beds of 3 to 18 inches at velocities of 20 to 80 knots. Test results confirmed the validity of the mathematical model.

Using this mathematical model, a phenolic foam arrestor system was designed to demonstrate the full-scale arrest of an aircraft. A foam bed 680 feet long by 48 feet wide by 18 inches deep was constructed on Taxiway A at the FAA Technical Center. Two demonstrations were conducted with the instrumented Boeing 727 aircraft. In the first demonstration, the aircraft traveling at 50 knots was safely stopped 420 feet into the arrestor bed. The aircraft was extracted, the bed repaired, and a second demonstration was conducted. The Boeing 727 traveling at 60 knots was safely stopped 540 feet into the bed. Airport rescue and firefighting equipment and personnel maneuvered on the bed without difficulty.

## 1. INTRODUCTION.

On February 28, 1984, a Scandinavian Airline System DC-10-30 aircraft overran after landing on runway 4R at John F. Kennedy (JFK) International Airport and plunged into Thurston Basin. The accident report indicated that the DC-10 departed the end of the runway at about 75 knots and entered Thurston Basin 600 feet later still moving at about 38 knots.

Overruns such as this one often result in loss of life, serious injury to passengers and crew, and extensive damage to aircraft. An overrun, by definition, occurs anytime an aircraft passes beyond the end of a runway during an aborted takeoff or while landing. There are many reasons for an overrun: engine failures which result in insufficient power to complete the takeoff, thrust reverse failures, brake failures, improper flap settings, pilot misjudgments, and snow/ice/water on the runway surface.

Accident reports published by the National Transportation Safety Board (NTSB) and the International Civil Aviation Organization (ICAO) have provided information on aircraft weight, speed, location, runway conditions, and injuries for many aircraft overrun accidents. Data (David, 1990) for the period from 1975 to 1987 are shown in figures 1 and 2.

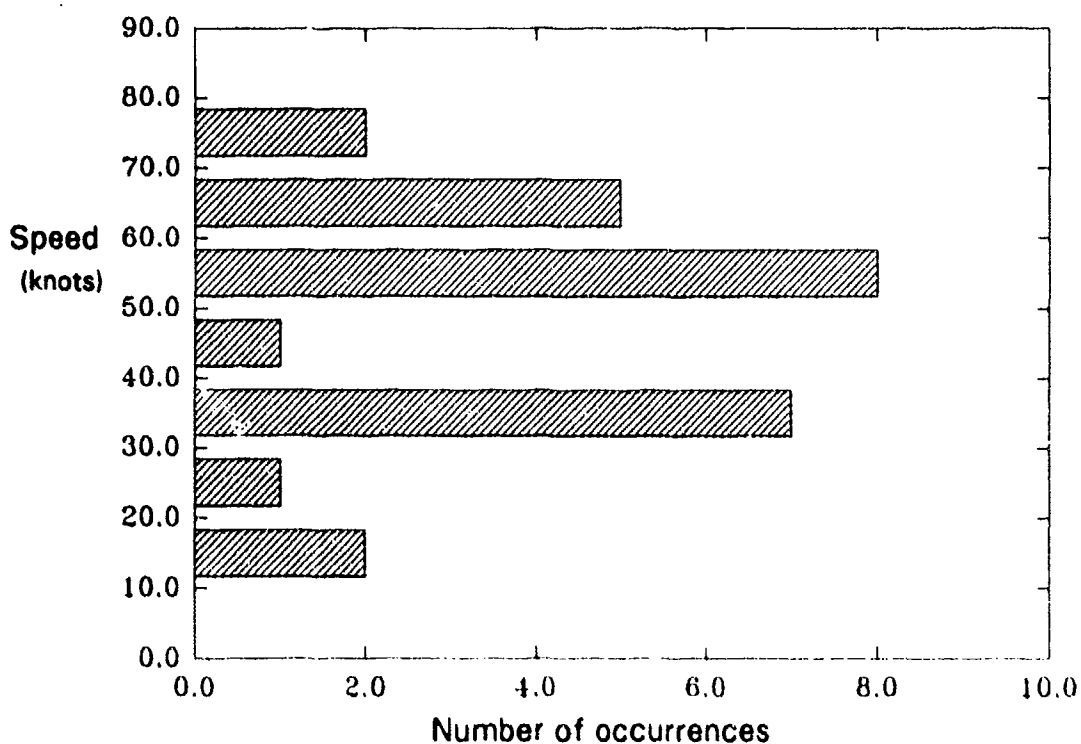


FIGURE 1. Runway Exit Speeds During an Overrun

Figure 1 shows the speed of the aircraft when it left the end of the runway during an overrun and the number of occurrences at this speed. This figure indicates that all



of the overrun accidents occurred at speeds under 80 knots and that a majority of the accidents occurred at speeds less than 60 knots.

Figure 2 shows the location of the aircraft after the accident. Note that the final locations of a majority of the aircraft were very close to the extended runway centerline (those enclosed in the rectangle within the chart).

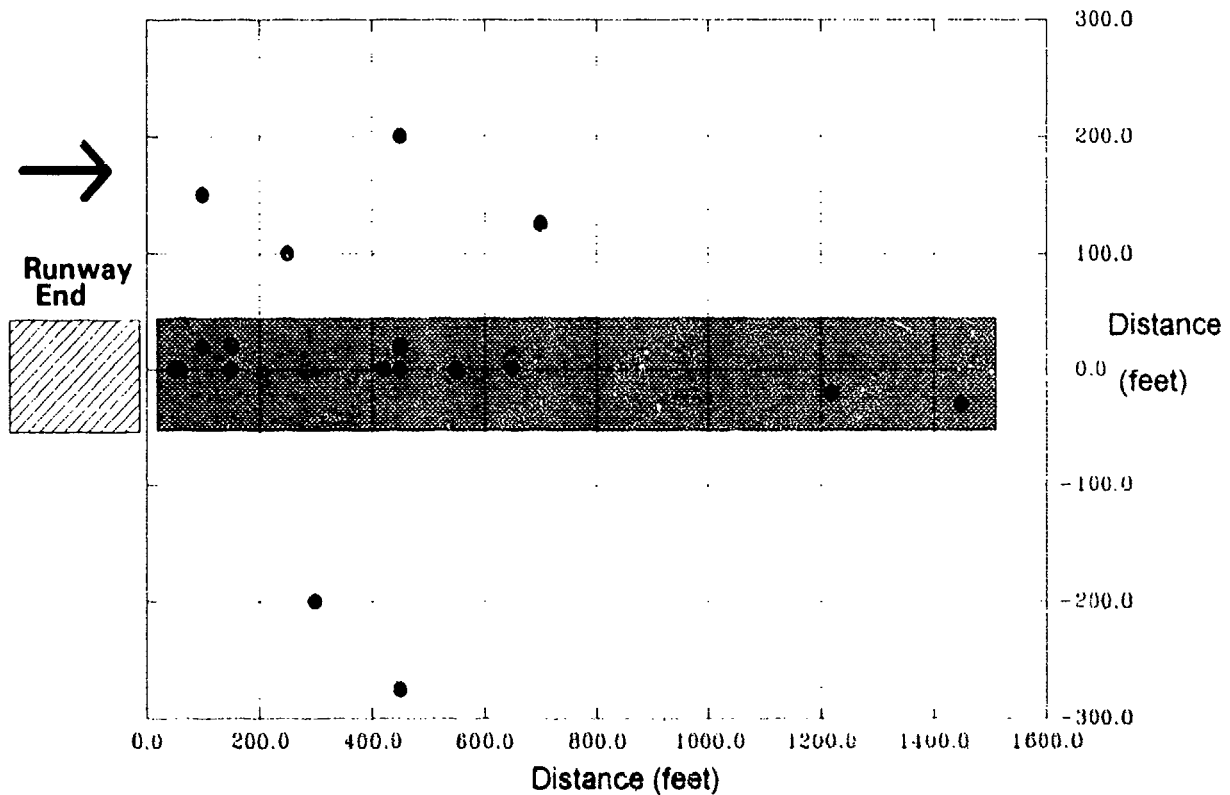


FIGURE 2. Aircraft Overrun Accident Locations Beyond the Runway

In order to minimize the hazards of overruns the Federal Aviation Administration (FAA) requires a safety area of 1000 feet in length at the end of a runway (*Federal Aviation Administration, 1992*). A typical runway with safety area is shown in figure 3.

Many airports, which were constructed before the safety area became a standard, do not have the required 1000 feet of space at the ends of runways because of existing structures, bodies of water, large drop-offs, railroads, or highways. The relocation of these impediments is often economically impractical or environmentally unacceptable. Consequently, it is necessary to develop a means to stop an overrunning aircraft in less than 1000 feet so that safety at such airports could be ensured. A soft ground arresting system is one passive means that has been shown to accomplish this task.

The goal of these tests was to show the effectiveness of a soft ground arresting system in safely stopping an aircraft from a speed of up to 60 knots in less than 1000 feet. In order to achieve this goal, several objectives must be fulfilled. The objectives are to show:

- That a mathematical model representing the tire/foam interface can accurately predict landing gear loads, deceleration, and speed decay of aircraft during simulated overruns.
- That a jet aircraft traveling up to 60 knots can be safely stopped within a bed of phenolic foam less than 1000 feet long.
- That airport rescue and firefighting equipment and personnel can smoothly maneuver without difficulty on the foam following arrestment.
- That the aircraft can be extracted from the foam bed without damage.
- That the foam bed can be repaired following arrestment.

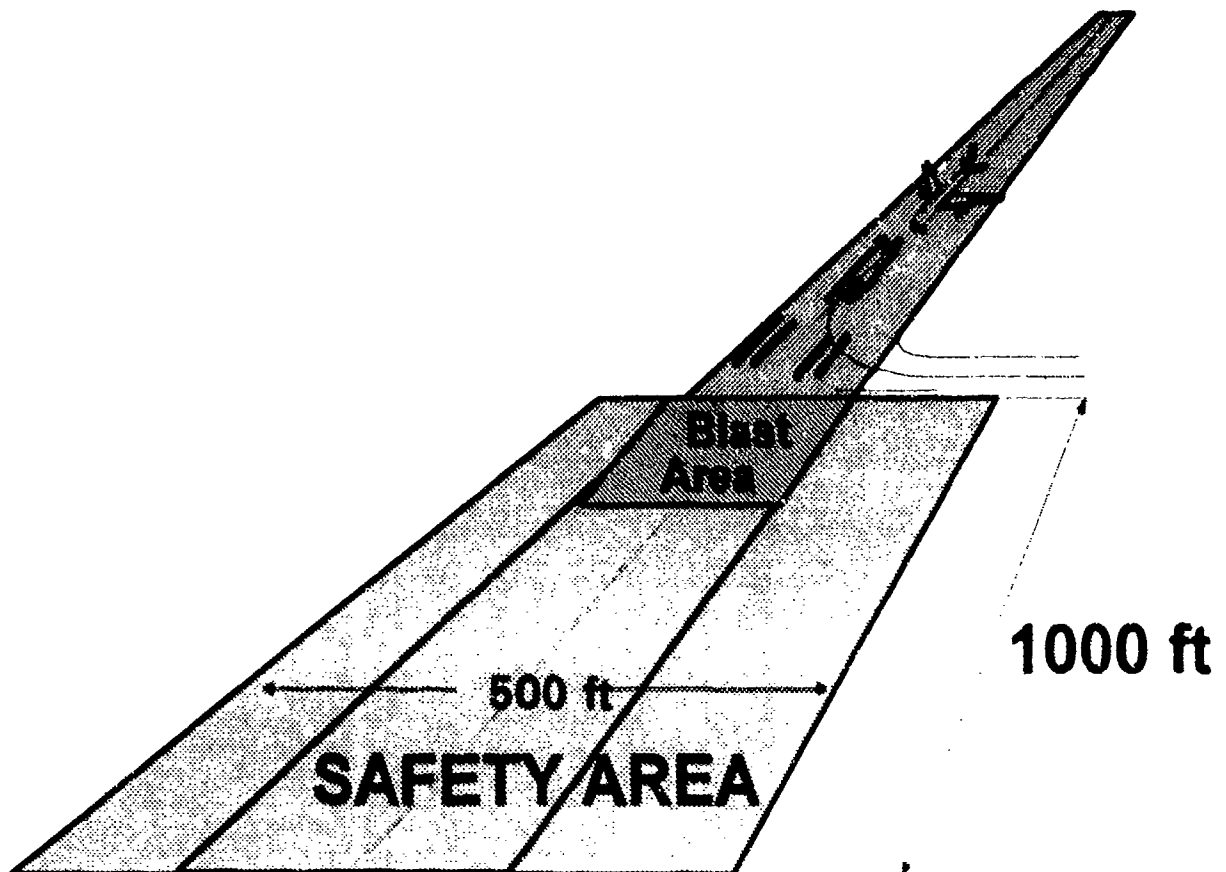


FIGURE 3. Typical Airport Safety Area with Required 1000' of Overrun

## 2. SOFT GROUND ARRESTING SYSTEMS.

Soft ground, in the context used here, means any material which will deform readily and in a predictable manner under an aircraft's tire path. As the tires crush the material, the drag forces decelerate the aircraft. The properties and physical dimensions of the material and the aircraft weight and speed may determine the effectiveness of a given material in stopping the aircraft. A general representation of a soft ground arresting system is shown in figure 4.

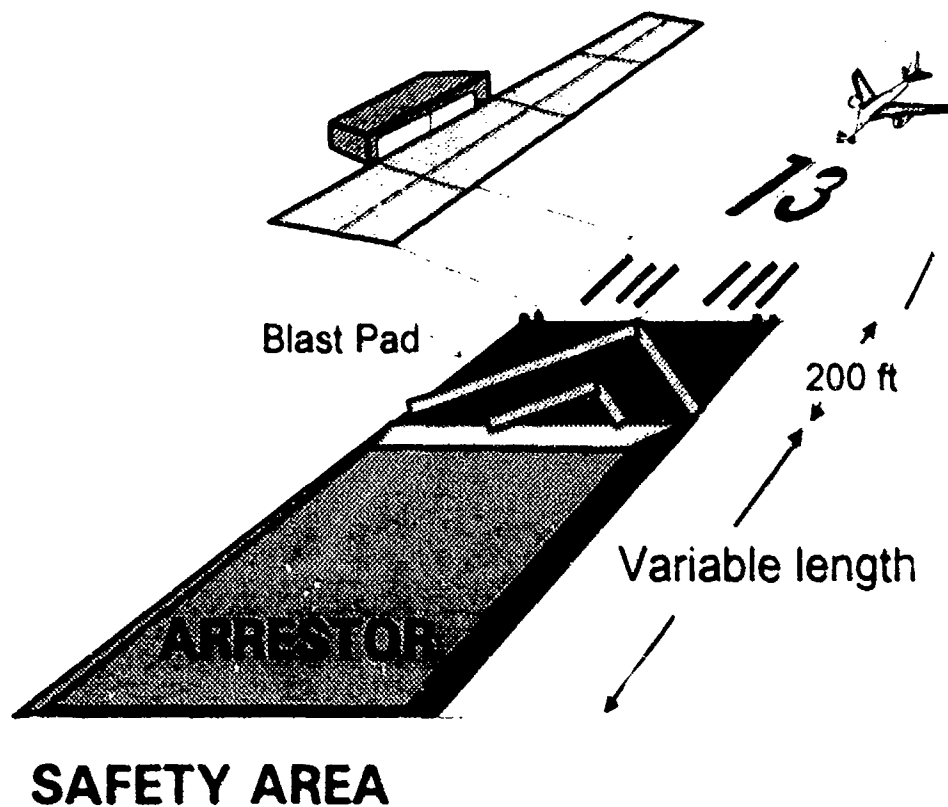


FIGURE 4. Soft Ground Arresting System Installation

### 2.1 PREVIOUS RESEARCH.

#### 2.1.1 Great Britain.

Great Britain conducted tests in the late 1960's and early 1970's to develop a soft ground aircraft arresting system (Bade, 1968 and 1969, Barnes, 1971). In 1974, the Royal Aircraft Establishment conducted trials with a Comet 3B aircraft at its

maximum landing mass of 120,000 pounds at speeds up to 56 knots in test beds of poured-in-place urea formaldehyde foam of varying depth, length, and density. The main conclusions from the trials are that deceleration of the aircraft in the arrestor bed is independent of entry speed, that significant drag is contributed by both the leading and trailing wheels and that this drag is predictable, that the foam causes no significant damage to turbine engines or aircraft structure, and that the addition of a foam ramp reduces the peak drag forces on the aircraft (Gwynne, 1974).

### 2.1.2 Military Arrestment Systems.

Arresting systems used by the military are primarily active systems. Most of these arrestors were developed for fighter aircraft. The U. S. Navy uses large hydraulic systems and cables across aircraft carrier decks for aircraft arrestment. This system requires that a very strong hook be attached to the aircraft to engage the cables that activate the hydraulic system and bring the aircraft to a stop. The Navy also uses large net barriers to capture aircraft which miss the arrestor deck cables. The nets pass over the cockpit and wings and the net ends are attached to an energy absorbing device which produces a drag large enough to stop the aircraft.

The U. S. Air Force uses large ship anchor chains for an arrestor. The chains are strung parallel to the runway sides with a cable attached to two chain ends at the departure end of the runway. The downwind ends of the chains are left free. The interconnecting cable lies transverse to the runway departure end so that a hook attached to the aircraft structure can engage the cable and drag the heavy chain links one after another until the aircraft stops.

The aircraft arresting systems currently utilized by the military cannot be easily adapted to civil aircraft. The installation of hook assemblies on existing commercial aircraft would require extensive structural modifications. General aviation aircraft would be similarly impacted, and each category would incur significant weight penalties. The installation of nets and cable systems present other obstacles such as high installation and maintenance costs, and the rapid deceleration associated with these systems could have a detrimental effect on passengers, crew, and aircraft integrity.

### 2.1.3 Research by Port Authority of New York and New Jersey (PANY&NJ)

After the February 28, 1984, accident at JFK International Airport, the Port Authority conducted a study (Horne, 1985) to develop a safety overrun area. This study concluded that a "Plastic Foam Covered Overrun" was the most promising of all the overrun types studied. An evaluation (Cook, 1988) of a foam arrestor bed for runway 4R/22L at JFK concluded that "The technical feasibility of a passive foam arrestor has been adequately demonstrated to assure a high probability of success"

## 2.2 FAA RESEARCH.

The FAA research program included: investigation of potential soft ground materials; development of the tire/material interface mathematical model; application of the mathematical model to gravel and foam; and, verification of the model with an instrumented Boeing 727 aircraft.

### 2.2.1 Soft Ground Materials.

The ability to predict the performance of a foam arrestor was furthered by an FAA sponsored study (Cook, 1987). This study was initiated to determine whether or not aircraft having gross weights of 114,000 to 630,000 pounds could be safely stopped in less than 1000 feet after overrunning the available length of runway at 70 knots. The study produced the following functional design criteria for an arrestment system:

- Gear loads must remain below design limits to minimize structural damage to the landing gear and reduce the possibility of wing fuel tank rupture.
- The system must permit airport rescue and firefighting vehicles easy access and maneuverability on the bed.
- The repair of the bed in the event of an incident must be simple and quick.
- The system performance must be tolerable of weather extremes.
- The system must not attract birds or other creatures which might present a hazard to airport operations.
- Maintenance to keep the system operational must be minimal.

This criteria was applied to several materials as viable candidates for use in the soft ground arresting system: water ponds present the dual problem of freezing in the winter and also of attracting water fowl. Sand must be kept dry and loose or it is susceptible to freezing or consolidation. Clay, to be effective, must be kept wet, and this is difficult to do under all weather conditions; gravel beds must be kept dry and loose, and the hard stones may be ingested by turbine engines and cause serious damage. The limitations of water, sand, and clay were considered to be excessive and these materials were excluded as candidates for further study. However, gravel was considered worthy of continued study.

Crushable materials like rigid plastic foams and aerated portland cement concrete or foamcrete were investigated as possible arrestor materials and found to have many desirable features although somewhat more expensive than sand, clay, or gravel. Rigid plastic foam and foamcrete are generally stable over a broad temperature range and are not susceptible to freezing or long term consolidation.

### 2.2.2 Mathematical Model.

In order to determine the stopping capability of the arresting materials, a tire/material interface model was developed. The model would also provide aircraft dynamic response during the arrestment.

The wheel/foam interface illustrated in figure 5 is one example of the model. This interface includes elements of the landing gear, arrestor material, and tires. The drag and vertical forces induced by foam are a function of the density of foam, velocity of wheel axle, and the surface area of the tire exposed to foam. Tire deflection also creates a vertical force related to tire stiffness. Force and moment balance can provide necessary equations to compute aircraft deceleration, gear loads, and dynamic response. The mathematical model was solved using a finite element procedure on a 386 based microcomputer. It can handle various aircraft weights, speeds, test bed configurations, soft ground materials, and other pertinent parameters.

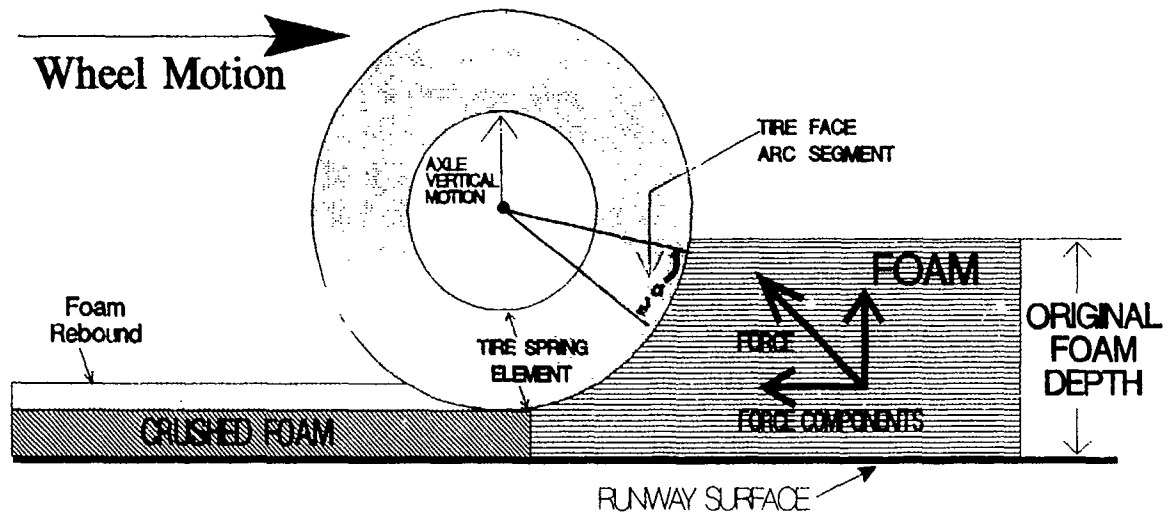


FIGURE 5. Wheel/Foam Interface Model

### 2.2.3 Soft Ground Material Response Prediction.

The model was applied to gravel and polystyrene foam to predict the response of these materials as a result of aircraft arrestment. Aircraft weighing from 114,000 pounds to 630,000 pounds were used. The aircraft speed at the beginning of the arrestment was 70 knots. Other input variables were the crushing strength, density, and thickness of the soft ground materials.

Results on gravel indicated that gravel was suitable for stopping commercial aircraft during an overrun at entry speeds of 70 knots or less. Although the material is inert with relatively low cost, gravel spray (*and possible ingestion by turbine engines*), and long term consolidation of the gravel beds are significant drawbacks; and in colder climates the bed is susceptible to freezing over.

Results on foam indicated two parameters of concern: the crushing strength and the amount of recovery after the foam was crushed (*foam rebound*, see figure 5). Products which showed little rebound were desired since this provides maximum energy dissipation. Compression tests indicated that the foam would compress to about 80 or 90 percent of its original depth after which it would act as a rigid surface. The five simulations utilized a 24-inch-deep composite foam bed consisting of a bottom 12 inch layer of foam with a crushing strength of 60 psi and a top 12 inch layer of foam with a strength of 45 psi. It was found that the foam bed was the most efficient of all materials tested as evidenced by the nearly constant deceleration of the aircraft over the complete arrestment. Foam particles loosened during arrest are not likely to cause damage, and the foam, although combustible, was self-extinguishing.

#### 2.2.4 Verification of the Mathematical Model.

The procedure for verifying the mathematical models involves actual measurement of the parameters pertinent to the output of the model. The measured and predicted results are then compared to establish the validity of the model. Because measured results may contain errors, redundancy is usually employed as a compensating procedure. In this study measurements of deceleration and pertinent forces were recorded in order to provide this necessary compensation.

The FAA in 1991 conducted a series of tests to verify the assumptions and simplifications in the mathematical model. These tests were conducted at the FAA Technical Center and consisted of taxiing an instrumented FAA Boeing 727 aircraft over several foam arrestor beds at various speeds and foam depths: Five at 6-inch depth, two at 12-inch depth, and one at 18-inch depth. During one of the 6-inch depth tests, the aircraft brakes were applied. Each of these tests are explained in greater detail in appendix A. The data presented in this section were generated during test 8. This test was conducted at 50 knots through an 18-inch-deep bed, and it most closely resembled a bed that would be required for actual airport operations.

All tests were conducted with aircraft weight of approximately 135,000 pounds. The speed range was from 20 to 80 knots. The test beds were designed to monitor the deceleration of the aircraft in addition to its velocity, landing gear loads, and brake torque. The results of these tests showed that the measured parameters from the aircraft were within 10 percent of the values predicted by the mathematical model. The 18-inch-deep bed provided the most effective deceleration without exceeding the stresses encountered by the aircraft during normal operation.

The test beds were fabricated by layering 4 foot by 8 foot by 3-inch-deep phenolic foam panels with a crushing strength of 35 psi. This particular phenolic foam was selected because it was readily available on the commercial market. The phenolic foam was also considered less of a fire risk than the polystyrene foam used in the

1986 simulations. The bottom layer of foam was bonded to the taxiway with silicone adhesive (to secure the bed during the test runs and in the event of high winds). Adjacent panels were fastened together with latex adhesives.

Figure 6 shows a time history plot of the aircraft center of gravity longitudinal deceleration during test 8 in 1991. The plot also contains the deceleration simulated by the mathematical model. The tracks of the two curves are similar. The noise along the measured curve results from the vibration of the landing gear in the drag direction. This noise does not contribute to aircraft deceleration because it is both positive and negative about a mean value with the net effect of zero.

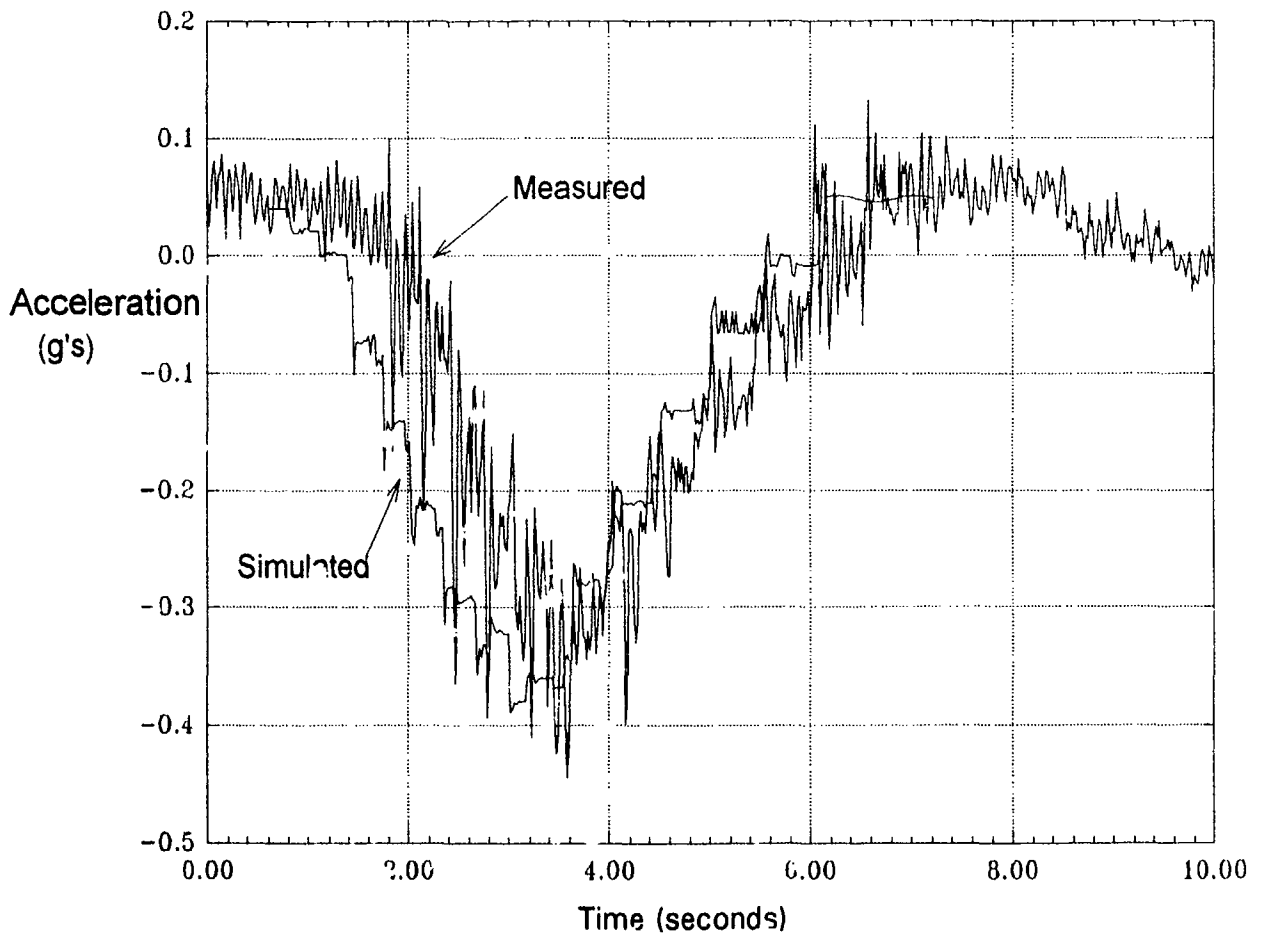


FIGURE 6. Longitudinal Acceleration Comparison

The aircraft entered the test beds with one engine at idle thrust of approximately 1200 pounds. The aerodynamic drag on the aircraft was assumed to be equal to but in the opposite direction of the engine thrust, with the net result of thrust and drag being zero. Therefore the deceleration of the aircraft in figure 6 is a result of the foam bed drag on the landing gear wheels. The similarity of the two curves indicate that the mathematical model can accurately predict the behavior of an aircraft in a foam arresting bed.



The landing gear forces were also measured and compared against the analytical model. Figures 7(a) and 7(b) present the nose gear drag and vertical loads as measured and simulated (again for test 8). The curves plot the forces exerted on the nose gear against time. The measured curve has been time shifted about 1 second for ease of evaluation.

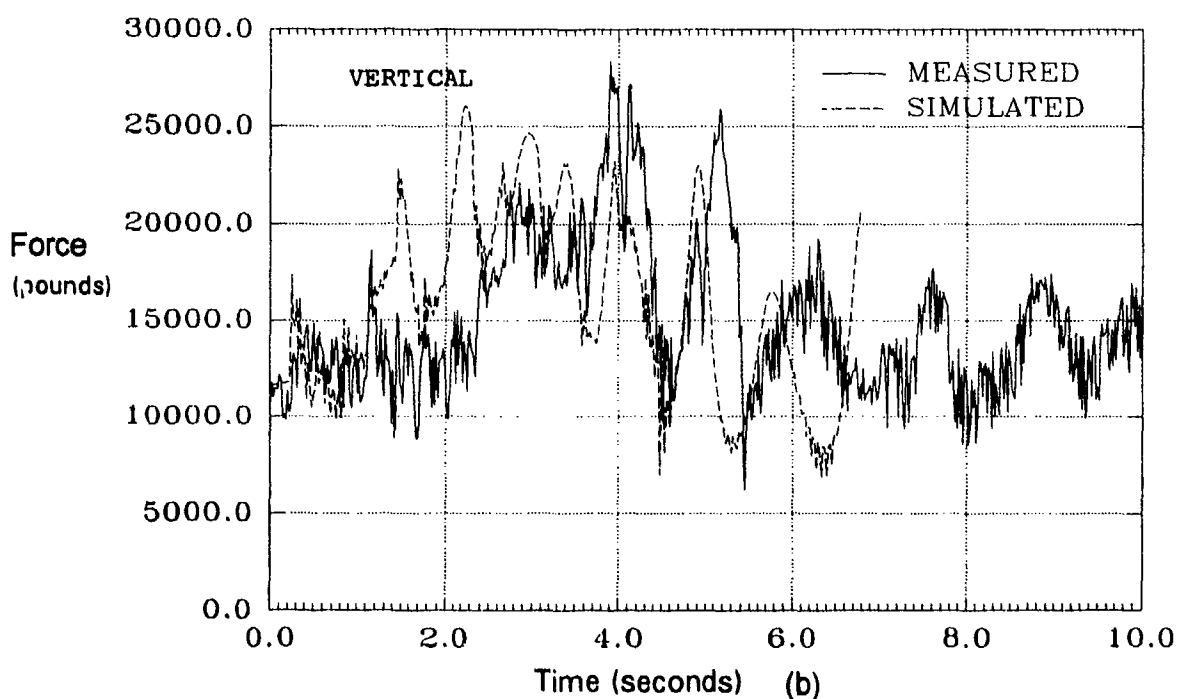
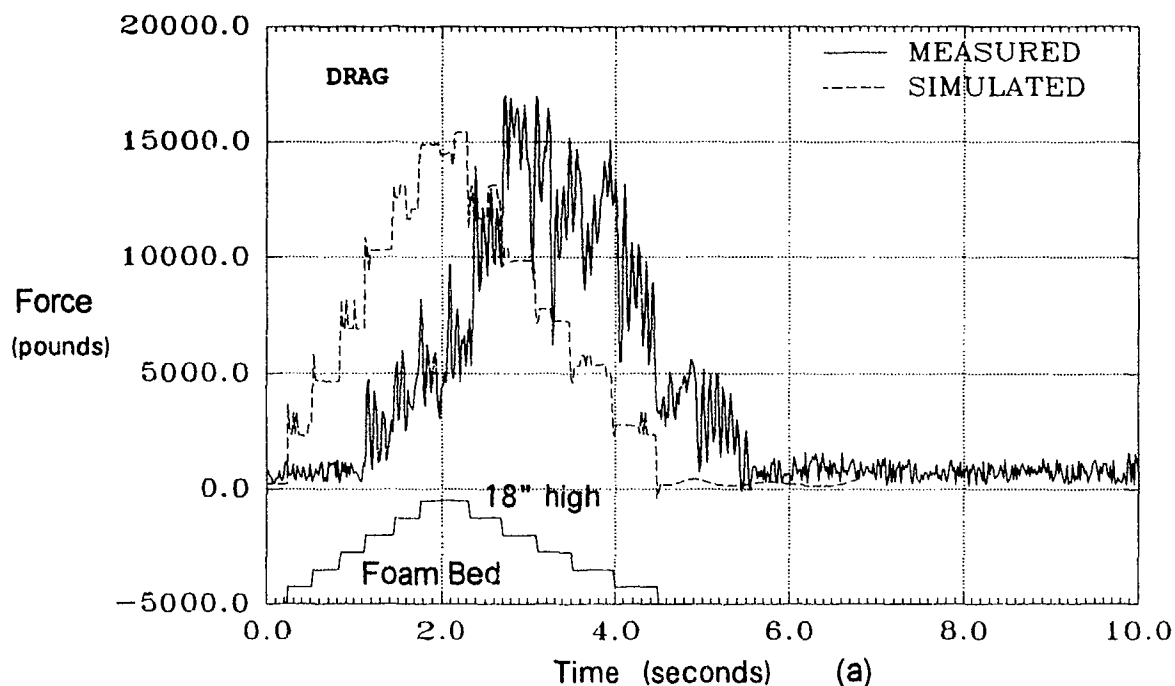


FIGURE 7. Nose Gear Drag and Vertical Loads

Figures 8(a) and 8(b) present curves which plot drag and vertical forces against time for the main gear of the aircraft. Once again the measured curves are shifted about one second in time.

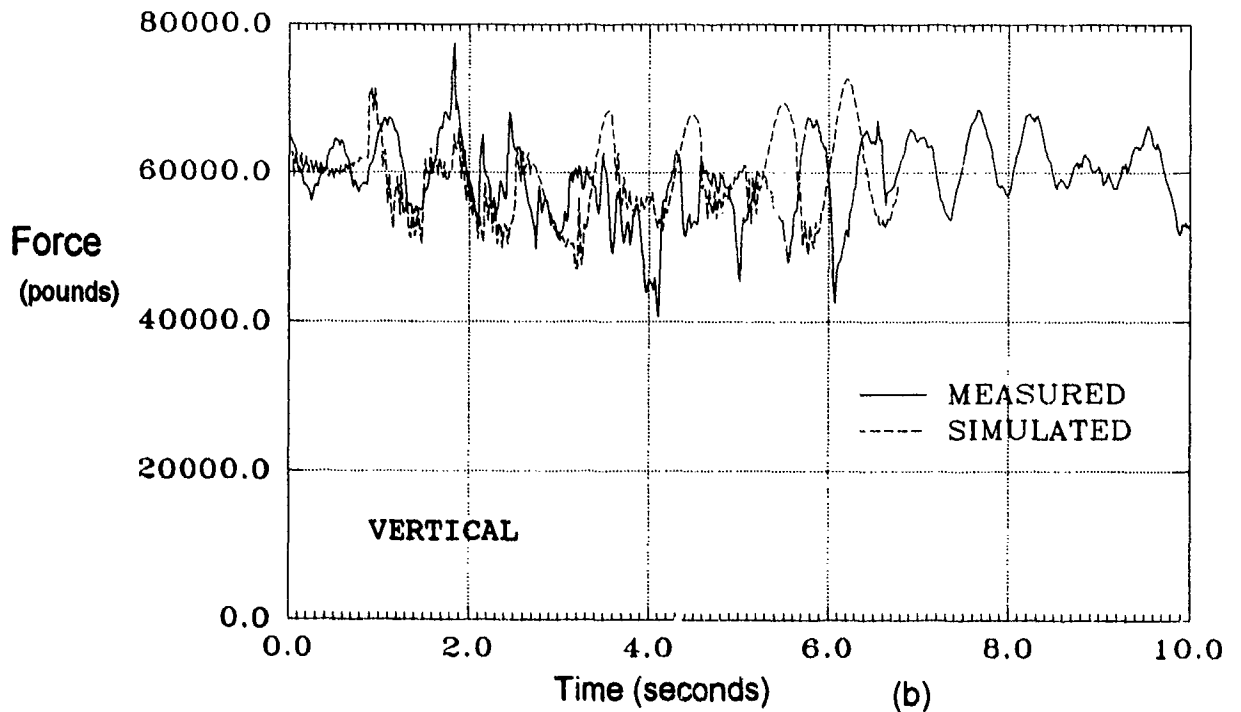
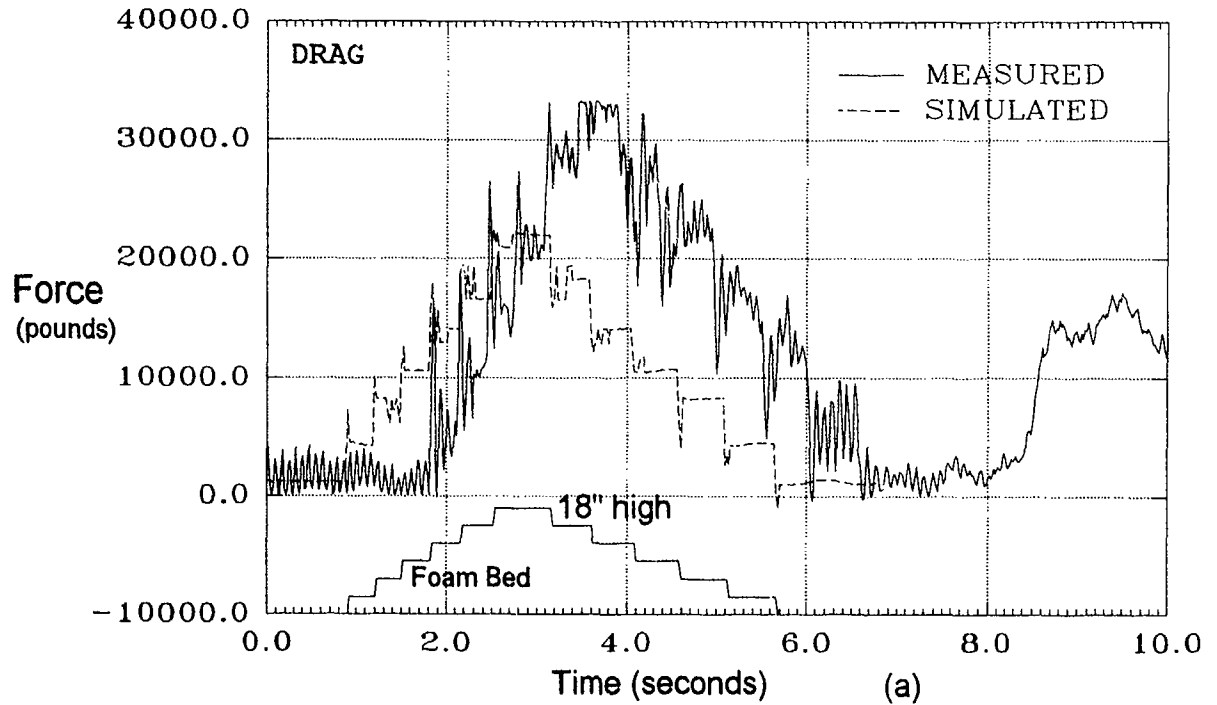


FIGURE 8. Main Gear Vertical and Drag Loads

The simulated and measured vertical loads on the main gear are similar in both magnitude and dynamic response (*figure 8(b)*). However, the drag on the main gear measured about 10,000 pounds higher than simulated. In this case there is evidence to support the simulated value over the measured value. First, the nose gear measured and predicted drag results were similar. Second, the measured acceleration curve of figure 6 shows that the maximum deceleration was about 0.4 g's at a time of 3.6 seconds into the test. This deceleration would require a total drag on the aircraft of about 53,700 pounds. The nose gear drag at that time was about 13,000 pounds so that the total drag on the main gear should be about 40,700 pounds or 20,350 pounds on each gear. Figure 8(a) shows that the measured drag load was about 32,000 pounds at the 3.6 second time spot but the simulated main gear drag was only about 22,000 pounds (remember to subtract 1 second for the simulated curve). This analysis shows that the measured main gear drag is too large by about 10,000 pounds and that the simulated drag is probably correct.

Another item concerning the accuracy of the computer simulation is its ability to predict the ground speed of the aircraft while in the arrestor test bed. Figure 9 shows the comparison of the measured and simulated ground speed prediction for test 8. The simulated reduction in speed appears to be about 2 knots lower than the measured value even though both started at the same speed. This is considered a minor error but may indicate an over estimate of the gear drag by the computer simulation.

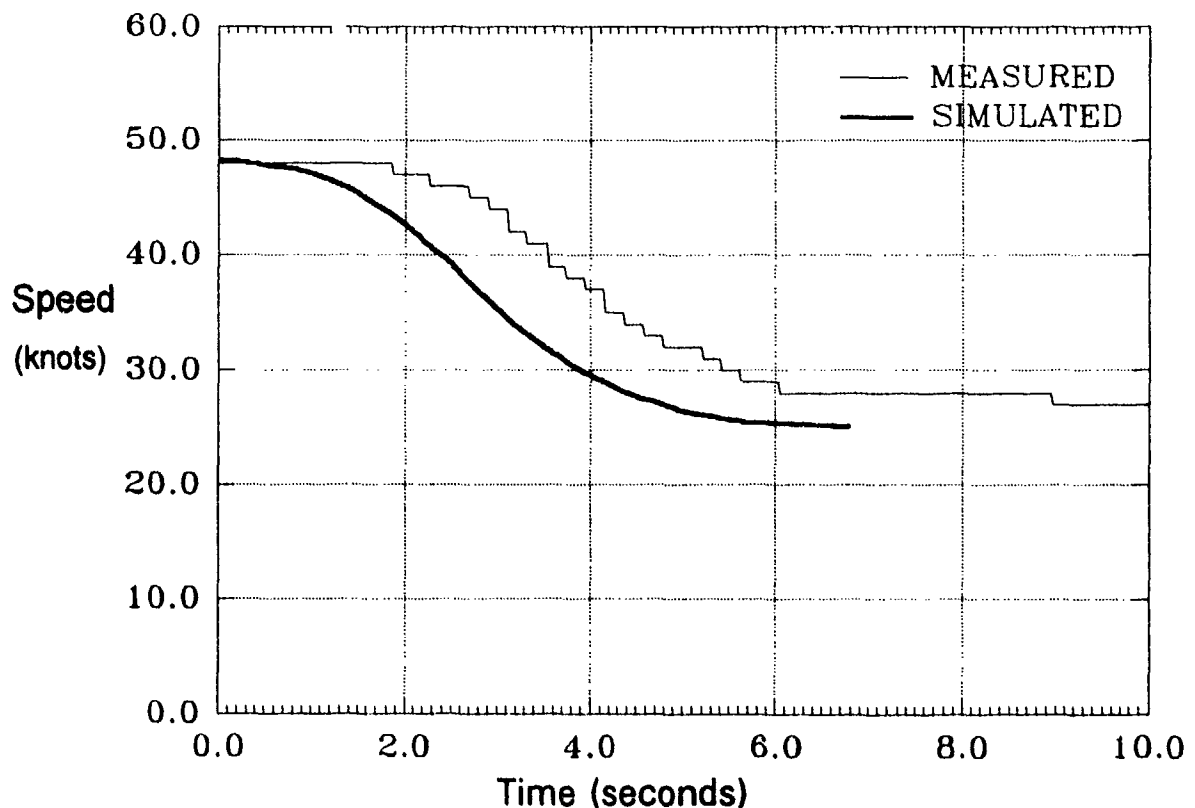


FIGURE 9. Comparison of Computed and Measured Ground Speed

As mentioned previously the aircraft brakes were applied during one of the test runs. The brakes were applied prior to and while passing through the 6-inch-deep bed. As expected the main gear drag increased to a "moderate" braking level just prior to bed entry. As the main gear wheels entered the bed there was a reduction in the measured drag, with this lower level being sustained throughout the extent of the bed. This value was close to the level achieved during a similar test with no brake application. These results indicate that braked wheels have little or no drag effect within the foam bed. Similar results were obtained during the British test program (*Bade, 1968 and 1969; Barnes, 1971; Gwynne, 1974*).

### 3. FULL-SCALE DEMONSTRATION OF SOFT GROUND ARRESTOR.

#### 3.1 FOAM BED DESIGN.

The results of the model verification tests prompted the FAA to plan a full scale demonstration of a soft ground arrestment system. The plan envisioned taxiing the instrumented FAA Boeing 727 aircraft at speeds up to 60 knots and bringing the aircraft to a complete and safe stop within the phenolic foam bed.

Using the previously developed mathematical model, the foam arrestor system for the demonstration was designed to be 496 feet long by 48 feet wide by 18 inches deep. An entry ramp 160 feet long would precede the full-depth bed. This stepped up portion would keep the loads exerted on the aircraft well below allowable design loads. An exit ramp 24 feet long was also added in the event the aircraft went beyond the available length of arrestor. Figure 10 shows the general layout of the arrestor configuration. Total bed length was 680 feet.

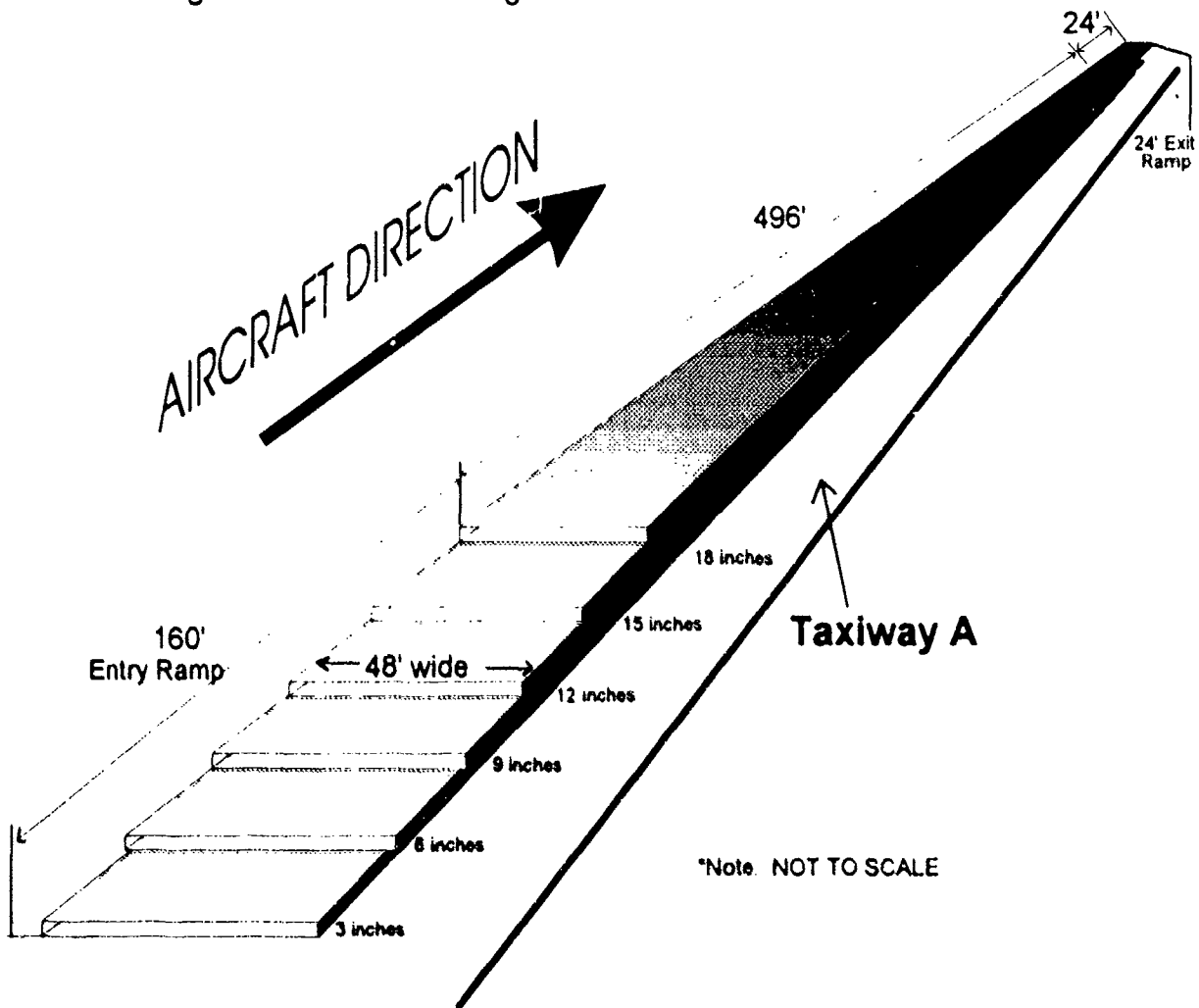


FIGURE 10. Soft Ground Arrestor System Layout

It was planned to conduct two demonstrations. The demonstrations would be conducted with aircraft entry speeds of 50 knots and 60 knots. Aircraft instrumentation system would record accelerations at the center of gravity and at the cockpit, velocity, and gear loads. Rut depths would be measured and final aircraft location recorded. Numerous video and still photography perspectives were employed. Aircraft extraction procedures would be field tested and the bed would be repaired for a second demonstration. After the second aircraft arrest and final measurements, airport rescue and firefighting equipment and personnel would enter and maneuver on the bed.

### **3.2 FOAM BED CONSTRUCTION.**

The arrestor was installed on Taxiway A at Atlantic City International Airport, NJ. Some 5,200 phenolic foam panels (4 feet by 8 feet by 3 inches) were stacked to meet the design configuration. The bottom layer of foam was bonded to the taxiway with silicone adhesive. Successive layers of foam were slightly offset from each other to break up the long vertical and horizontal joints and then bonded together with a silicone adhesive. The exterior surface joints between the panels were caulked and the entire bed was coated with a silicone sealer. The silicone products successfully protected the foam from moisture intrusion and ultraviolet degradation. However, the panels were subject to random splitting apparently due to thermal stresses which exceeded the tensile strength of the foam. Also, the panels displayed significant warping prior to the application of the sealer. This was due to uneven drying of the top side of the panels versus the bottom side. During the repair of the bed after the first demonstration, smaller panels (4 feet by 4 feet by 3 inches) were used. This significantly reduced the amount of random cracking, and the warping was also reduced.

### **3.3 AIRCRAFT ARREST AT 50 KNOTS.**

Prior to conducting the first demonstration the solution for the mathematical model insured that gear loads would not exceed any load limits specified for the aircraft. The model also predicted that the aircraft would come to rest 330 feet into the arrestor bed (*figure 11*).

The Boeing 727 aircraft entered the foam bed at 50 knots with two engines shut down, center engine at idle thrust, and flaps set at 15 degrees. It was assumed that the thrust of the single engine at idle would be offset by the aerodynamic drag of the aircraft. The aircraft came to a complete stop 420 feet into the bed (*figure 11*). Accelerations, velocity, and landing gear loads were recorded. Measurement of the ruts depths revealed deformations which were significantly less than expected. As the wheels were dug out of the foam it was observed that there was considerable foam rebound on the aft side of the tires. This indicated that the foam was rebounding on the back side of the tires and producing a forward thrust which canceled some of the drag on the wheels. This would cause an increased stopping

distance for the aircraft. Foam rebound had not been evident during the model verification tests. However foam used in the 1991 verification tests had a compressive strength of 35 psi whereas the foam for the full-scale demonstration had a compressive strength of 55 psi. The strength of the foam was increased for the demonstration in order to increase the drag on the aircraft and thereby shorten the foam bed. However the rebound strength was not adequately represented as an input parameter to the analytical model, and the simulation overestimated the net drag force and underestimated the stopping distance. Appendix C describes the analytical model elements in greater detail.

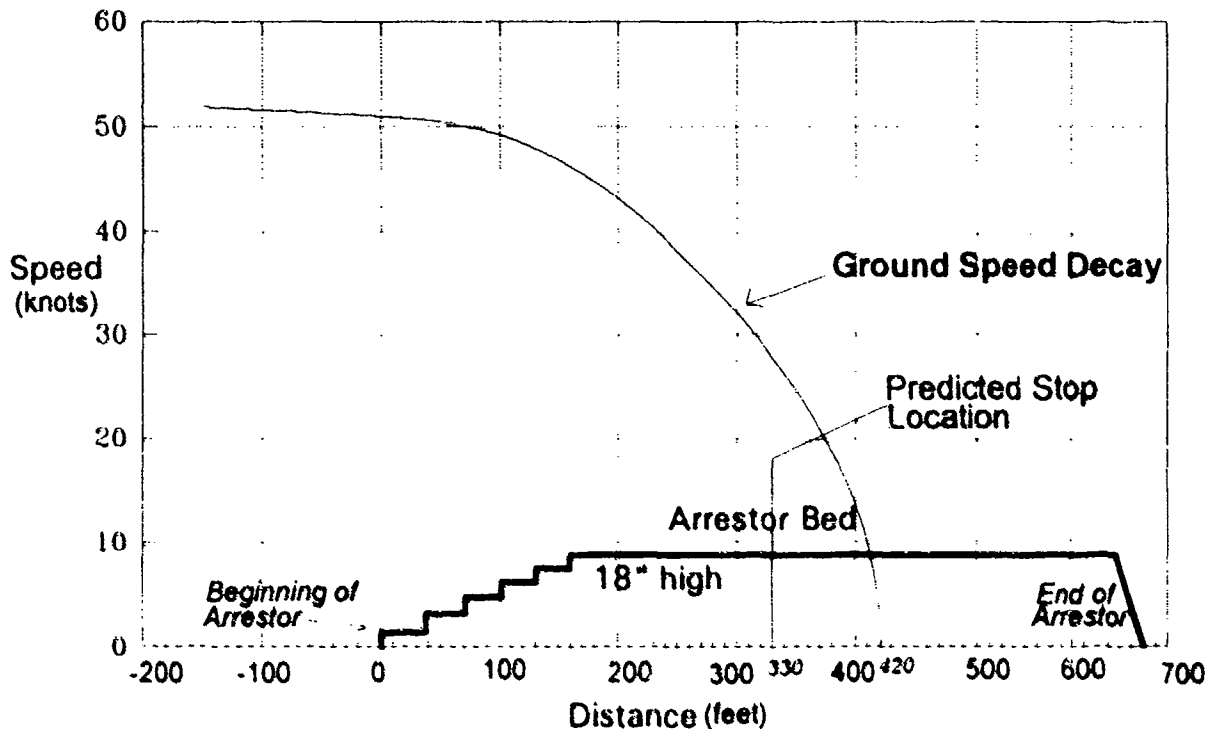


FIGURE 11. Nose Gear Travel Distance - 50-Knot Demonstration

Figure 11 also shows the speed decay in the foam bed and identifies both the predicted and actual location of the fully arrested aircraft. Appendix B provides additional data related to accelerations, gear loads, and drag ratio.

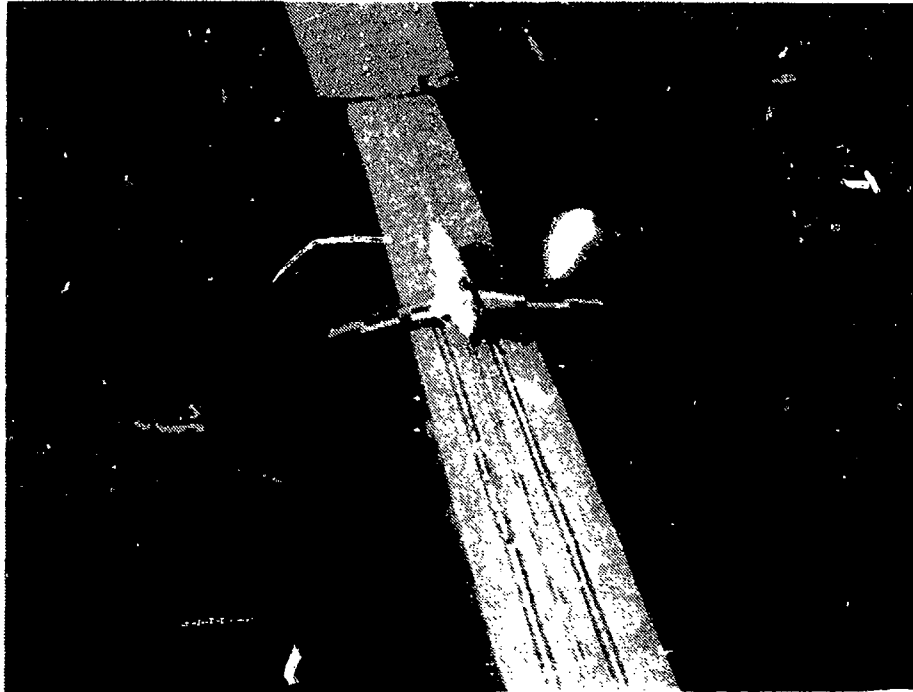


FIGURE 12. Overhead View of Arrested Aircraft

### **3.4 AIRCRAFT EXTRACTION AND FOAM BED REPAIR.**

After rut measurements were completed, the damaged foam was removed and the aircraft was pushed out of the bed. The entire process took about 8 hours. The bed was repaired with panels which were smaller than the original. The 4 foot by 4 foot by 3 inch panels were less susceptible to the random cracking and warping than the original 4 foot by 8 foot by 3 inch panels. The repaired bed was secured in place and sealed with silicone adhesives and sealant.

### **3.5 AIRCRAFT ARREST AT 60 KNOTS.**

The analytical model predicted the stopping distance with an entry speed of 60 knots to be 536 feet. The instrumented Boeing 727 aircraft entered the bed at 60 knots with one engine at idle and flaps at 15 degrees. The aircraft came to a complete stop 540 feet into the bed (*figure 13*). Accelerations, velocity, and gear loads were recorded. Rut depths were measured and recorded.

Figure 13 shows the speed decay in the foam bed and identifies both the predicted and actual location of the fully arrested aircraft. Appendix B provides additional data related to accelerations, gear loads, and drag ratio.



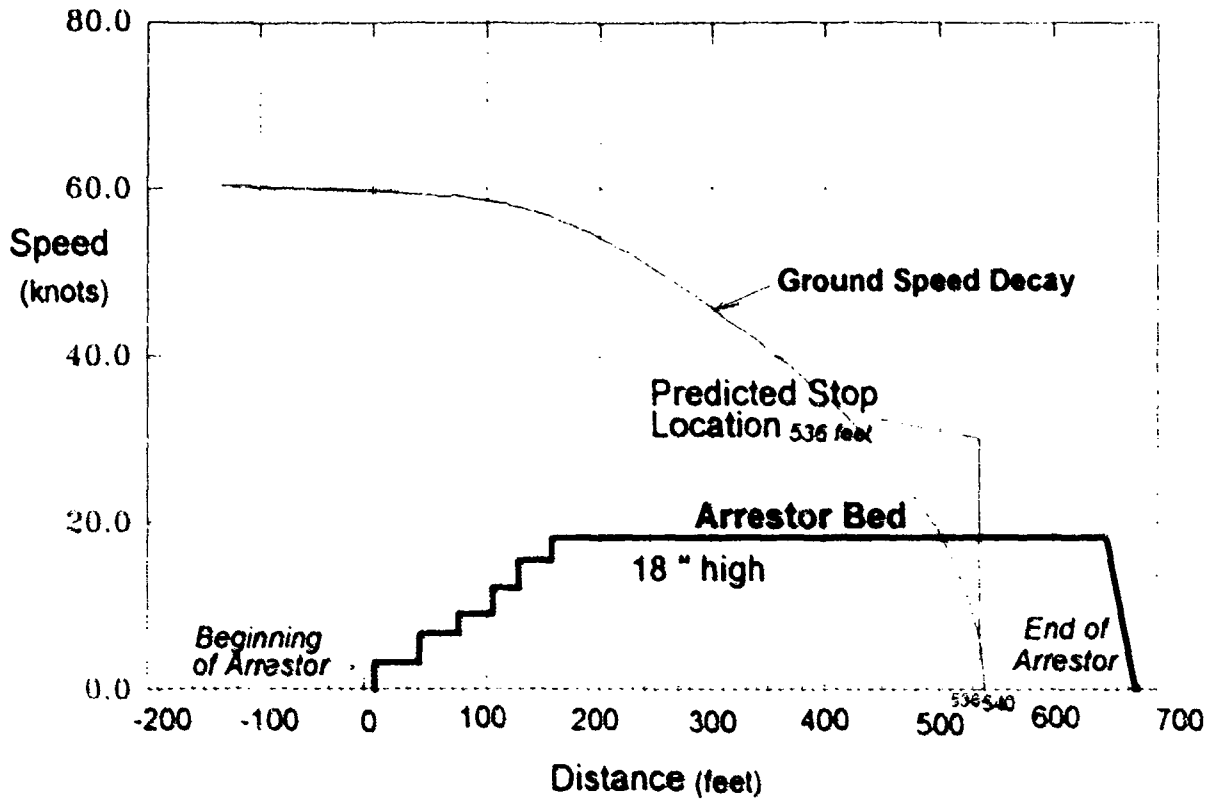


FIGURE 13. Nose Gear Travel Distance in Feet - 60-Knot Demonstration

After rut measurements were complete, airport rescue and firefighting equipment and personnel entered the foam bed and maneuvered within the bed without difficulty. Figure 14 shows fire truck operating on the arrestor bed

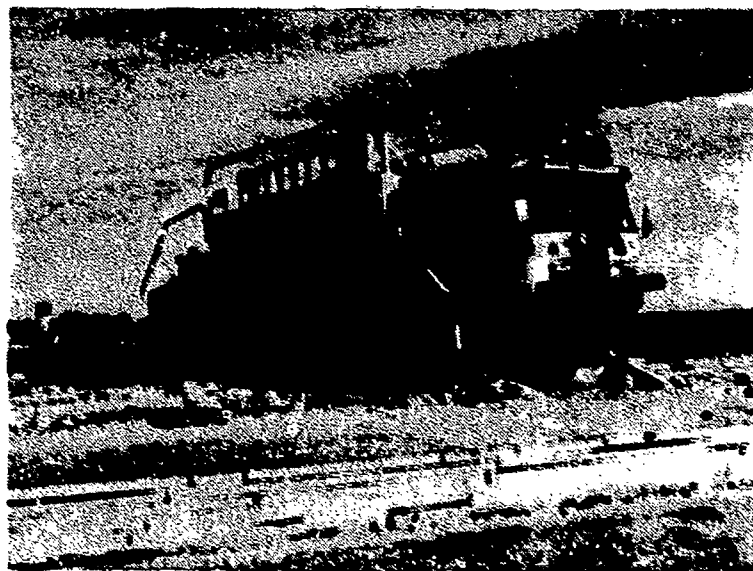


FIGURE 14 P-19 Airport Rescue / Firefighting Truck Operating in Arrestor Bed

#### **4. CONCLUSIONS.**

- The validity of a mathematical model representing a tire/foam interface to accurately predict the landing gear loads, deceleration of aircraft center of gravity, and aircraft speed decay was confirmed by eight tests with the use of the FAA Boeing 727 aircraft.
- Aircraft arrestment on a full-scale soft ground bed was accomplished with entry speeds of 50 knots and 60 knots: at 50 knots the aircraft came to a complete stop in 420 feet and at 60 knots in 540 feet. In each case the bed was 680 feet long, 48 feet wide, and 18 inches deep.
- Airport rescue and firefighting equipment and personnel were able to maneuver without difficulty on the foam following the arrestment.
- Aircraft was successfully extracted from the foam bed following arrestment.
- The foam bed was successfully repaired following the arrestment.

## 5. REFERENCES.

Bade, E. (1968). Soft Ground Arresting of Civil Aircraft. (Technical Report 68032). Ministry of Technology, Farnborough, Hants.

Bade, E. (1969). Soft Ground Arresting of Civil Aircraft - Influence of Gravel Depth and Tire Inflation Pressure. (Technical Report 69001). Ministry of Technology, Farnborough, Hants.

Barnes, J.R. (1971). Development of a Model Technique for Investigating Performance of Soft Ground Arrestors for Aircraft. (Technical Report 71231). Royal Aircraft Establishment.

Cook, R. F. (1987). Soft Ground Aircraft Arresting Systems. (Report DOT/FAA/PM-87/27). Department of Transportation/Federal Aviation Administration.

Cook, R. F. (1988). Evaluation of a Foam Arrestor Bed for Aircraft Safety Overrun Areas. (UDR-88-07). University of Dayton Research Institute, Dayton Ohio. (Prepared for the Port Authority of New York and New Jersey).

Cook, R. F. (1993). Soft Ground Arresting System for Commercial Aircraft. (Department of Transportation/Federal Aviation Administration/CT-TN 93/4).

David, Robert E. (1990). Location of Commercial Aircraft Accidents/Incidents Relative to Runways. (Department of Transportation/Federal Aviation Administration/AOV-90-1).

Federal Aviation Administration (1992). Airport Design. (FAA Advisory Circular 150/5300-13). February 24, 1992.

Gwynne, G. M. (1974). Urea Formaldehyde Foamed Plastic Emergency Arresters for Civil Aircraft. (Technical Report 74002). Royal Aircraft Establishment.

Horne, Walter B. (1985). JFKIA - Runways 4R-22L Safety Overrun Study. (Prepared for the Port Authority of New York and New Jersey).

**APPENDIX A**

**MATHEMATICAL MODEL VERIFICATION TESTS**

**APRIL - JUNE 1991  
ATLANTIC CITY INTERNATIONAL AIRPORT  
POMONA, NJ**

## 1. INTRODUCTION.

An experimental program using an instrumented FAA Boeing 727 aircraft was conducted at the FAA Technical Center to determine the effectiveness of a plastic (phenolic) foam material as an arrestor for aircraft which overrun the available length of runway during takeoff, abort, or landing. The program consisted of eight foam test beds ranging from 6 inches deep to 18 inches deep, all having foam ramps to reduce the aircraft gear loads and dynamic response. The aircraft traversed these foam beds at speeds of 20 to 80 knots to determine the deceleration and loads produced on the aircraft by the foam.

A computer program was used to simulate each of the tests prior to the actual test. This computer program is capable of simulating the aircraft nonlinear landing gear characteristics, the aircraft flexible structural dynamic response, the ramp/taxiway surface modification caused by the addition of the foam, the landing gear drag and vertical loads and the aircraft deceleration resulting from the foam arrestor, and the wheel axle displacement (rut depths) in the foam.

The aircraft was instrumented to measure landing gear loads in three mutually perpendicular axes and moments about the axle of the main gear, accelerations at the center of gravity in three directions, wheel speeds, ground speed and other parameters. The instrumentation was calibrated prior to arrestor testing and the test data obtained were recorded on 5.25 inch high density floppy disks in ASCII format. Initial static, braking, and turning tests were conducted to verify the computer program accuracy prior to foam bed tests. As a result of the initial tests only the nose gear and right main gear loads are analyzed; the left gear loads were found to be in error.

## 2. MEASURED AND SIMULATION RESULTS.

The experimental program consisted of eight tests of an instrumented Boeing 727 aircraft traversing phenolic foam arrestor beds as summarized in table A-1. Results from these tests and comparisons with the computer simulated results along with a broad description of the test bed design and installation are discussed in this section of the report.

TEST (ORDER)	GW (LB)	CG (IN)	ENTRY VELOCITY (KNOTS)	BED DEPTH (IN)
T1-S1-20K (1)	135,067	901	20	6
T1-S2-40K (2)	134,267	901	40	6
T2-S2-60K (3)	132,267	900	62	6
T1-S1-BRK-40K (4)*	131,267	900	40	6
T2-S2-80K (5)	134,882	901	80	6
T4-S2-30K (6)	135,965	891	33	12
T4-S2-50K (7)	134,625	894	50	12
T5-S2-50K (8)	134,249	896	49	18

*Note: Speeds were read visually from the INS for the first four tests because the ground speed indicator was inoperative.*

### 2.1 TEST BED CONSTRUCTION AND INSTALLATION.

The test beds were constructed so that the deepest test section had an approach ramp and a sloped exit ramp to provide gradual exit. The ramp lengths were variable depending on the test speed and the maximum depth of the test section. These ramps were provided to assure that excessive gear loads would not be imposed on the aircraft.

The phenolic foam test beds were installed by bonding 3 inch thick, 4- by 8-foot panels to the FAA ramp and Taxiway A at Atlantic City International Airport sites. The foam panels were bonded to the surface and each other with a latex based adhesive. Some panels were pre-bonded at the manufacturer's facility to provide 6-inch-deep panels. The upper panel of these preformed panels was offset 3 inches in two directions to provide overlap between adjoining panel joints. Four bed configurations and three depths (6, 12, and 18 inch) were tested and each bed is shown on figure A-1.

## 2.2 AIRCRAFT TESTS ON 6-INCH-DEEP FOAM BEDS.

Six-inch-deep foam beds were used initially to reduce the potential for damage to the aircraft in the event that the analytical results were erroneous.

### 2.2.1 Test T1-S1-20K Description.

The first test was made on a Type-1 phenolic foam test bed on the FAA ramp. The aircraft was accelerated with all three engines until it reached a speed of about 30 knots and then the speed was allowed to decay, with the engines shut down (thrust=0.0), to about 20 knots before entering the foam bed. No flaps or spoilers were deployed for the test run.

A mild bump was felt in the cockpit upon nose wheel entry to the foam bed. A small, but noticeable, longitudinal deceleration was also noted.

The aircraft was braked to a stop after clearing the test bed and the aircraft was visually inspected. Although a large amount of foam material had been thrown into the nose wheel well by the nose wheel and some was caught in areas of joints and other capture areas, no physical damage was noted anywhere to the aircraft. There was no evidence that any foam had entered the engines; however, a review of the video coverage indicated that lowering the flaps to 15 degrees and use of only the number 2 engine when possible might be advantageous for future tests.

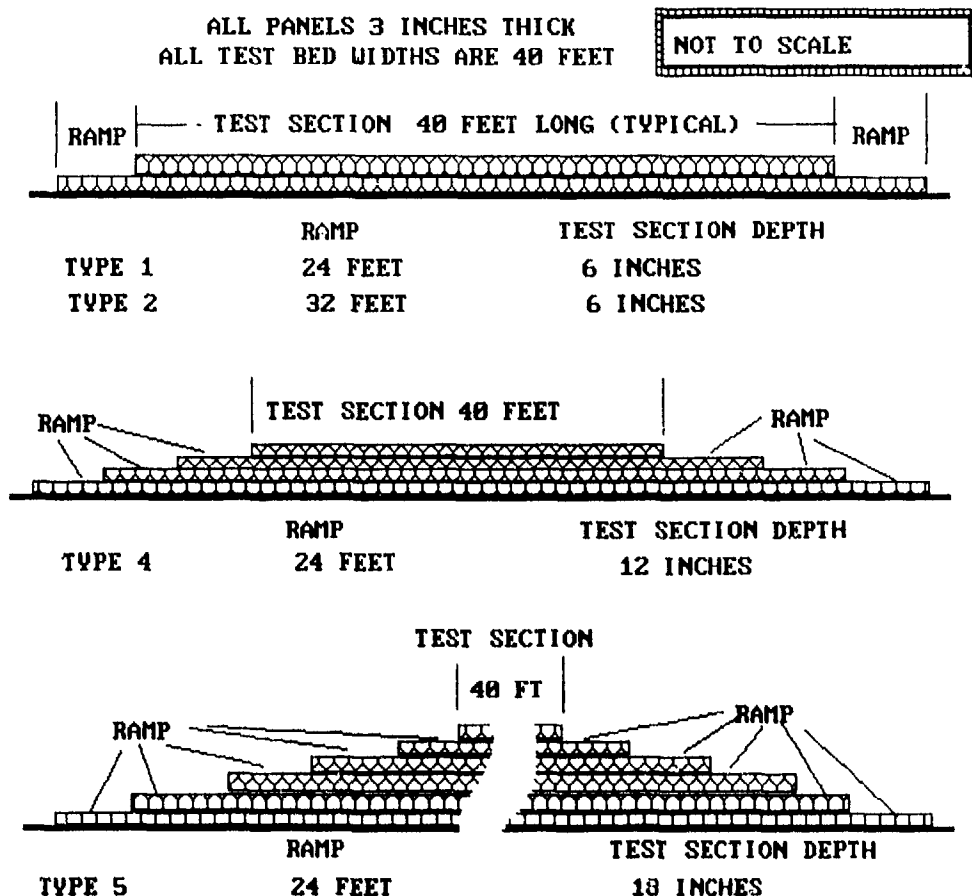


FIGURE A-1. Test Bed Layouts

The test bed was inspected and it was evident that deep rutting had occurred. The rut depths (deformation/percentage full depth) were recorded and the results are given in table A-2. This rutting was expected since it is the deep rutting that allows the arrestor to provide forces that decelerate the aircraft.

Table A-2. Average of Rut Depths in Type-1 Foam Arrestor Bed			
T1-S1-20K	PART 1-Inches	PART 2-Inches	PART 3-Inches
Nose Gear	2.0 (66%)	4.7 (78%)	2.2 (72%)
Right Main Gear	2.0 (66%)	4.2 (69%)	1.7 (55%)
Left Main Gear	2.0 (66%)	4.6 (76%)	2.0 (66%)

### 2.2.2 Recorded Data Results T1-S1-20K.

Once satisfied that the aircraft was not damaged and the test bed had performed as desired, the recorded data were reduced and compared to the simulated results previously computed and stored in the onboard computer. The results obtained are shown on figures A-2 to A-4.

Figure A-2 shows a comparison of the measured deceleration along with the simulated deceleration. The simulated deceleration vertical scale was shifted vertically .07 g's to match the measured value and the simulated value was also shifted left by about .5 seconds in order to provide an easier comparison. The initial undisturbed 0.05 g's acceleration measured value is a result of zero being offset slightly. Free rolling deceleration would be about -0.02 g's. The simulated deceleration curve is also shifted horizontally for clarity. From figure A-2 it is clear that the measured and simulated deceleration values are in agreement. It should be noted that the measured value was truncated somewhat early by the event marker during the recording but it is clear that the two curves are quite comparable. The nominal measured deceleration in the bed center section was about 0.1 g.



## LONGITUDINAL ACCELERATION

B-727 GW=135067 LB CG=901 INCHES

TEST T1S120K 6-INCH-DEEP FOAM BED

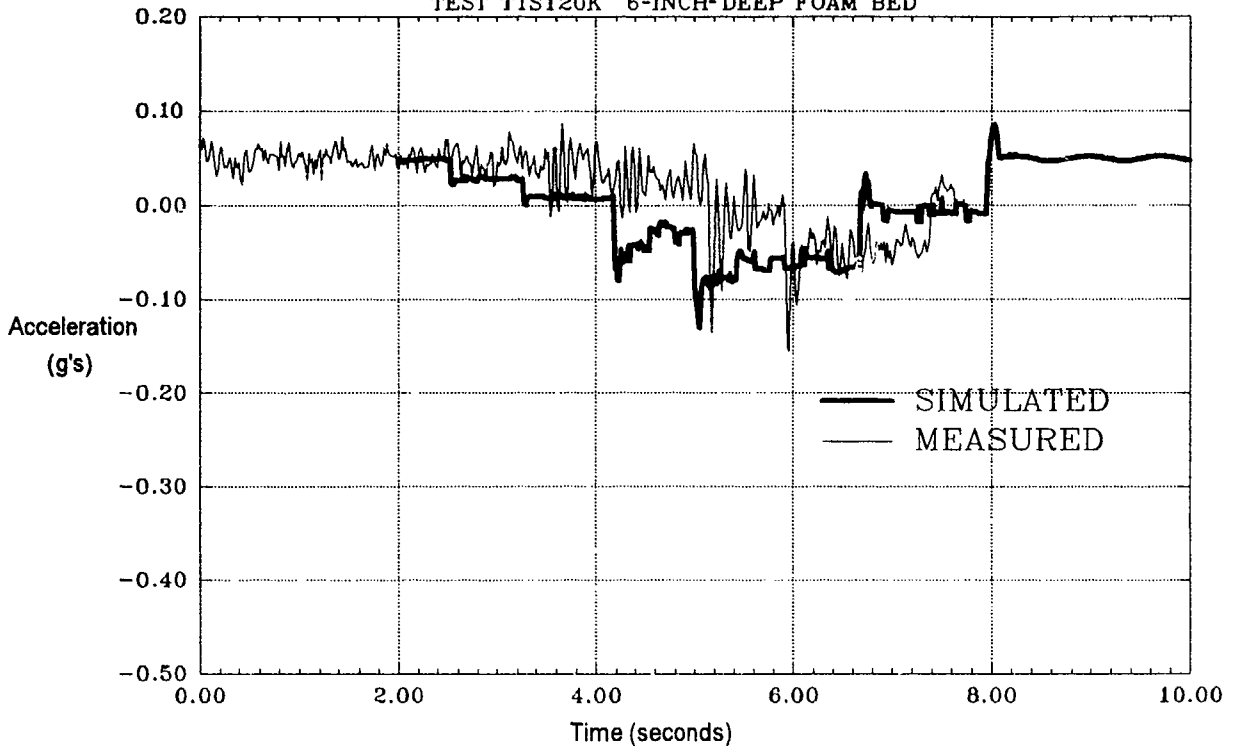


FIGURE A-2. Deceleration of Aircraft at 20 Knots

The next comparison of measured and simulated data is for the nose gear vertical and drag loads resulting from the wheels traversing the foam bed. Figure A-3 gives this comparison and again it is noted that the values are quite close. As in figure A-2 the curves are translated horizontally but the similarity is clear. The maximum measured nose gear vertical load was about 25,000 pounds which is considerably below the 40,300 pound load limit and the maximum measured drag load was about 7,500 pounds although the nominal drag load after the peak was about 4000 pounds, both of which are much lower than the 25,500 pound limit value. The nose gear nominal drag load was about 1000 pounds less than the simulated value. Also note that the measured drag trace shape follows the shape of the foam bed longitudinal cross-section.

A comparison of the measured and simulated main gear loads is shown in figure A-4. The vertical loads are quite similar as in the nose gear comparison. The nominal drag values are also very close but differ in that the measured value has a large peak at the beginning of each change in arrestor height. An investigation of these initial peak loads showed that they were caused by the natural frequency of the landing gear. Actual aircraft modal and generalized mass data are not available for the FAA aircraft but figure A-5 shows the results of a simulation where the mass and modal frequency were estimated and this effect was simulated. It is clear that a similar spike is produced even though the amplitude of the spike is somewhat smaller. The amplitude of the spike is controlled by the amount of damping and modal mass in the vibrating mode. It should be noted that this condition holds for both the nose and main gears. Since the gear loads were relatively small there is no concern of exceeding load limits from this source.

### 2.2.3 Test T1-S2-40K Description.

The test was conducted on Taxiway A. The aircraft flaps were lowered to 15 degrees and engines 1 and 3 were plugged to prevent any possibility of loose foam entering the nacelle. The aircraft was accelerated to approximately 40 knots and just before entering the test bed the power was cut (thrust=0.0). After passing through the test bed the aircraft was braked to a stop. An inspection of the nose wheel area showed that there was no significant amount of foam material on the wheel or in the wheel well.

The rut depths (deformation) in the foam bed were measured at several locations in each section of the bed and the average of the results is shown in table A-3.

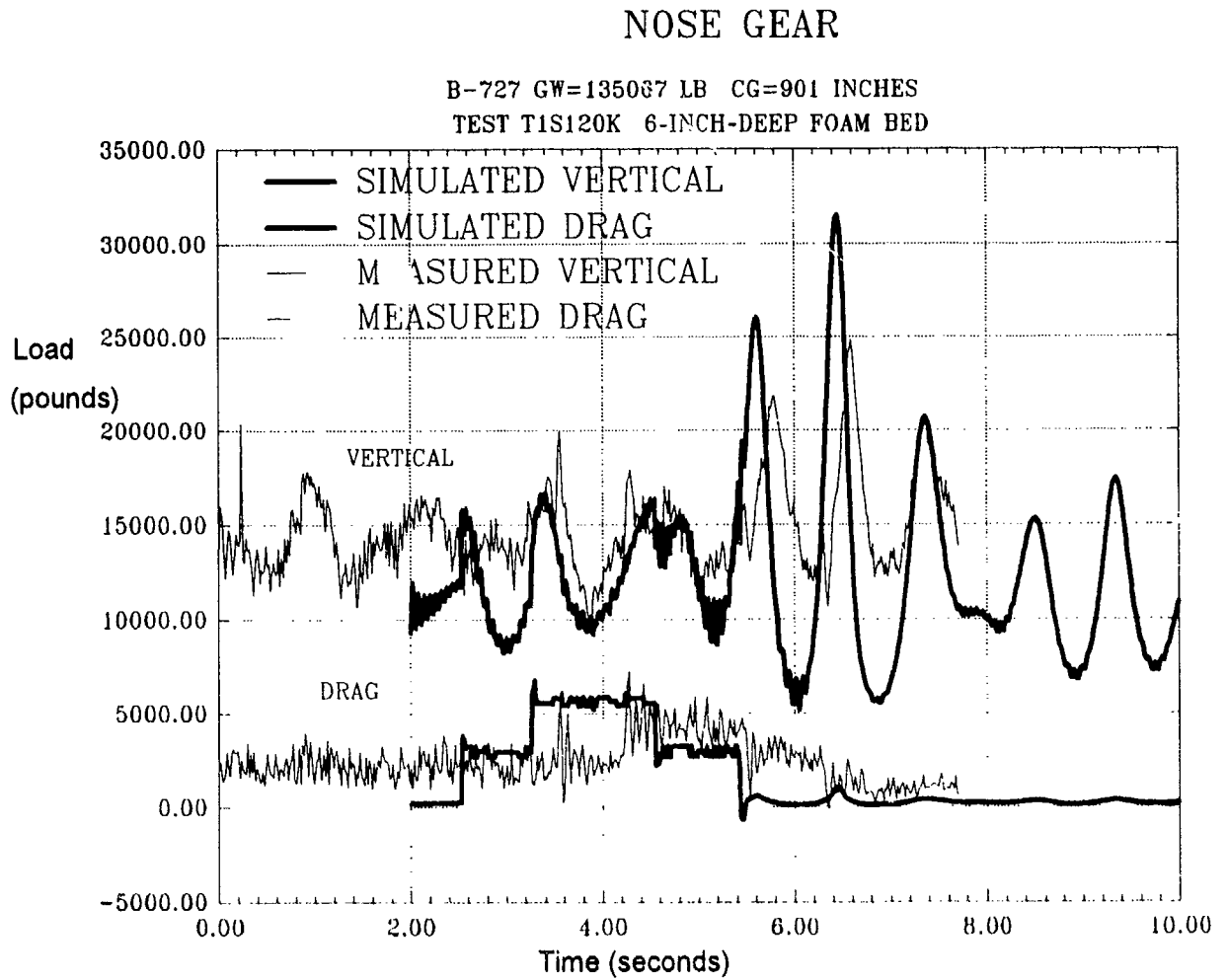


FIGURE A-3. Nose Gear Load Comparison

### RIGHT MAIN GEAR

B-727 GW=135067 LB CG=901 INCHES  
TEST T1S120K 6-INCH-DEEP FOAM BED

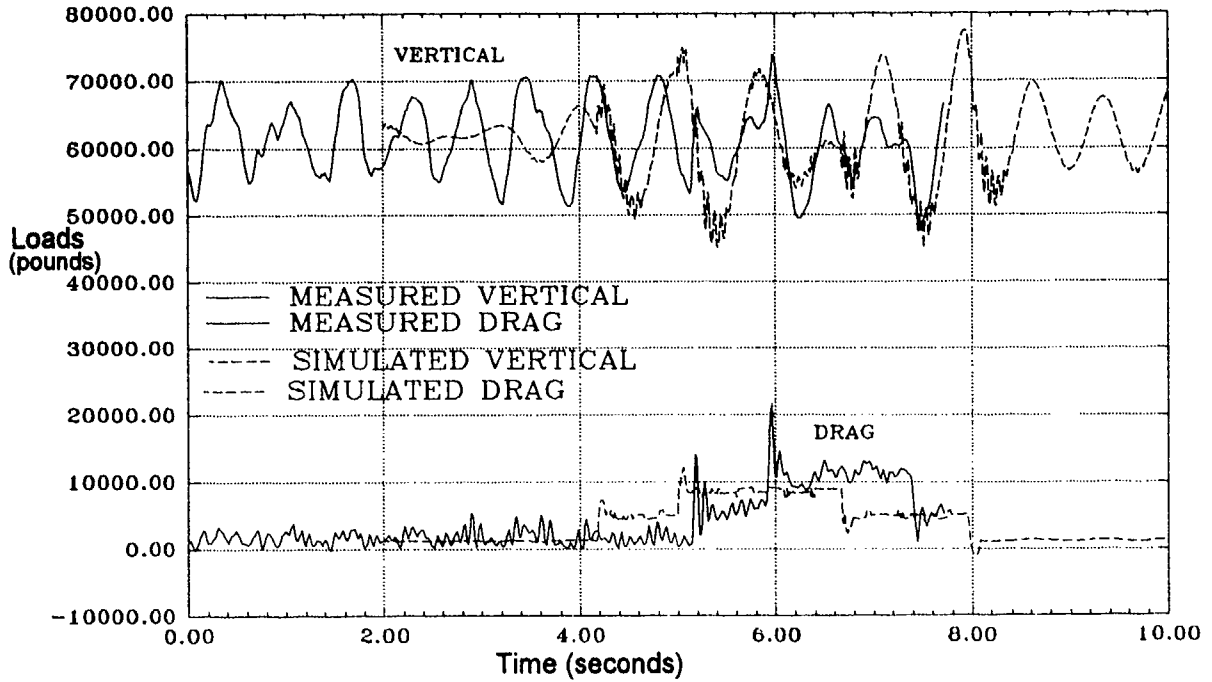


FIGURE A-4. Main Gear Load Comparison

### RIGHT MAIN GEAR

B-727 GW=135067 LB CG=901 INCHES  
TEST T1S120K 6-INCH-DEEP FOAM BED

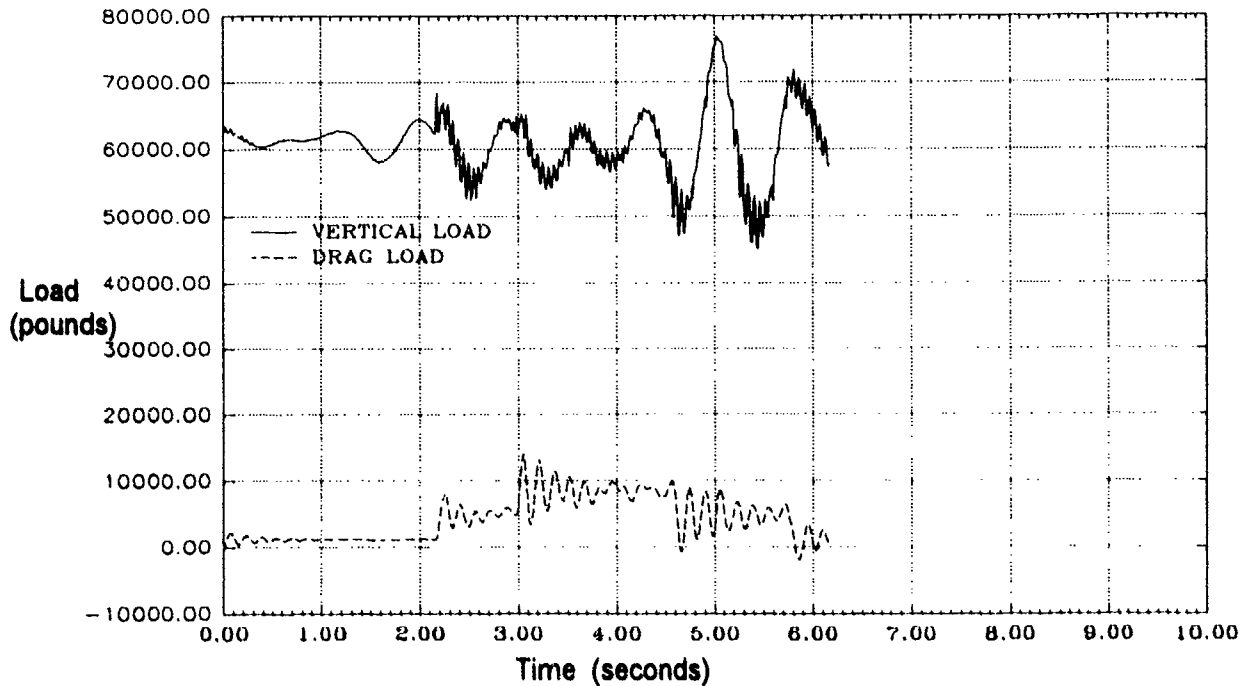


FIGURE A-5. Drag Load Spikes During Initial Entry into Foam Bed

Table A-3. Average Rut Depths For Type-1 Foam Arrestor Bed			
T1-S2-40K	Section 1 Inches	Section 2 Inches	Section 3 Inches
Nose Gear	2.46 (82%)	3.675 (61%)	2.09 (69%)
Right Main Gear	2.07 (69%)	4.11 (68%)	2.42 (80%)
Left Main Gear	1.89 (63%)	4.11 (68%)	2.18 (73%)

#### 2.2.4 Recorded Data Results T1-S2-40K.

Figure A-6 shows a comparison of the longitudinal acceleration of the aircraft during the test. The simulated longitudinal acceleration is also shown. Again, the measured and simulated values are nearly the same except for the noise on the measured trace. The nominal measured deceleration was about 0.1 g.

Figure A-7 shows a comparison of the measured and simulated nose wheel loads while in the foam test bed. The nose gear vertical loads compared quite favorably in both magnitude and curve shape. The nominal drag load was only about 3500 pounds while the simulated value was about 6000 pounds, both of which are much below the nose gear limit value. The difference in the drag load values could be due to a lesser nose gear penetration into the foam bed as a result of aircraft dynamics.

The comparison of the measured and simulated main gear loads is shown on figure A-8. The vertical loads compared quite well as did the nominal drag loads.

#### 2.2.5 Test T2-S2-60K Description.

The aircraft flaps were lowered to 15 degrees and the aircraft accelerated with all engines to about 66 knots on Taxiway A. The engine thrust was reduced to idle (thrust about 3600 pounds) just before entry into the Type-2 test bed. The speed was about 62 knots at entry. A mild thump was felt as the aircraft passed over the foam bed. The aircraft was braked to a stop and the aircraft inspected. A visual inspection indicated no visible damage to the aircraft.

The test bed was inspected and found to have deep, but ill defined, ruts formed by the aircraft wheel passage. The rut depths available are recorded in table A-4.

Table A-4. Average Rut Depths in Type-2 Foam Arrestor Bed			
T2-S2-60K	Section 1 Inches	Section 2 Inches	Section 3 Inches
Nose Gear	NO DATA	2.2 (36%)	NO DATA
Right Main Gear	2.0 (66%)	NO DATA	NO DATA
Left Main Gear	NO DATA	NO DATA	NO DATA

### LONGITUDINAL ACCELERATION

B-727 GW=134267 LB CG=901 INCHES  
TEST T1S240K 8-INCH-DEEP FOAM BED

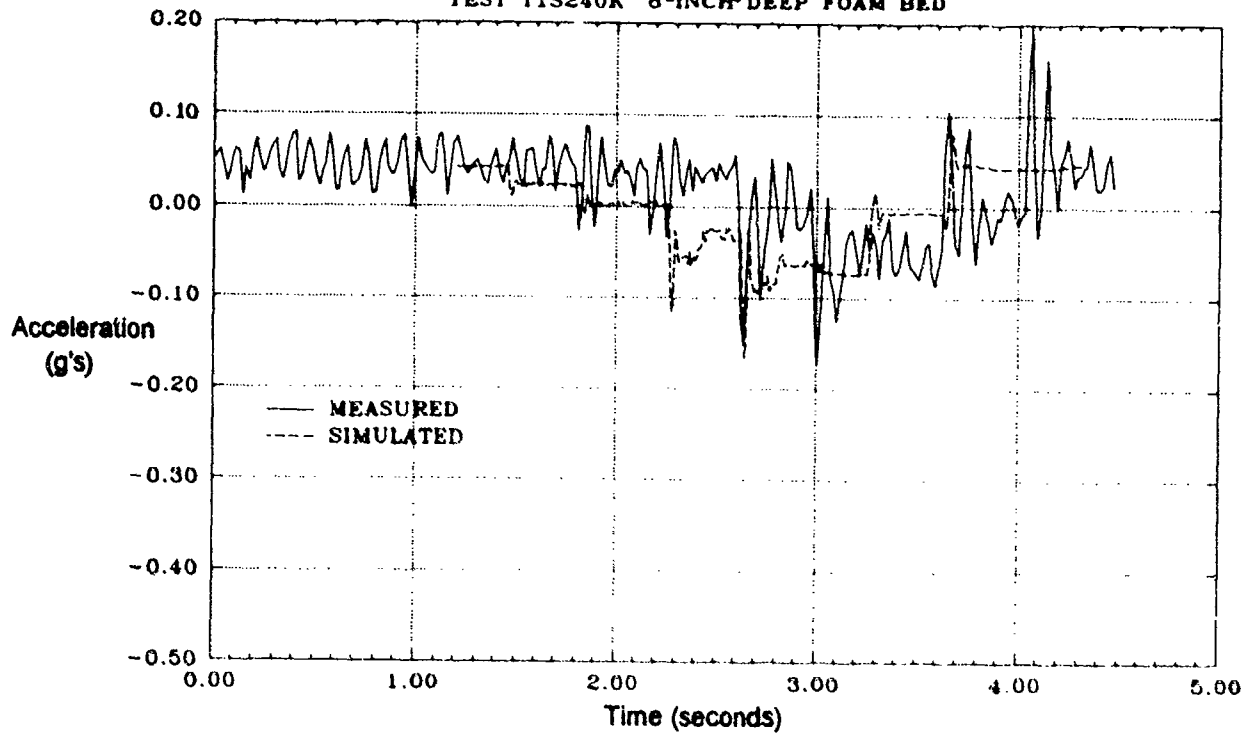


FIGURE A-6. Comparison Test T1S240K Measured and Simulated Longitudinal Acceleration

### NOSE GEAR

B-727 GW=134267 LB CG=901 INCHES  
TEST T1S240K 6-INCH-DEEP FOAM BED

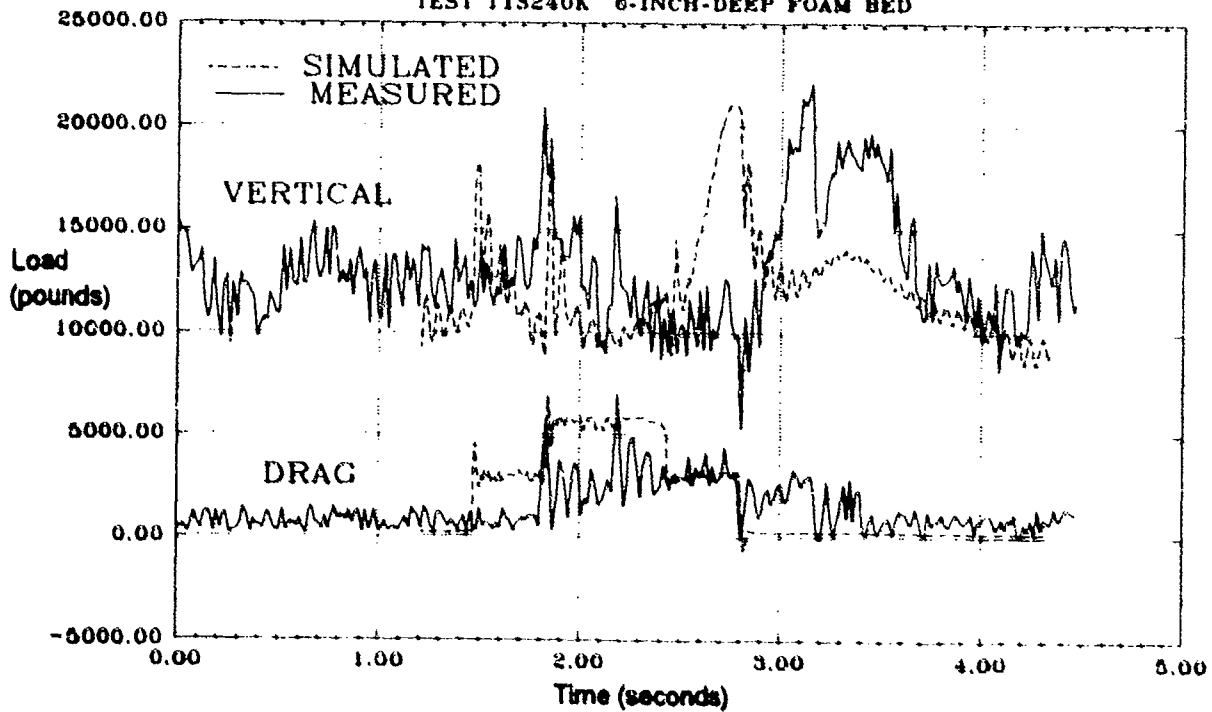


FIGURE A-7. Comparison of Test T1S240K Measured and Simulated Nose Gear Loads

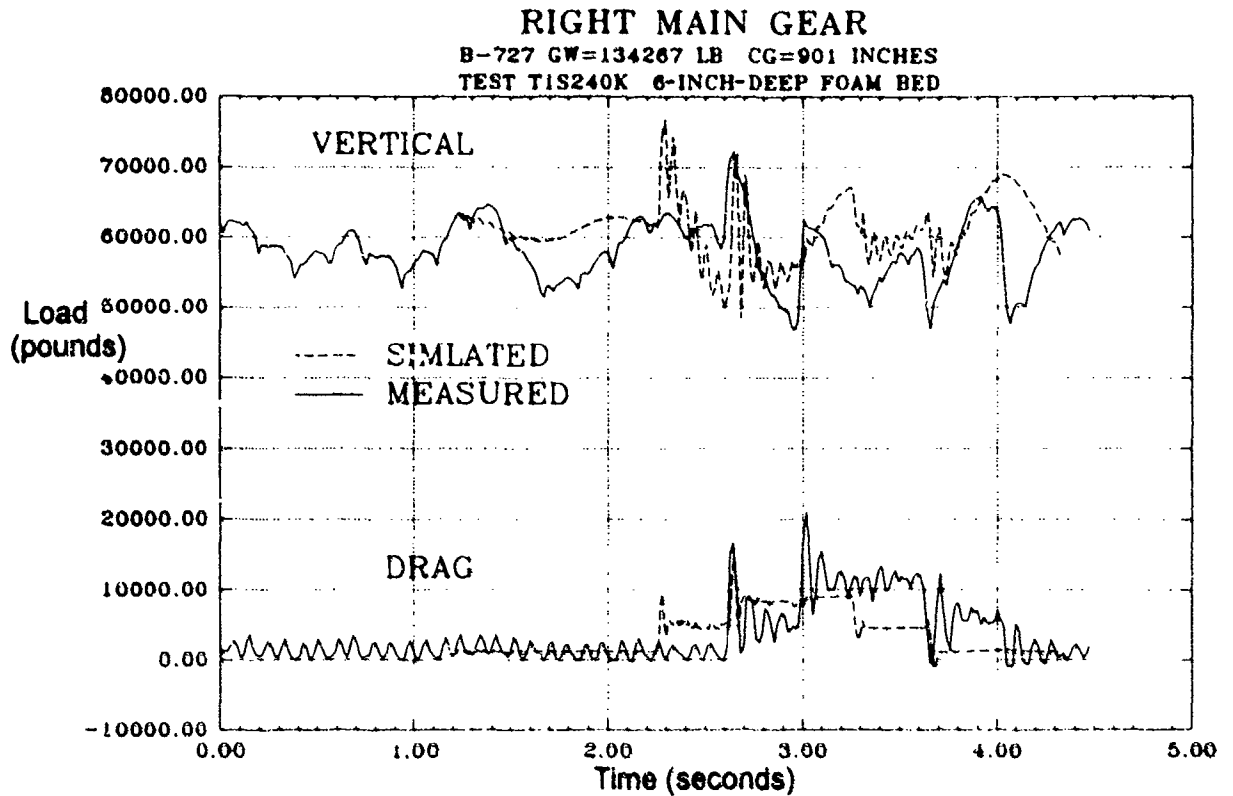


FIGURE A-8. Comparison of Test T1S240K Measured and Simulated Right Main Gear Loads

2.2.6 Recorded T2-S2-60K Data Results.

The measured longitudinal aircraft acceleration is shown in figure A-9 along with the simulated trace. The average deceleration in the center section of the bed was about 0.1 g as in the previous tests.

Figure A-10 shows the nose gear load comparison for the measured and simulated results. The vertical loads compared quite favorably but the measured drag was lower than the simulated trace. The average measured drag in the center section of the test bed was about 3000 pounds as compared to the simulated 6000 pounds.

Figure A-11 gives a comparison of the vertical and drag loads for the right main gear. The measured vertical load is slightly lower than the simulated trace. This is probably due to a small amount of lift since the flaps were lowered to 15 degrees. To compensate for this additional lift the aircraft spoilers will be deployed in future high speed runs. The measured drag load is slightly higher than the simulated trace which seems to be characteristic of all runs thus far.

### 2.2.7 Test T2-S2-80K Description.

The aircraft was accelerated using all three engines to a speed of 80 knots. The flaps were lowered to 15 degrees prior to starting the test run. Just prior to entering the Type-2 test bed the engine thrust was reduced to idle and the wing spoilers were deployed to reduce the wing lift and to provide a realistic landing or takeoff abort configuration.

A mild thump was felt in the cockpit as the aircraft crossed the foam bed as in previous test runs.

The aircraft was braked to a stop and a visual inspection made. There was no damage evident and only a small amount of foam caught up in aircraft parts. The foam bed was inspected and found to look similar to the previous beds with deep ruts corresponding to the wheel tracks. The rut depths were recorded and the average values are shown in table A-5.

T2-S2-80K	Section 1 Inches	Section 2 Inches	Section 3 Inches
Nose Gear	2.3 (77%)	4.0 (66%)	1.8 (60%)
Left Main Gear	2.2 (73%)	4.2 (69%)	2.0 (66%)
Right Main Gear	2.2 (73%)	4.2 (69%)	2.1 (68%)

### LONGITUDINAL ACCELERATION

B-727 GW=132267 LB CG=900 INCHES

TEST T2S260K 6-INCH-DEEP FOAM BED

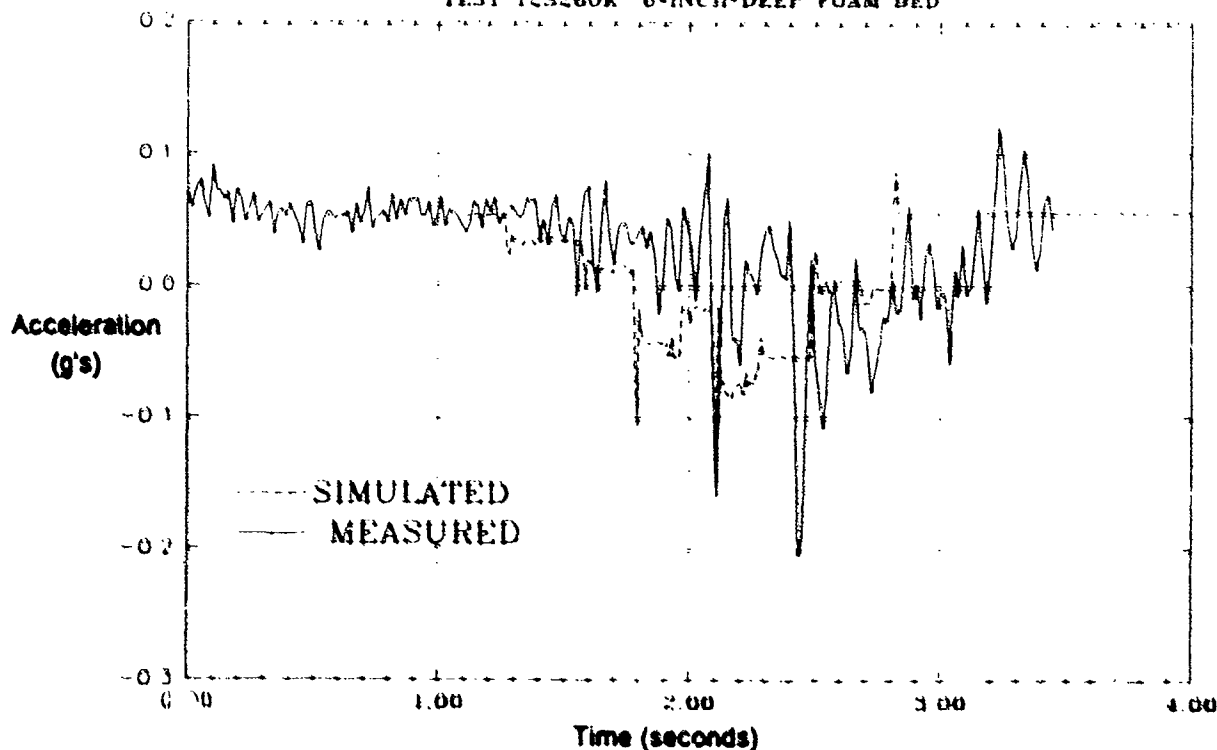


FIGURE A-9. Comparison of T2S260K Measured and Simulated Longitudinal Acceleration

### NOSE GEAR

B-727 GW=132267 LB CG=900 INCHES  
TEST T2S260K 6-INCH-DEEP FOAM BED

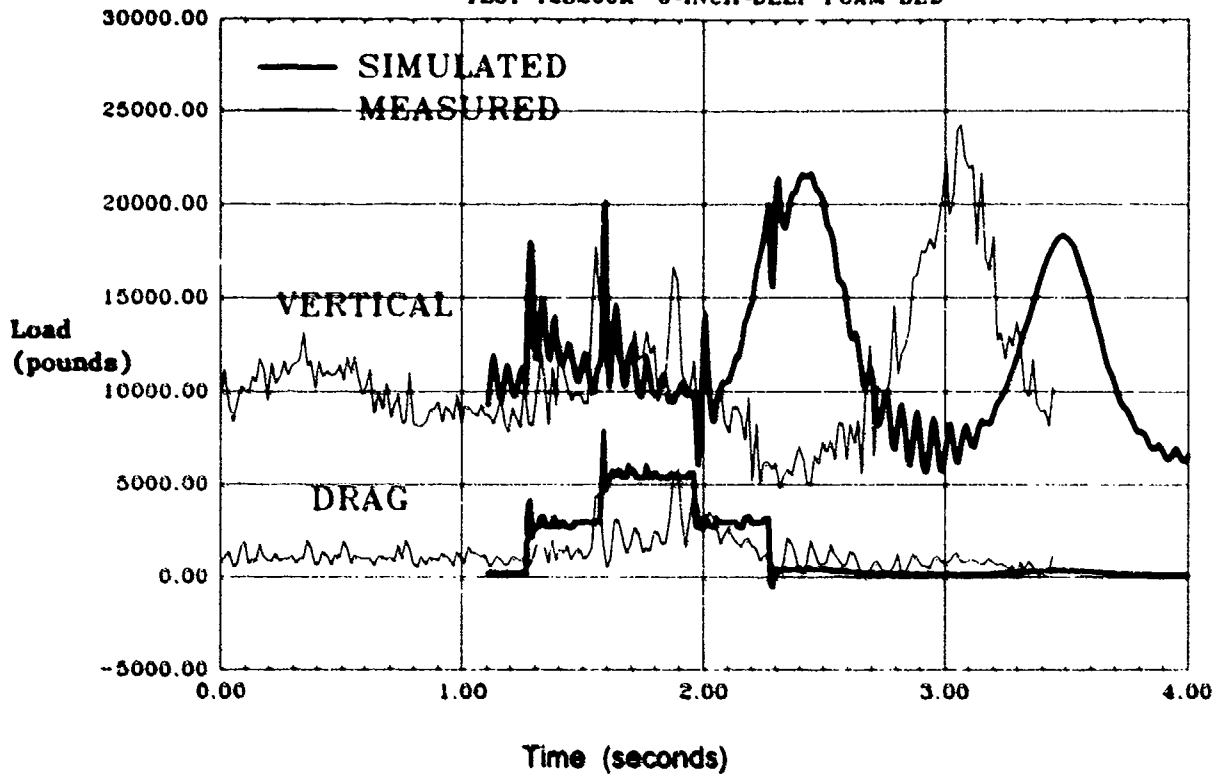


FIGURE A-10. Comparison of Test T2S260K Measured and Simulated Nose Gear Loads

### RIGHT MAIN GEAR

B-727 GW=132267 LB CG=900 INCHES  
TEST T2S260K 6-INCH-DEEP FOAM BED

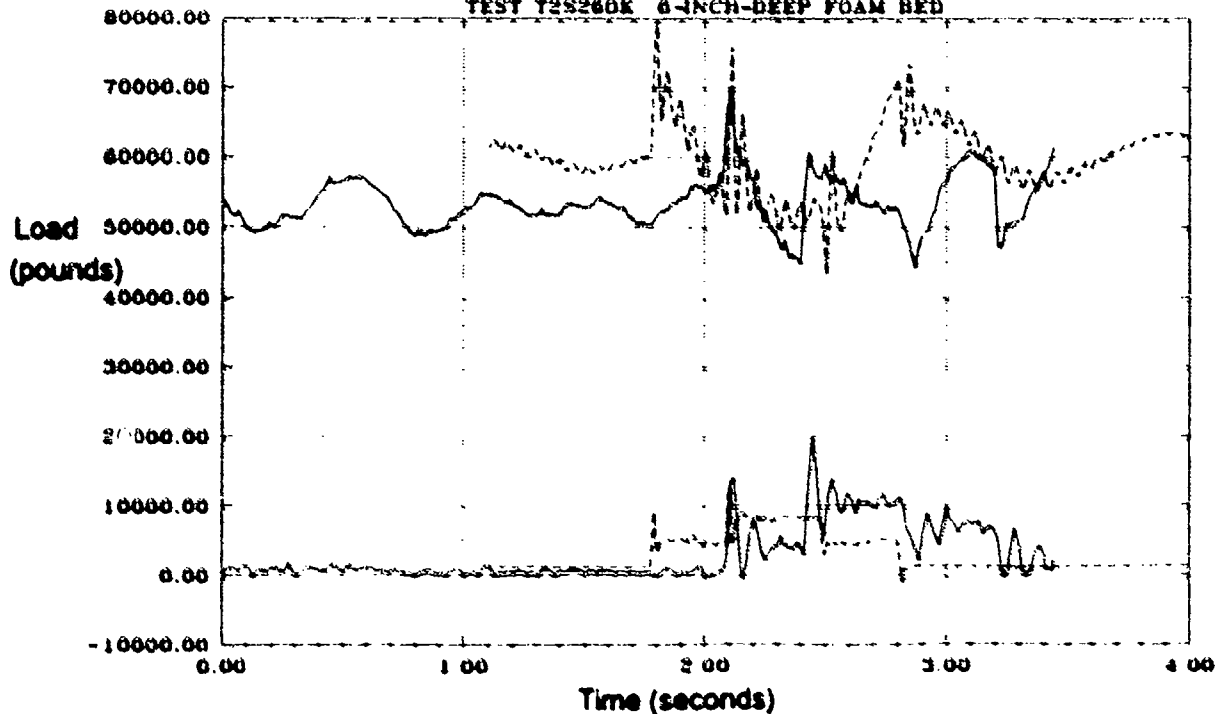


FIGURE A-11. Comparison of T2S260K Measured and Simulated Right Main Gear Loads



## 2.2.8 Recorded Data Results T1-S1-80K.

Figure A-12 shows the longitudinal acceleration at the aircraft cg. The deceleration in the foam bed was essentially the same as on previous test runs, about 0.1 g. The measured and simulated values compared favorably when the measured acceleration noise was averaged.

Figure A-13 shows a comparison of the measured and simulated nose gear vertical and drag loads resulting from aircraft passage over the foam test bed. The two traces are quite similar indicating good agreement. Neither load approaches limit value.

Figure A-14 presents the measured and simulated vertical and drag loads for the right main gear for the test run. Here it is evident that by deploying the spoilers the wing lift was reduced sufficiently to correspond to the simulated trace which assumes that the spoilers are deployed. The measured and simulated traces are in reasonable agreement in terms of shape and magnitude.

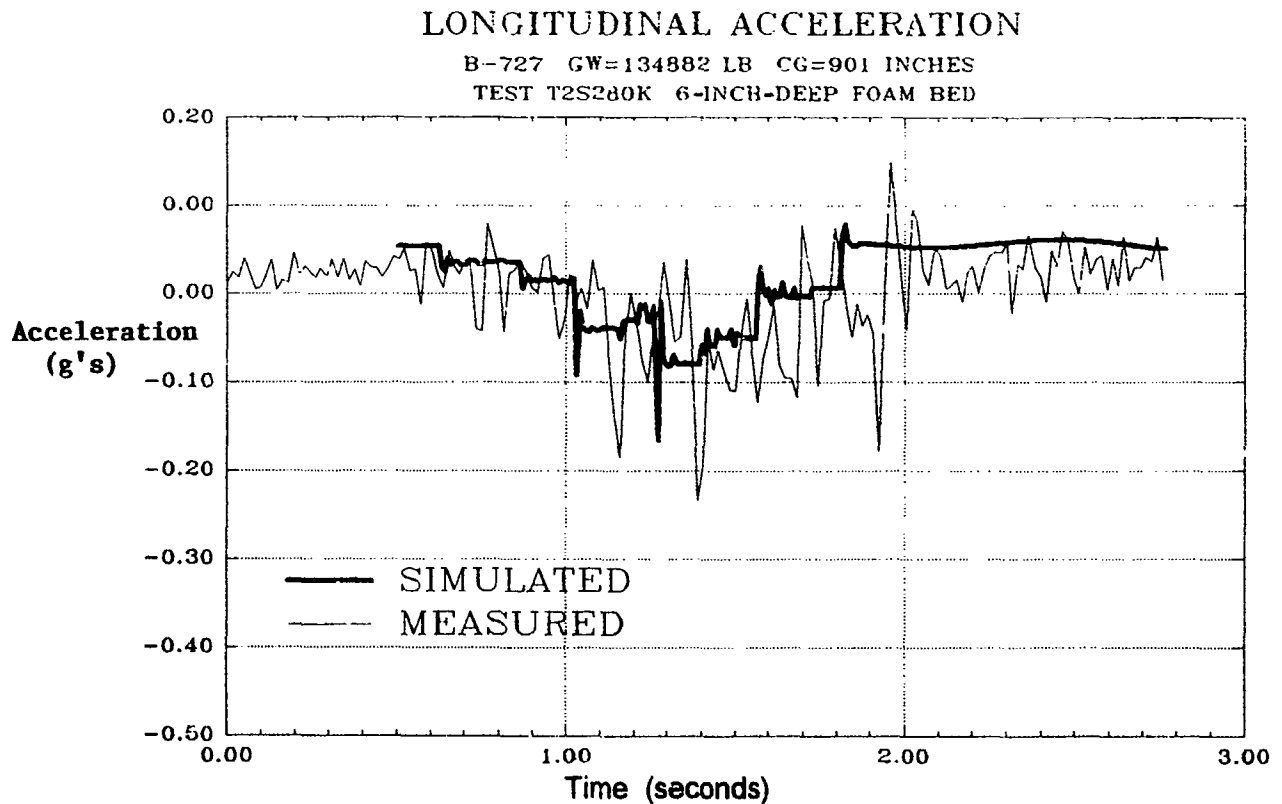


FIGURE A-12. Comparison of T2S280K Measured and Simulated Longitudinal Acceleration

### NOSE GEAR

B-727 GW=134882 LB CG=901 INCHES  
TEST T2S280K 6-INCH-DEEP FOAM BED

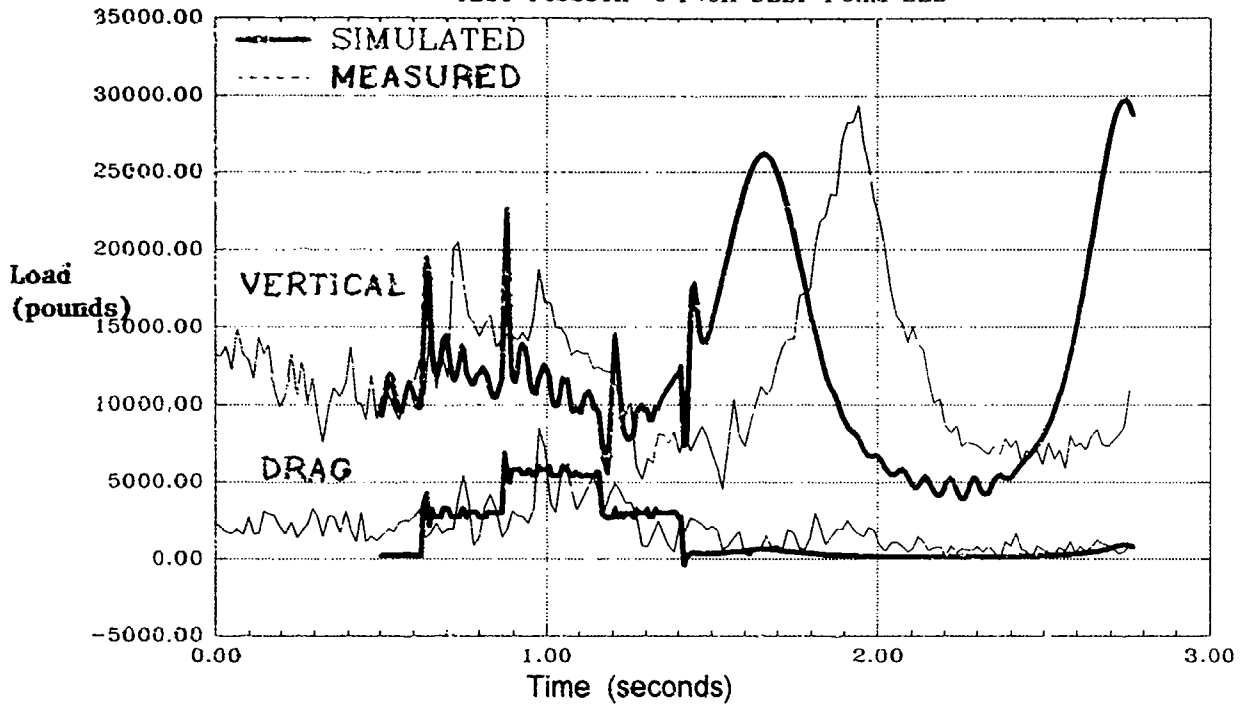


Figure A-13. Comparison of Measured and Simulated Nose Gear Vertical and Drag Loads

### RIGHT MAIN GEAR

B-727 GW=134882 LB CG=901 INCHES  
TEST T2S280K 6-INCH-DEEP FOAM BED

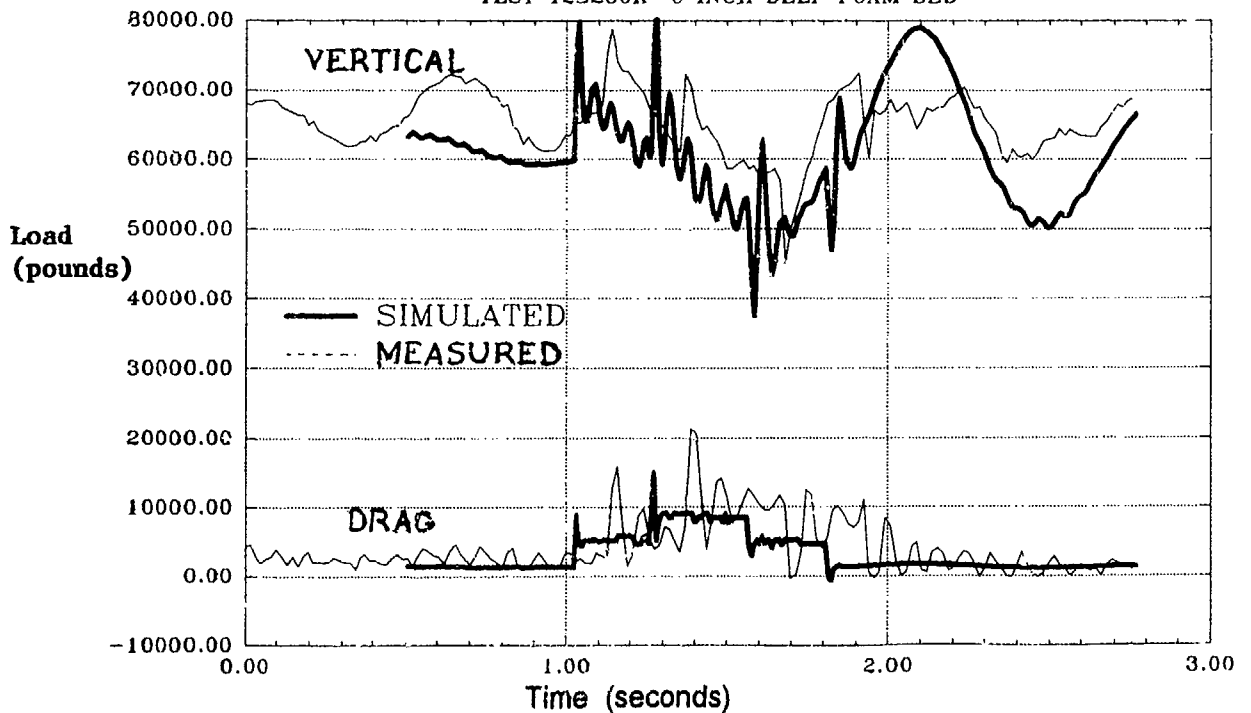


FIGURE A-14. Comparison of T2S280K Measured and Simulated Right Main Gear Loads

## 2.3 AIRCRAFT TESTS on 12-INCH-DEEP FOAM BEDS.

### 2.3.1 Recorded Data Results T4-S2-30K.

Figure A-15 Shows the longitudinal acceleration at the cg of the aircraft resulting from traversing the Type-4 foam test bed. It is immediately obvious that increasing the depth of foam causes a significant increase in aircraft deceleration. The maximum deceleration in the 12-inch-deep foam bed was about 0.23 g's.

A comparison of the measured and simulated nose gear loads in the vertical and drag directions is shown in figure A-16. The traces for these loads are quite comparable indicating that the simulation is sufficiently accurate. None of the measured loads approached the nose gear limit values (paragraph 2.2.2).

Figure A-17 is a comparison of the right main gear vertical and drag loads resulting from passage through the foam bed. The measured main gear drag is somewhat higher than the simulated value. It is believed that the measured drag is probably in error as can be shown by comparing the drag force required to obtain the deceleration shown on figure A-15. This discrepancy will be discussed further in the next section of the report.

Figure A-18 shows a comparison of the aircraft ground speed decay as resulting from passing through the foam bed. The measured ground speed showed a decay of about 13 knots while the simulated ground speed decay is about 18 knots or about a 15 percent difference. This item will also be discussed further in the next section of the report.

### 2.3.2 Test T4-S2-50K Description.

The aircraft was accelerated to 50 knots with only the center engine operating. The flaps were lowered to 15 degrees prior to the test run. The wing spoilers were deployed to negate lift and the engine thrust was set to idle just before test bed entry.

After a short time past nose wheel entry into the test bed a very noticeable longitudinal deceleration was felt in the cockpit. As soon as the aircraft cleared the test bed, brakes were applied and the aircraft stopped. The aircraft was visually inspected and there was no damage evident.

The foam test bed was inspected and as in previous cases there were deep ruts where the wheels passed through. Measurements of the ruts were made and the results are shown in table A-6.

T4-S2-50K	Sec 1	Sec 2	Sec 3	Sec 4	Sec 5	Sec 6	Sec 7
Nose Gear	2.1 (69%)	3.5 (58%)	3.7 (40%)	3.8 (30%)	4.0 (44%)	3.3 (55%)	1.6 (55%)
Left Main Gear	2.0 (66%)	3.6 (60%)	4.9 (55%)	5.9 (50%)	4.0 (44%)	3.0 (50%)	2.0 (66%)
Right Main Gear	2.6 (86%)	3.7 (62%)	5.1 (56%)	5.9 (50%)	4.7 (52%)	3.2 (53%)	1.25 (42%)

# LONGITUDINAL ACCELERATION

B-727 GW=135965 LB CG=891 INCHES  
TEST T4S230K 12-INCH-DEEP FOAM BED

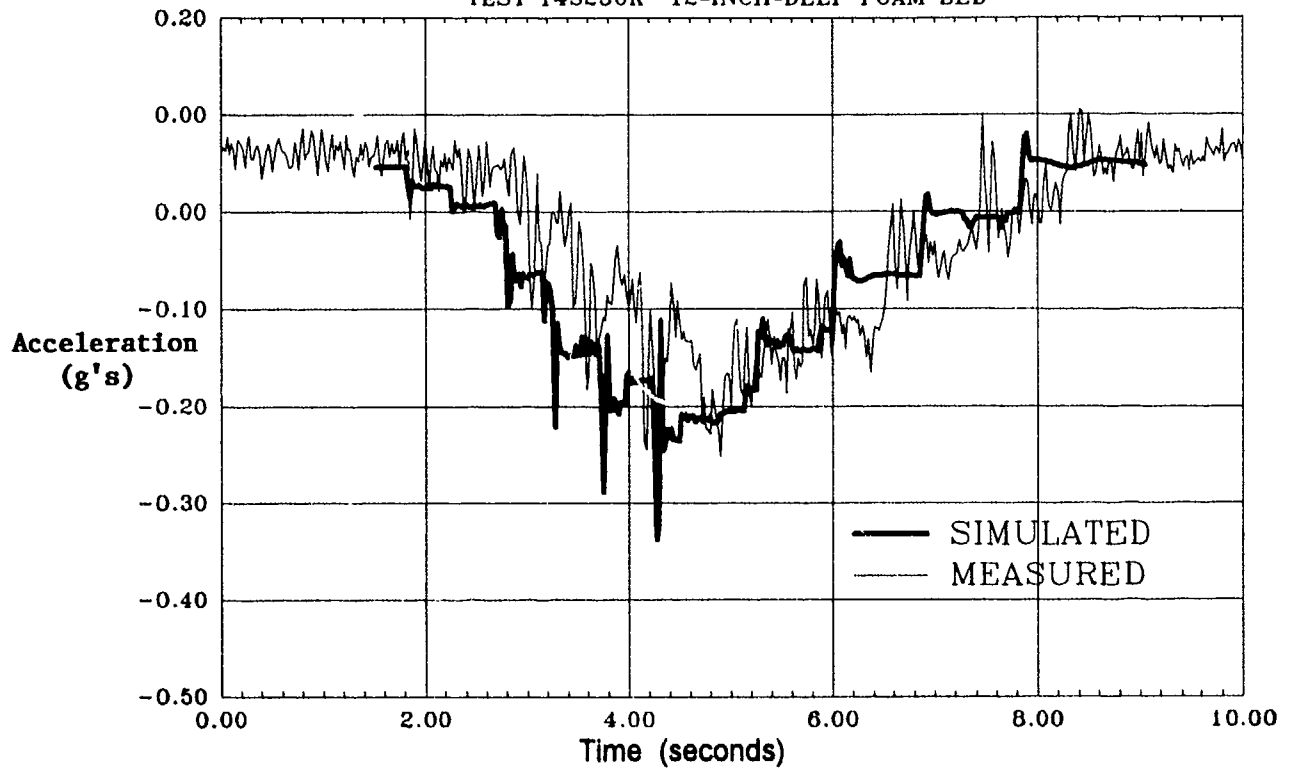


FIGURE A-15. Comparison of T4S230K Measured and Simulated Longitudinal Acceleration

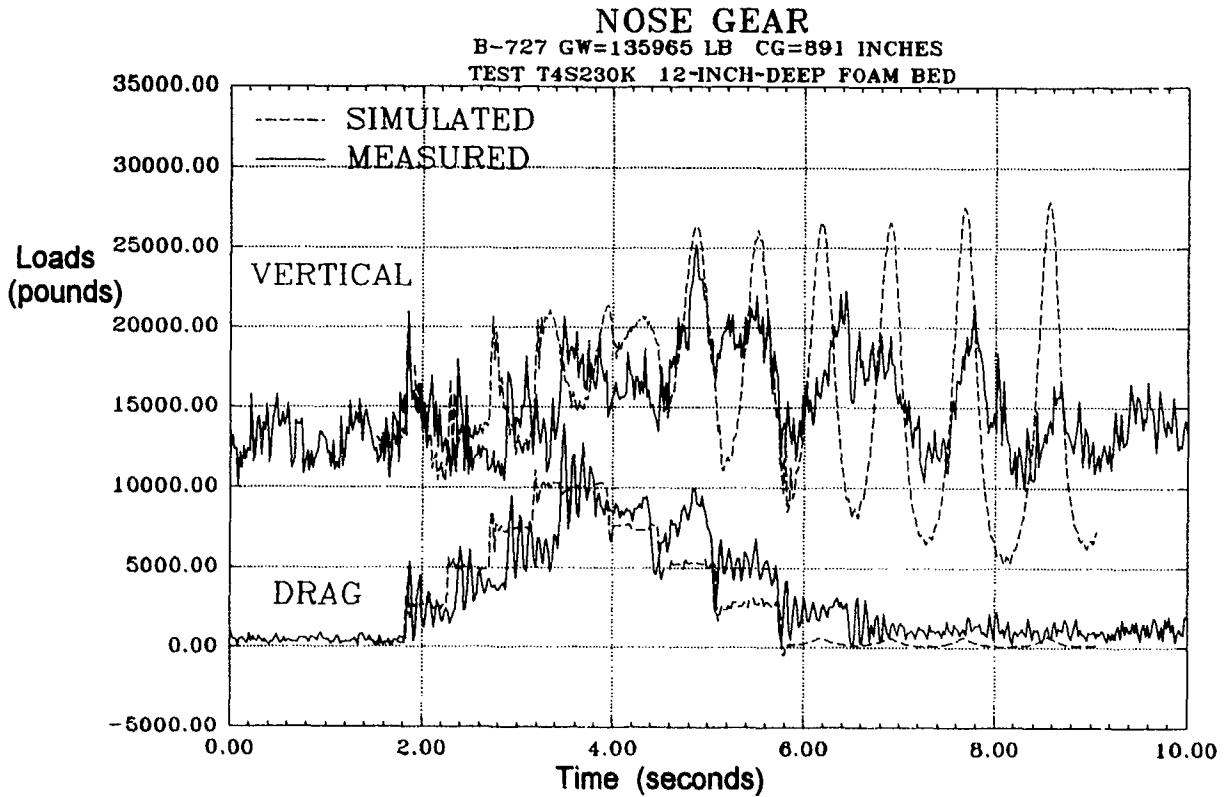


FIGURE A-16. Comparison of Test T4S230K Measured and Simulated Nose Gear Loads

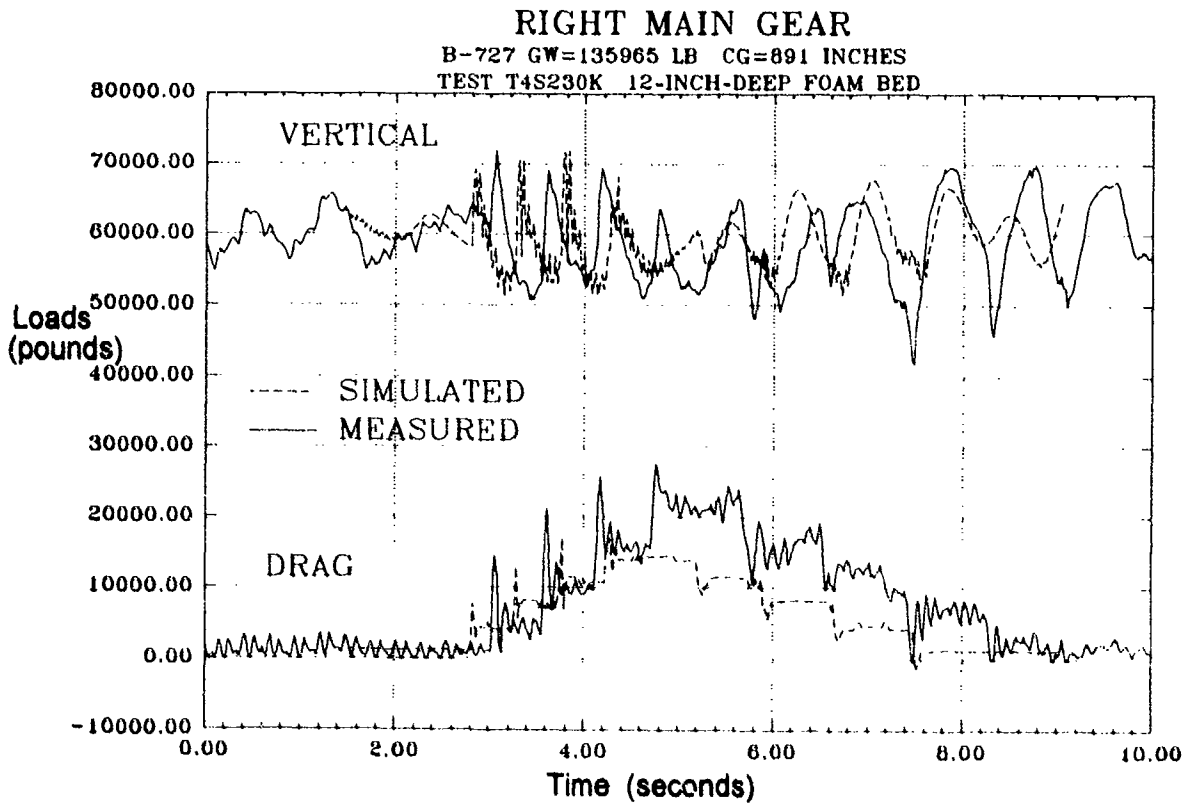


FIGURE A-17. Comparison of T4S230K Measured and Simulated Right Main Gear Loads

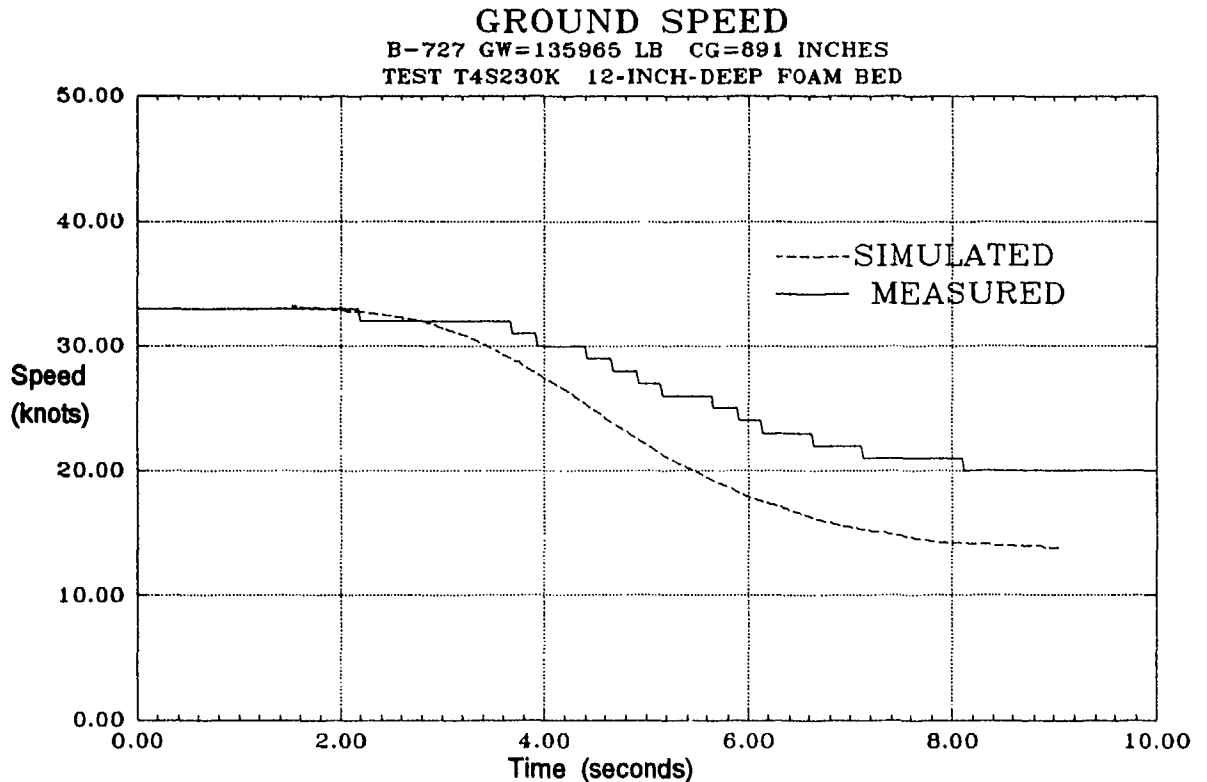


FIGURE A-18. Comparison of Test T4S230K Measured and Simulated Ground Speed

### 2.3.3 Recorded Test Data T4-S2-50K.

Figure A-19 shows the measured and simulated longitudinal acceleration of the aircraft for this test. The measured level of deceleration agrees with that obtained from the previous test in a 12-inch-deep foam bed, that is, about 0.23 g's.

Figure A-20 provides a comparison of the nose gear vertical and drag results. The vertical load results are quite similar but the drag loads show considerable difference. The simulated drag load is much higher than the measured drag load. It appears that the nose gear tended to ride over the foam rather than penetrate as had been the usual case. This can happen when the aircraft dynamics allow pitching and the main gear drag is not sufficient to pull the nose gear into the foam. In the normal arrestor design, the main gear drag would rotate the nose gear into the foam because the bed length would be much longer, i.e., equal or greater than 400 feet. The vertical and drag loads were below limit values.

The main gear measured and simulated loads are compared in figure A-21. The vertical loads are comparable but the measured drag load is slightly higher than the simulated drag load which has remained consistent for all test runs thus far.

Figure A-22 gives a comparison of the measured and simulated ground speed decay resulting from the foam test bed. The two traces are similar indicating good correlation between measured and simulated values.

### LONGITUDINAL ACCELERATION

B-727 GW=134625 LB CG=894 INCHES

TEST T4S250K 12-INCH-DEEP FOAM BED

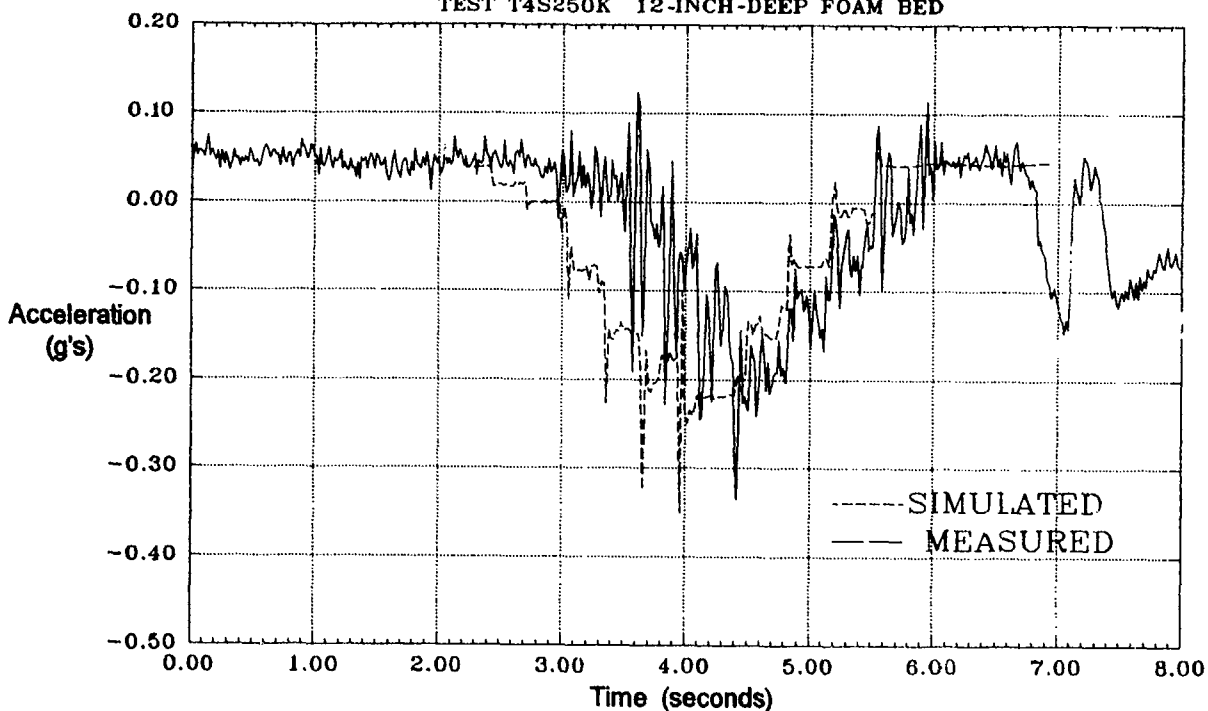


FIGURE A-19. Comparison of T4S250K Measured and Simulated Longitudinal Acceleration

### NOSE GEAR

B-727 GW=134625 LB CG=894 INCHES

TEST T4S250K 12-INCH-DEEP FOAM BED

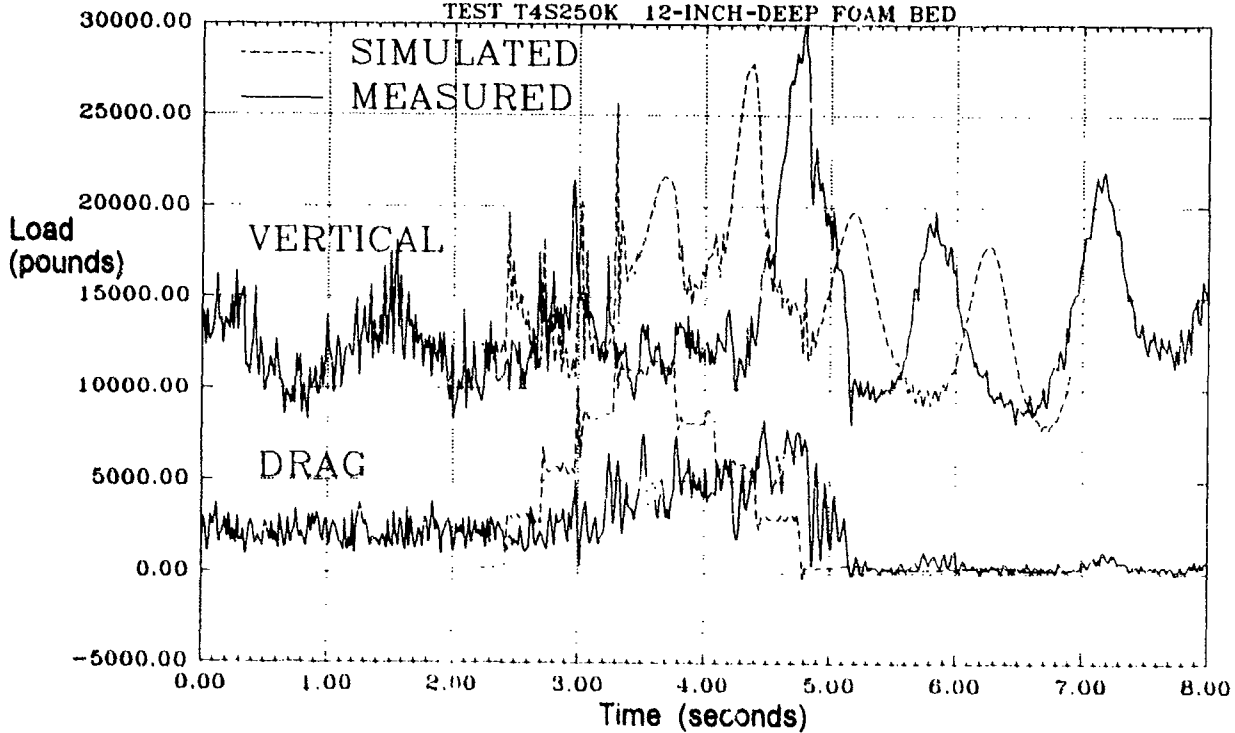


FIGURE A-20. Comparison of T4S250K Measured and Simulated Nose Gear Loads

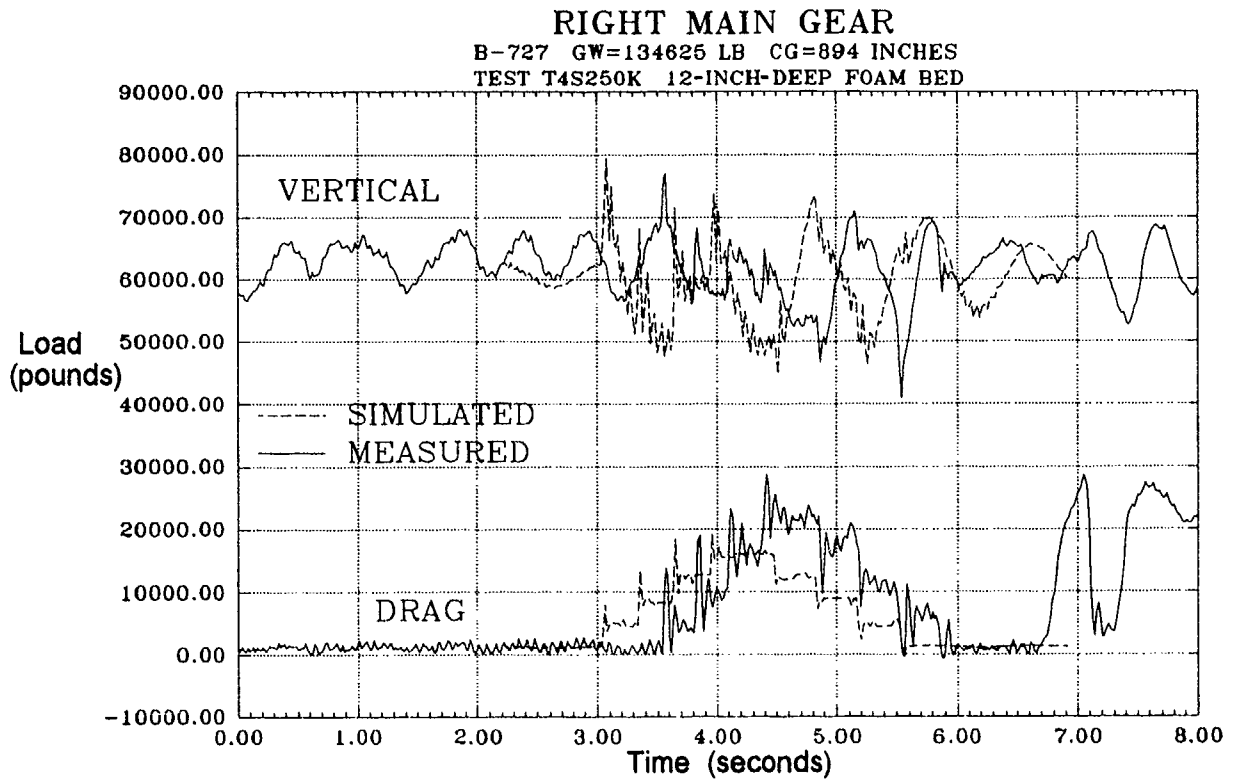


FIGURE A-21. Comparison of T4S250K Measured and Simulated Right Main Gear Loads

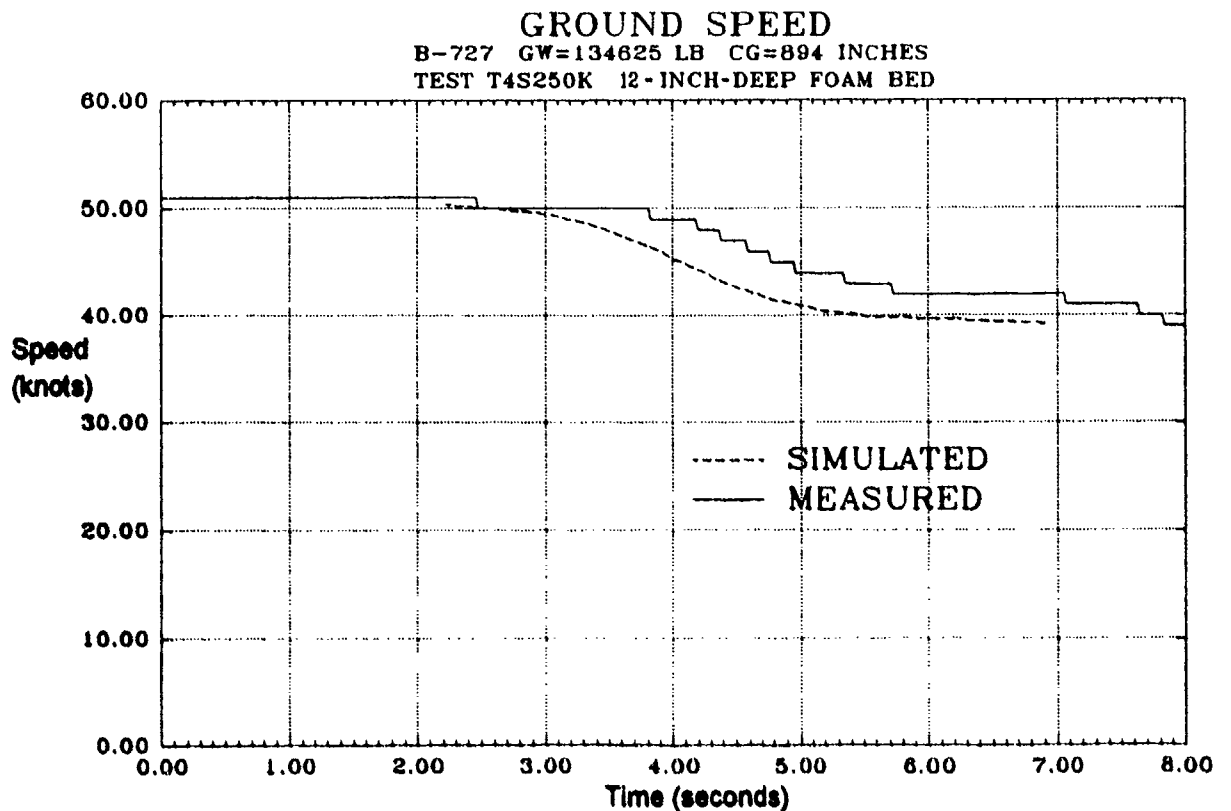


FIGURE A-22. Comparison of Test T4S250K Measured and Simulated Ground Speed



## 2.4 AIRCRAFT TESTS ON EIGHTEEN-INCH-DEEP FOAM BED.

The eighteen-inch-deep bed was designed to obtain the data necessary to assure that a full depth arrestor bed would perform as indicated by analysis. This bed depth (actually 20 inches) is required for any full scale arrestor.

### 2.4.1 Test T5-S2-50K Description.

As in the previous tests, the flaps were lowered to 15 degrees and the aircraft accelerated to 50 knots using only the center engine. Just prior to engaging the test bed the spoilers were deployed and the engine thrust reduced to idle.

On bed entry there was a mild thump as before and then when the main gear engaged the foam a very noticeable deceleration was felt in the cockpit. After the main gear cleared the test bed the aircraft was braked to a stop and a visual inspection of the aircraft was made. There was no evidence of any damage.

An inspection of the test bed was made and it was determined that the aircraft wheels had made deep ruts indicating that good penetration into the foam had occurred. The rut depths were measured and they are reported in table A-7.

T5-S2-50K	Left Main Gear	Nose Gear	Right Main Gear
Section 1	2.0 (66%)	1.9 (63%)	No Data taken since results appeared symmetrical
Section 2	4.3 (75%)	4.0 (66%)	
Section 3	5.5 (61%)	5.5 (61%)	
Section 4	7.0 (58%)	6.3 (52%)	
Section 5	10.0 (66%)	8.4 (55%)	
Section 6	13.0 (72%)	12.0 (66%)	
Section 7	10.3 (68%)	13.5 (90%)	
Section 8	11.0 (91%)	7.3 (60%)	
Section 9	5.3 (59%)	7.5 (83%)	
Section 10	3.8 (63%)	3.0 (50%)	
Section 11	2.0 (66%)	2.5 (83%)	

### 2.4.2 Recorded Data Test T5-S2-50K

Figure A-23 shows the longitudinal acceleration of the aircraft resulting from the Type-5 foam test bed. The maximum deceleration was about 0.4 g's when averaging through the trace noise. The measured and simulated accelerations were similar in shape and magnitude.

Figure A-24 shows the measured and simulated vertical and drag loads on the nose gear closely correlate. The drag load traces are similar in shape but the magnitude of the measured trace is less than the simulated trace.

Figure A-25 shows the comparison of the measured and simulated right main gear vertical and drag loads. The loads are well correlated, and the only discrepancy is in the magnitude of the drag load. The drag load is slightly higher for the measured curve.

A comparison of the measured and simulated ground speed is provided in figure A-26. The simulated ground speed change is about 24 knots while the measured change is only 20 knots. This 10 percent error is a reasonable value for experimental results.

## 2.5 FIRE/RESCUE VEHICLE MOBILITY.

An Oshkosh P-19 fire/rescue truck with a gross weight of about 30,000 pounds was driven across all depths of the foam beds. A visual indication of these tests was that airport rescue and firefighting equipment could operate on the foam surface satisfactorily. The fire truck crew indicated that they had no problem steering while operating on the foam bed. Rut depths were less than 3 inches in the undisturbed test bed areas.

## 2.6 PASSENGER MOBILITY ON FOAM ARRESTOR.

After each test, personnel walked around on the test bed to observe the test results and to make measurements of rut depths. There was no difficulty in walking on the material and there was good foot traction on the surface. There was no fuel spilled on any of the test beds to determine traction under these circumstances.

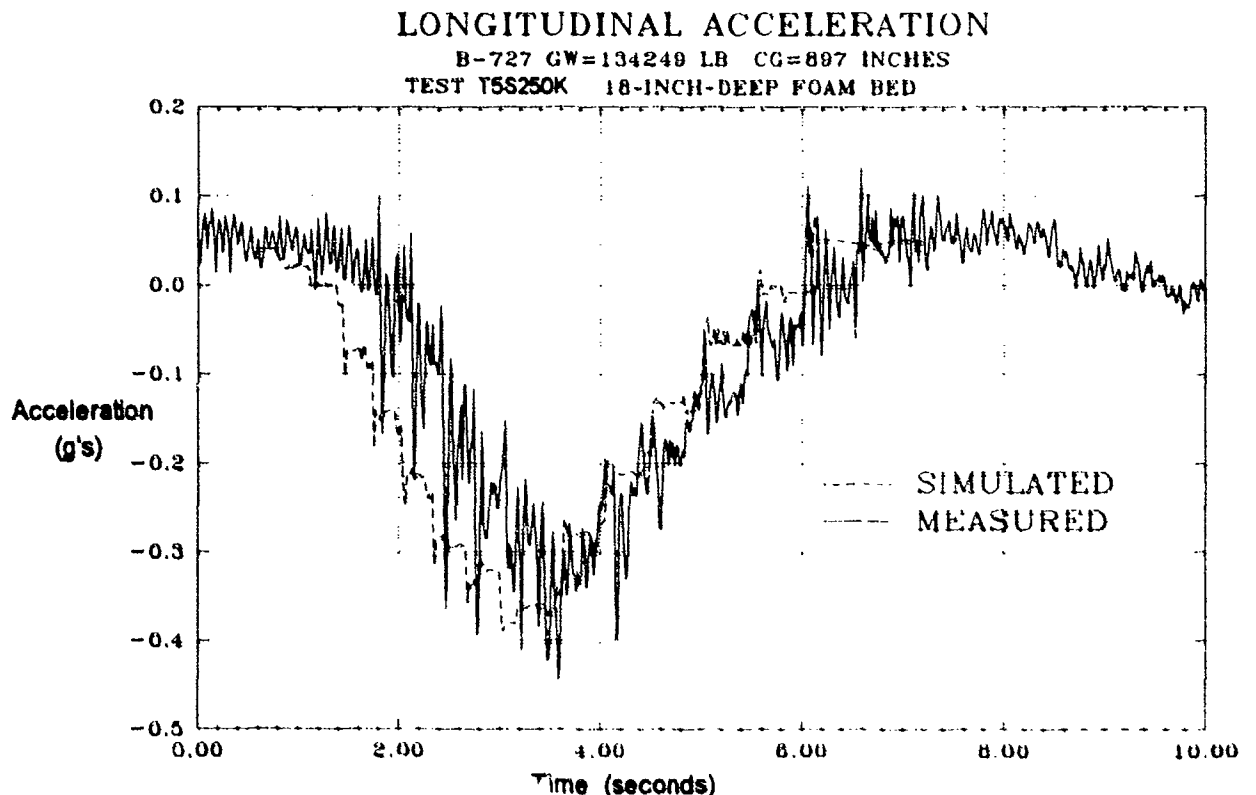


FIGURE A-23. Comparison of Measured and Simulated Longitudinal Acceleration

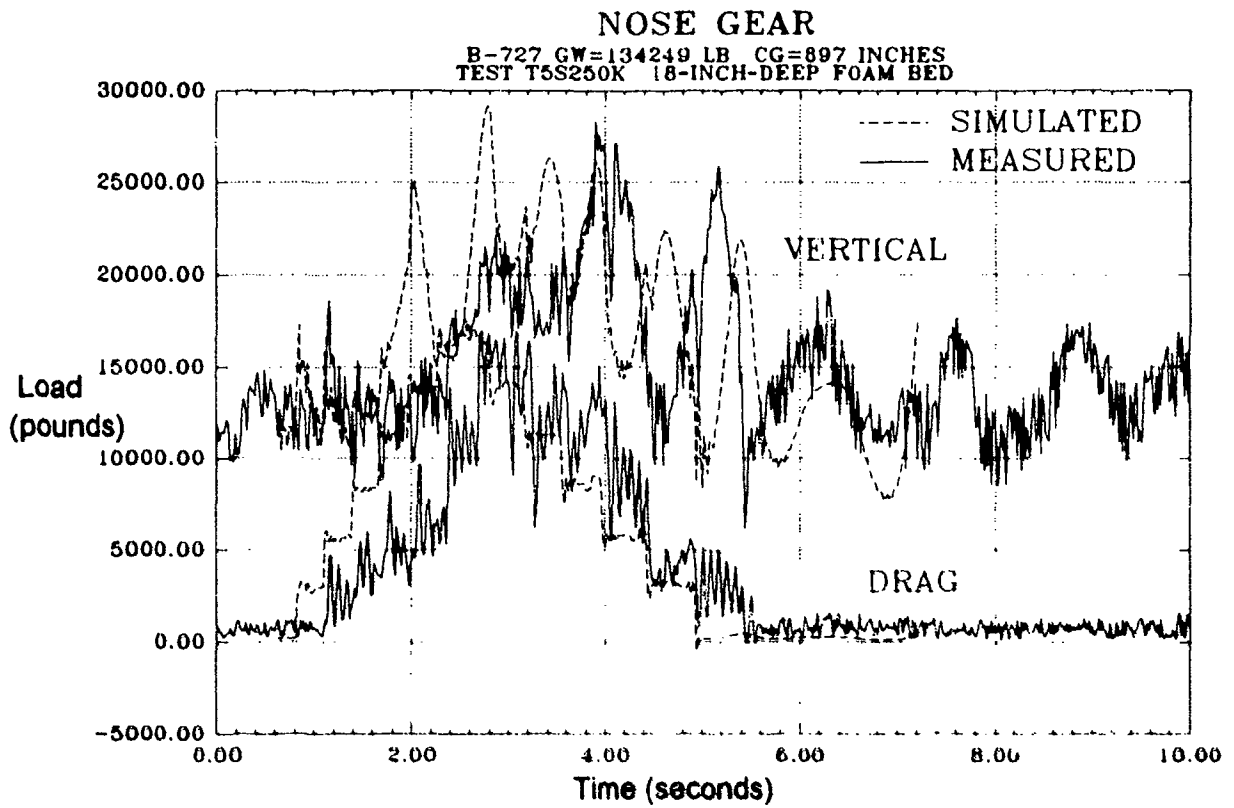


FIGURE A-24. Comparison of Test T5S250K Measured and Simulated Nose Gear Loads

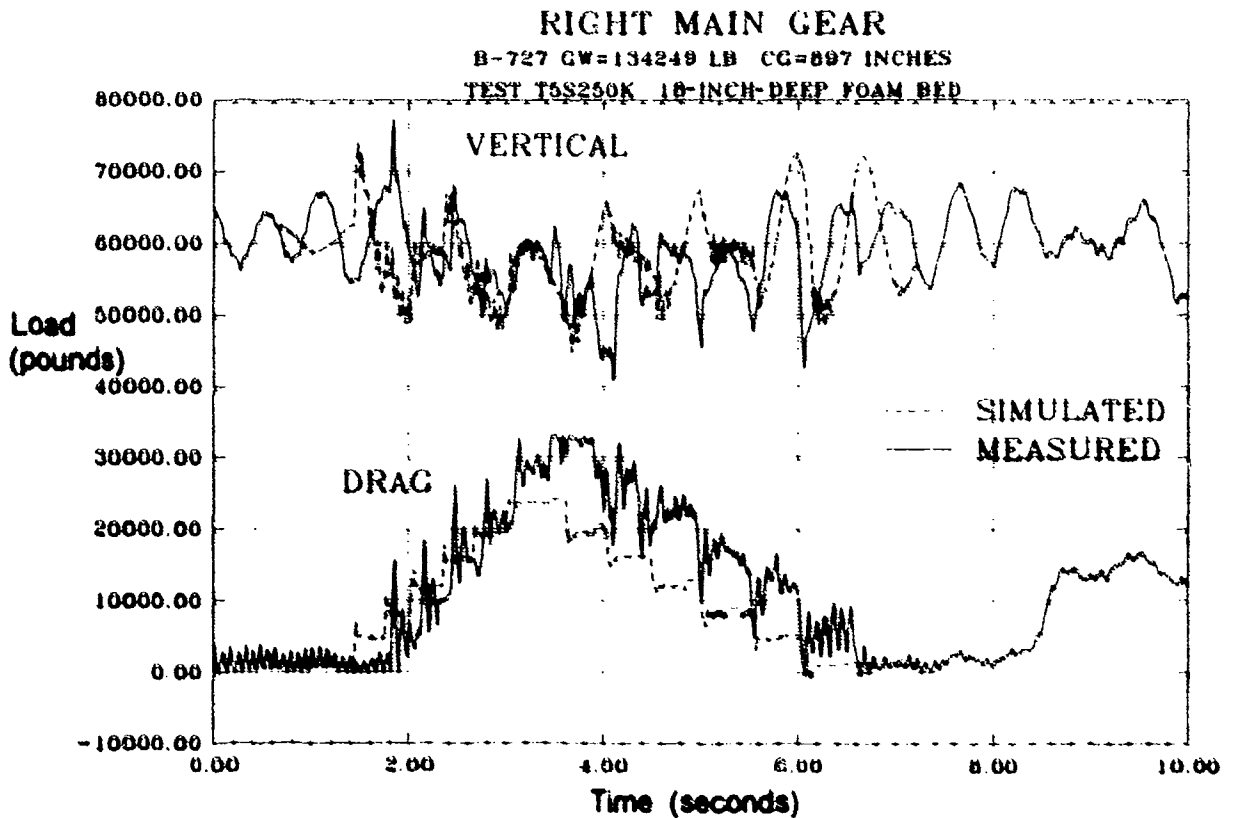


FIGURE A-25. Comparison of T5S250K Measured and Simulated Right Main Gear Loads

# GROUND SPEED

B-727 GW=134249 LB CG=897 INCHES  
TEST T5S250K 18-INCH-DEEP FOAM BED

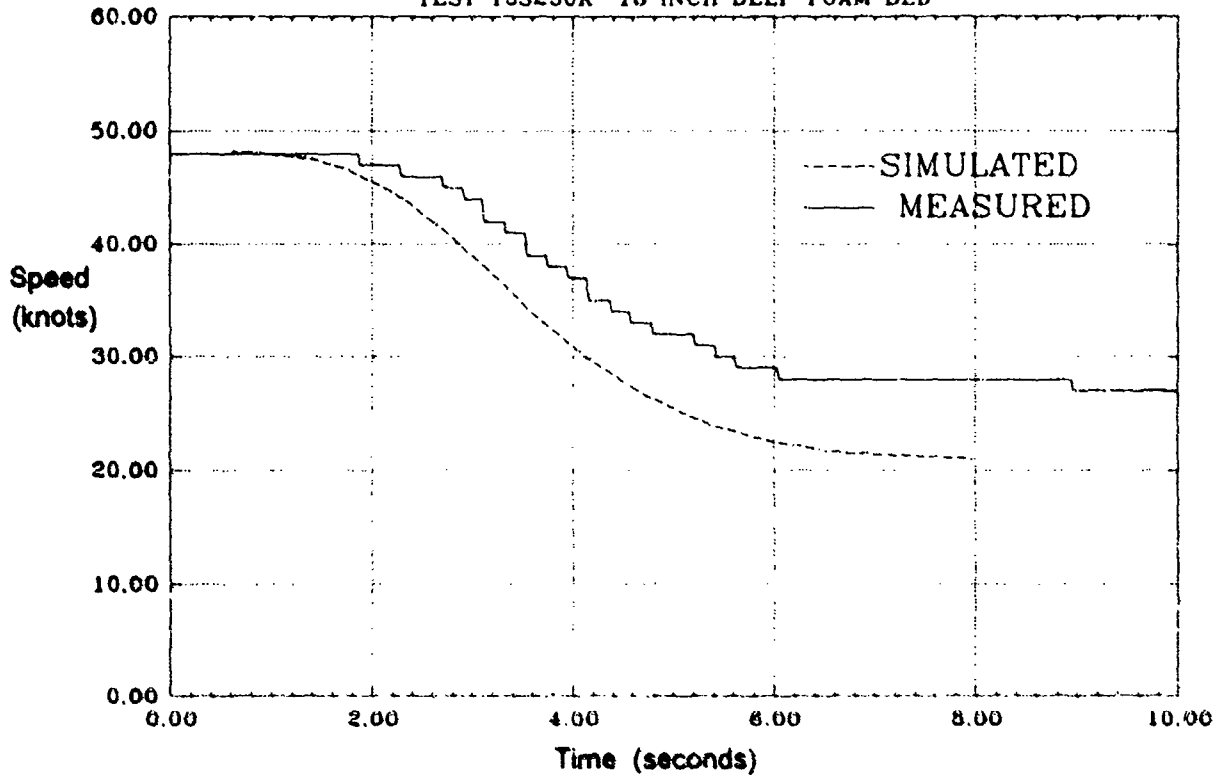


FIGURE A-26. Comparison of Test T5S250K Measured and Simulated Ground Speed

### 3. ANALYSIS OF RESULTS (1991 TESTS).

The effectiveness of the foam arrestor can be evaluated by comparing its performance with aircraft braking. When aircraft are braked the longitudinal deceleration obtained, in general terms, is a function of the brake pressure applied and the airfield surface coefficient of friction. The drag generated at the tire/runway surface is a function of the surface condition. That is, if the surface is dry a coefficient of friction as high as 0.8 might be obtained although 0.5 to 0.6 is much more common on runway surfaces. On a wet runway the available coefficient may not be higher than about 0.2 to 0.35 and on icy or snow covered runways the coefficient may be only .02 to 0.1. The analysis of the phenolic foam bed tested will be stated in this form so that the performance corresponds directly.

#### 3.1 TEST DATA DRAG RATIO.

In the previous section of this report landing gear vertical and drag load data from the aircraft tests and simulations were compared. Test gear load data were obtained from 6-, 12-, and 18-inch-deep foam beds. The 6- and 12-inch-deep beds were tested to provide incremental steps for aircraft safety in terms of landing gear loads since this was the first time aircraft tests on a phenolic foam arrestor had been made. The tests were also used to establish the accuracy of the simulation technology for foam arrestors. The 6- and 12-inch-deep foam beds would not be considered as appropriate for an actual operational arrestor but the results are provided here for demonstrating the computer simulation accuracy and how foam depth contributes to wheel drag. Only three cases will be presented, one for each foam bed depth.

Foam bed effectiveness is demonstrated by dividing the instantaneous drag load by the instantaneous vertical load for each landing gear or by dividing the total instantaneous gear drag on all wheels by the aircraft weight. The designation of these ratios are  $\mu_{EFF}$ . Although the ratios are not precisely equivalent they will be labeled the same in the following discussions. The latter definition is the one used in aircraft braking studies.

### NOSE GEAR DRAG RATIO

B-727 GW=134267 LB CG=901 INCHES  
TEST T1S240K 6-INCH-DEEP FOAM BED

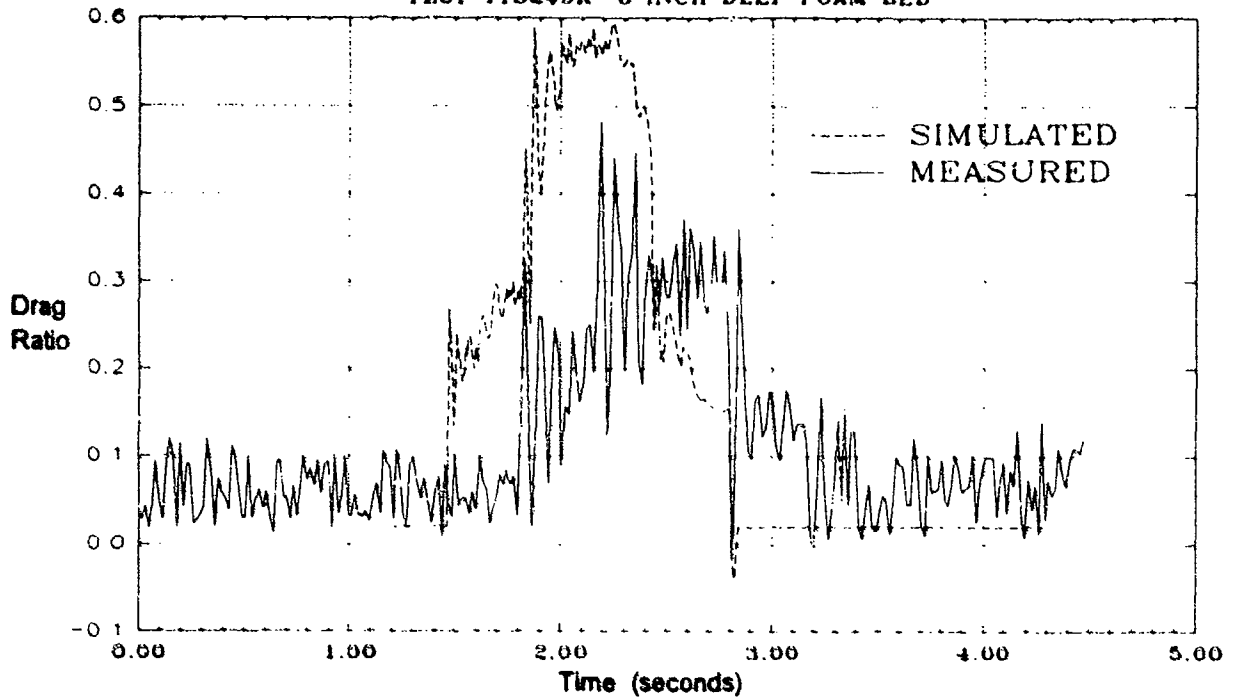


FIGURE A-27. Nose Gear Drag Ratio from Test T1S240K

### RIGHT MAIN GEAR DRAG RATIO

B-727 GW=134267 LB CG=901 INCHES  
TEST T1S240K 6-INCH-DEEP FOAM BED

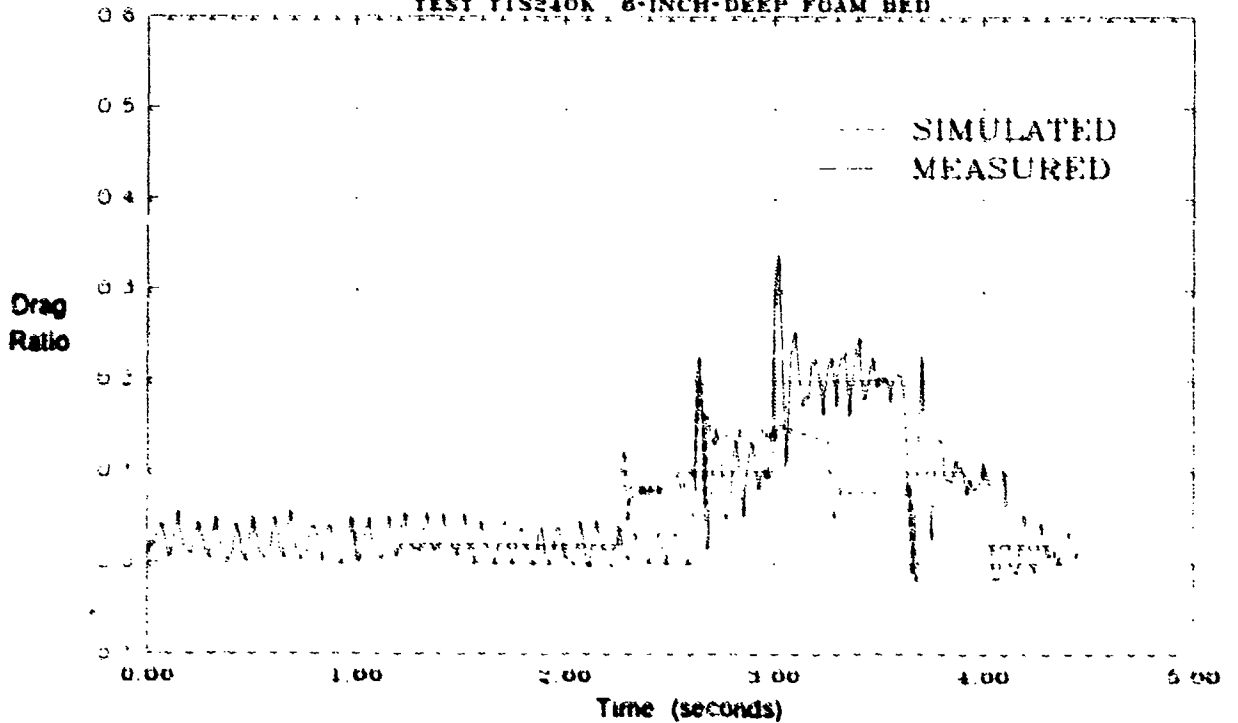


FIGURE A-28 Right Main Gear Drag Ratio from Test T1S240K

## TOTAL GEAR DRAG/GROSS WEIGHT

B-727 GW=134267 LB CG=901 INCHES  
TEST T1S240K 6-INCH-DEEP FOAM BED

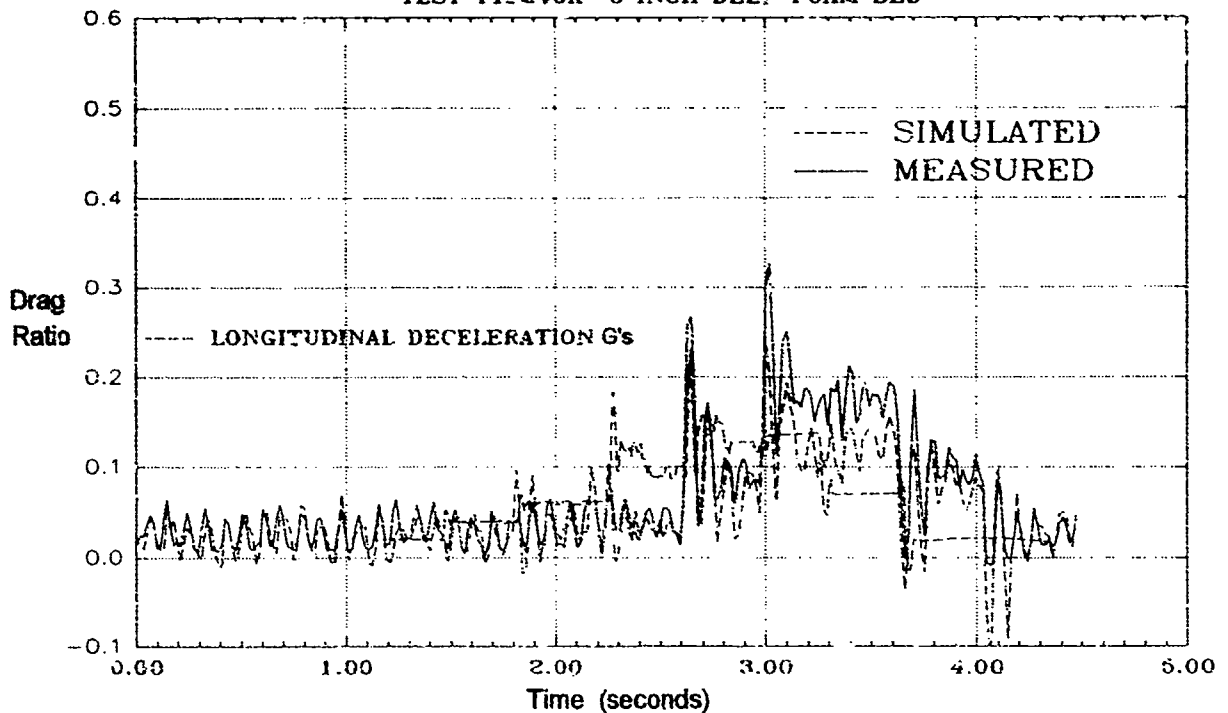


FIGURE A-29. Total Drag Ratio Compared to Deceleration for Test T1S240K

### 3.1.1 Six-Inch-Deep Foam Bed.

Figure A-27 shows the nose gear drag ratio obtained from the Type-1 foam bed. The simulated nose gear drag ratio is also shown. The measured drag ratio is somewhat smaller than the simulated value. The measured high nominal value of  $\mu_{EFF}$  is about 0.3 while the simulated value is about 0.55. Figure A-28 shows  $\mu_{EFF}$  for the right main gear for the same foam bed. The measured high nominal drag ratio is about 0.2 while the simulated value is about 0.15. Figure A-29 shows the total gear drag ratio, both measured and simulated, and the aircraft longitudinal deceleration which agrees well with  $\mu_{EFF}$ .

In this example only the gear drag was relevant because the engine was shut down (see paragraph 2.2.3) and at 40 knots the aerodynamic drag, even with the flaps at 15 degrees, is negligible compared to the gear drag forces in the foam bed. Therefore, the measured longitudinal acceleration is a good indicator of the aircraft drag force and  $\mu_{EFF}$ .

### 3.1.2 Twelve-Inch-Deep Foam Bed.

The measured nose gear drag ratio shown in figure A-30 is nearly equal to the simulated trace. The measured high nominal value is about 0.5 in the deepest part of the foam bed. The high nominal value for the simulated trace is about 0.55. Figure A-31 shows the measured and simulated drag ratio traces for the right main gear. The measured trace is somewhat higher than the simulated trace as in previous cases. Figure A-32 shows the total gear drag ratio which indicates a measured nominal  $\mu_{EFF}$  of about 0.35 but the simulated value is about 0.25 as is the high nominal deceleration.

The aircraft speed was about 30 knots so that the aerodynamic drag with flaps lowered to 15 degrees is negligible and the engine thrust is about 1200 pounds so that it is also considered negligible compared to the approximately 40,000 pounds of simulated (or 50,000 pounds measured) drag force produced by the foam bed (figures A-16 and A-17). Therefore, as above, the measured deceleration appears to be an accurate measure of the landing gear drag force and  $\mu_{EFF}$ .

### 3.1.3 Eighteen-Inch-Deep Foam Bed.

The last example of drag ratio results to be discussed will be from the 18-inch-deep foam bed. Figure A-33 shows that a high  $\mu_{EFF}$  of about 0.75 was obtained for the measured nose gear drag ratio and about 1.0 for the simulated case. Figure A-34 indicates that  $\mu_{EFF}$  values of 0.6 and 0.4 were obtained for the measured and simulated cases for the right main gear drag ratio. Figure A-35 shows a comparison of the total gear drag ratio and the measured deceleration obtained during the test. The high nominal value of  $\mu_{EFF}$  was about 0.4 which is considered a good braking capability. Again, the best correlation is obtained with the simulated values.

For this test the aerodynamic drag and the engine thrust are opposing so that their net effect on the deceleration is considered negligible, particularly when the gear drag forces are about 75,000 pounds.

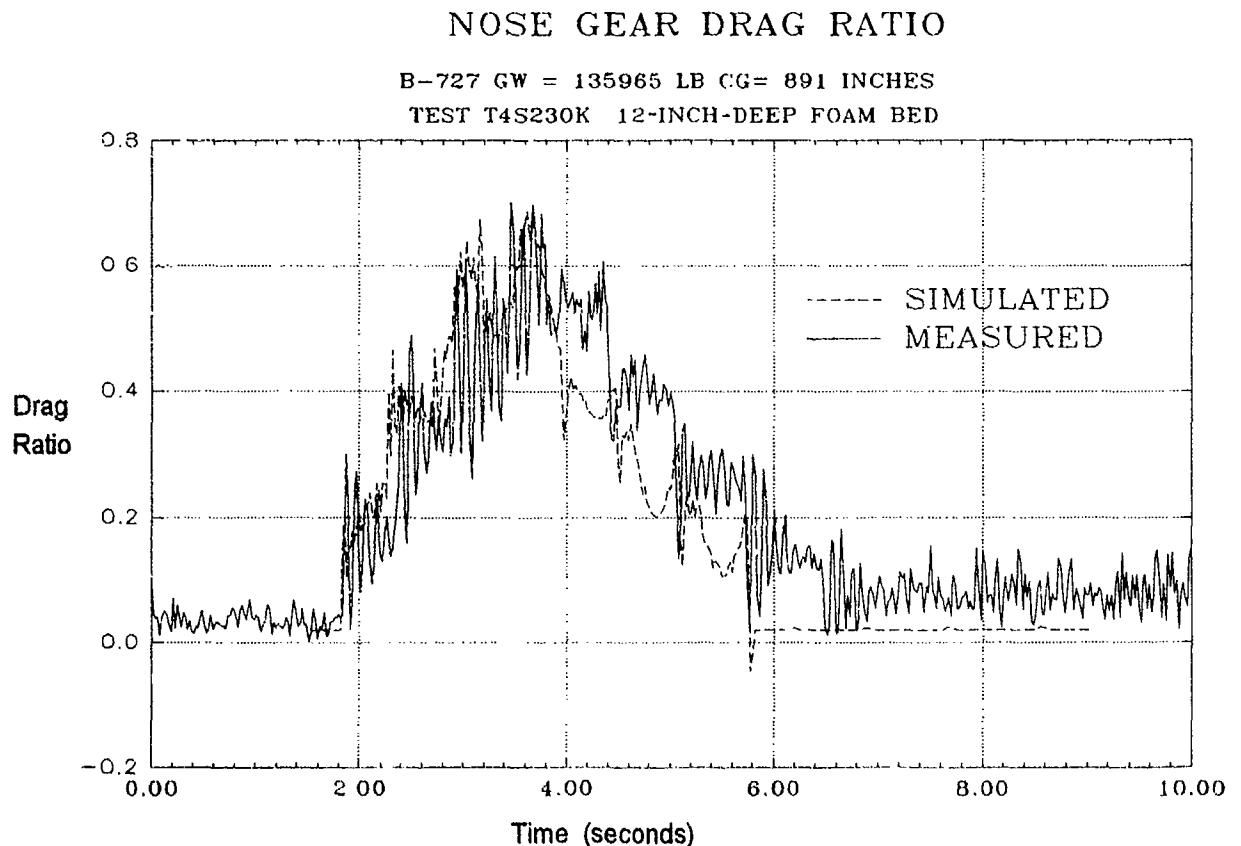


FIGURE A-30. Nose Gear Drag Ratio from Test T4S230K



### RIGHT GEAR DRAG RATIO

B-727 GW = 135965 LB CG= 891 INCHES

TEST T4S230K 12-INCH-DEEP FOAM BED

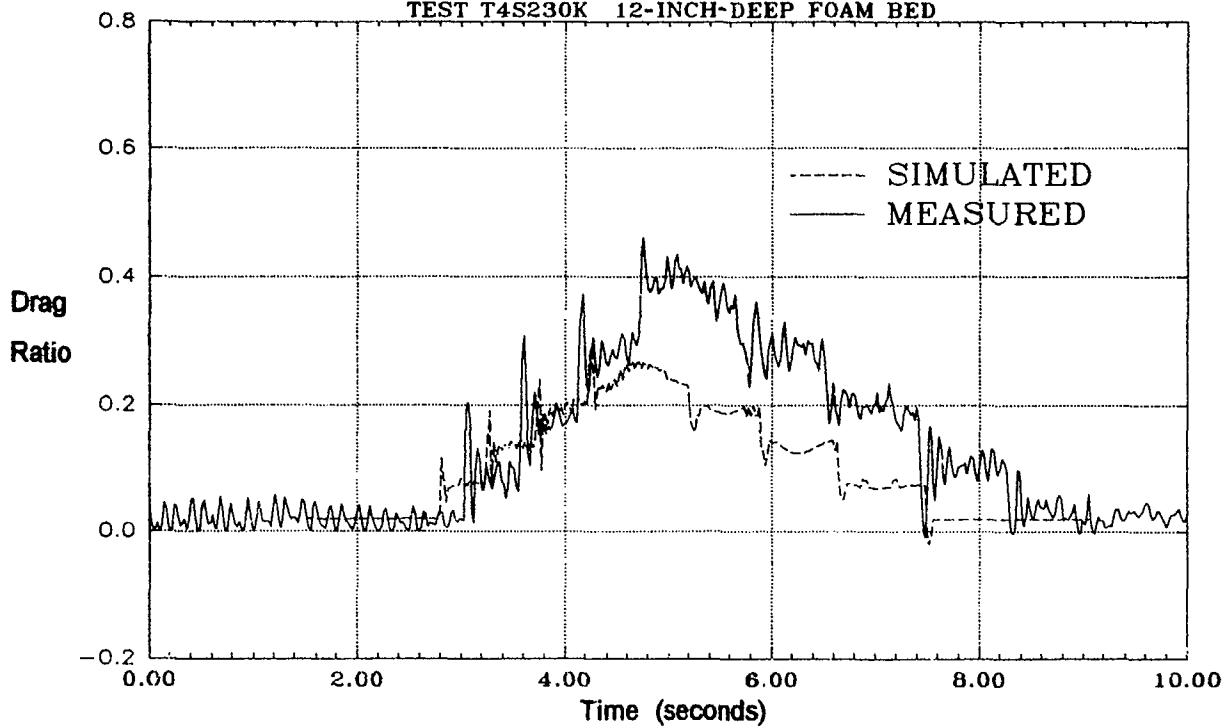
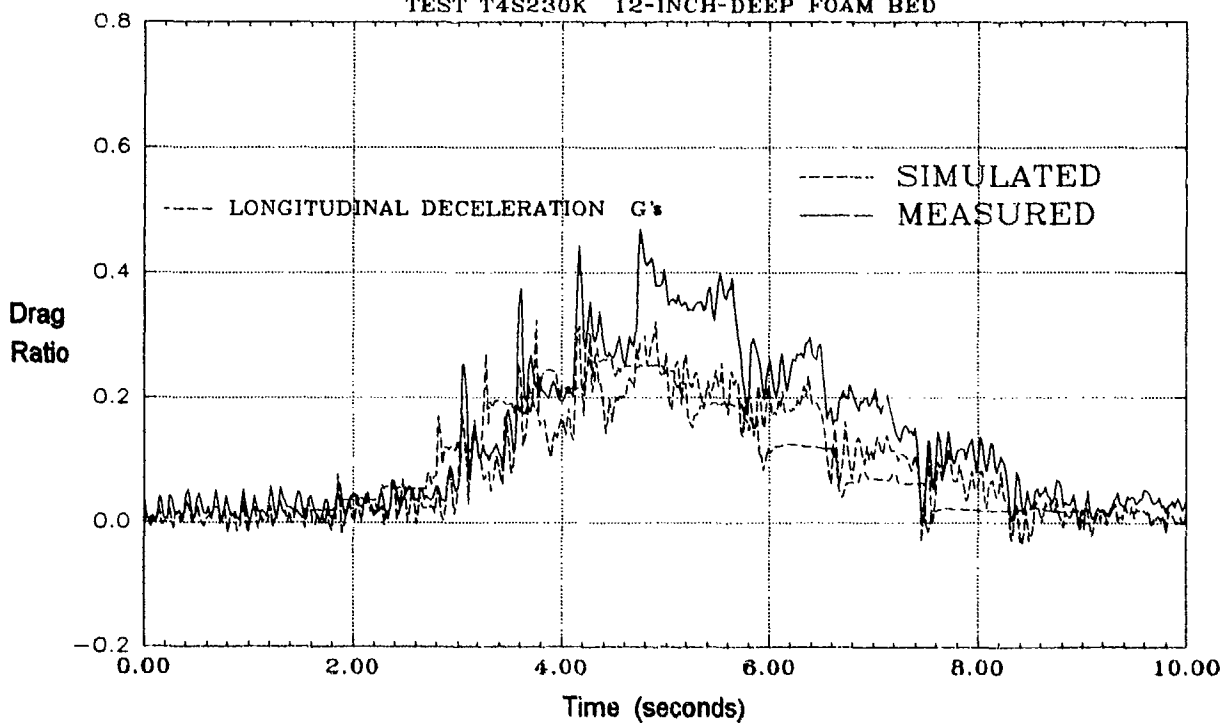


FIGURE A-31. Right Main Gear Drag Ratio from Test T4S230K

### TOTAL GEAR DRAG/GROSS WEIGHT

B-727 GW = 135965 LB CG= 891 INCHES

TEST T4S230K 12-INCH-DEEP FOAM BED



### NOSE GEAR DRAG RATIO

B-727 GW=134249 LB CG=897 INCHES  
TEST T5S250K 18-INCH-DEEP FOAM BED

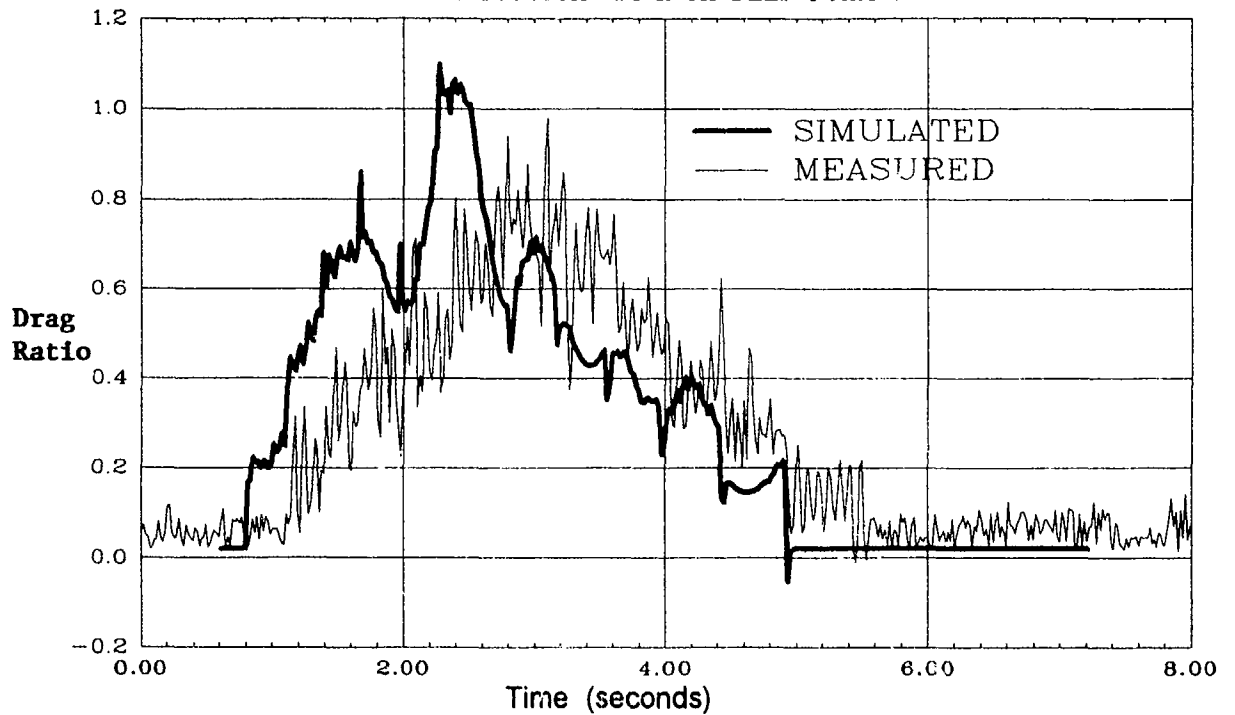


FIGURE A-33. Nose Gear Drag Ratio from Test T5S250K

### RIGHT MAIN GEAR DRAG RATIO

B-727 GW=134249 LB CG=897 INCHES  
TEST T5S250K 18-INCH-DEEP FOAM BED

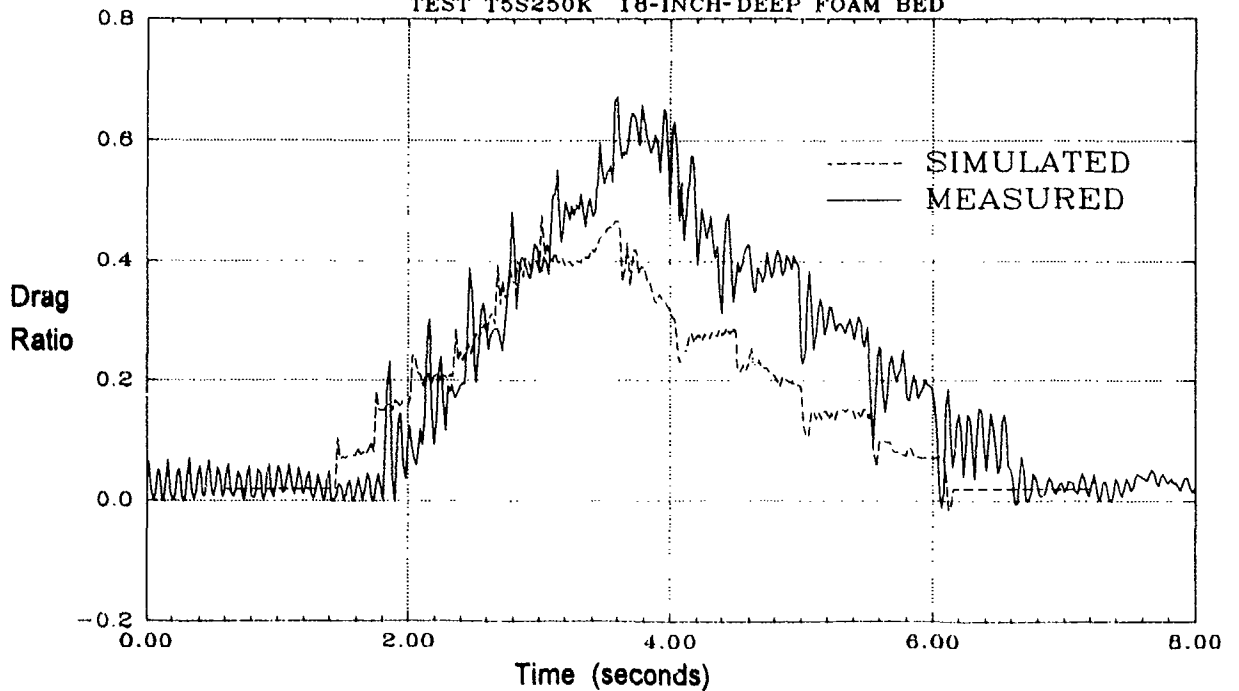


FIGURE A-34. Right Gear Drag Ratio from Test T5S250K

# TOTAL GEAR DRAG / GROSS WEIGHT

B-727 GW=134249 LB CG=897 INCHES

TEST T5S250K 18-INCH-DEEP FOAM BED

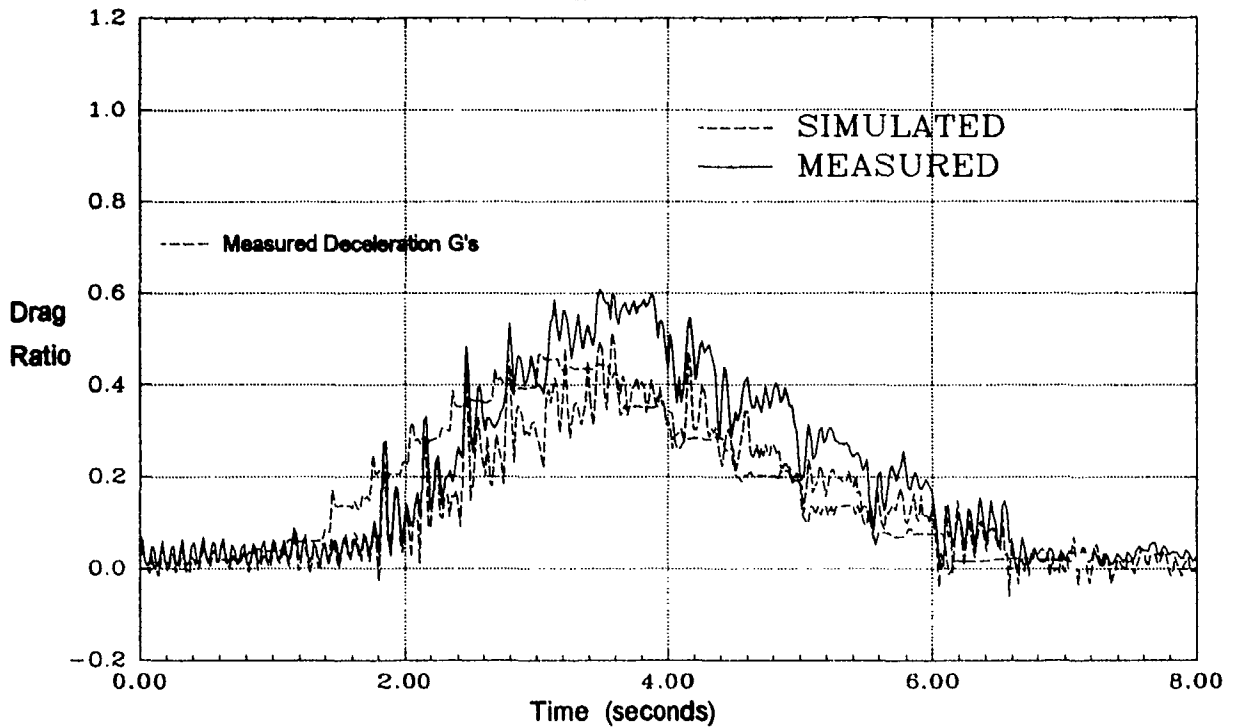


FIGURE A-35. Comparison of Total Gear Drag Ratio and Longitudinal Acceleration

**APPENDIX B**

**FULL-SCALE ARRESTING SYSTEM DEMONSTRATIONS**

**JUNE-JULY 1993**

**FEDERAL AVIATION ADMINISTRATION**

**TECHNICAL CENTER**

## 1. DATA ANALYSIS FOR 50-KNOT ARRESTMENT.

Aircraft arrestment with a 50-knot entry speed was simulated on the mathematical model. The nose gear drag and vertical loads for this simulation are plotted against time in figures B-1(a) and B-1(b). The actual loads as measured during the 50-knot demonstration are also shown on these figures. The representation of the foam bed is added for reference only. The mathematical model simulated, on average, a nose drag load approximately 2000 pounds higher than was actually measured during the demonstration. The simulated and measured vertical loads are within 10 percent of each other.

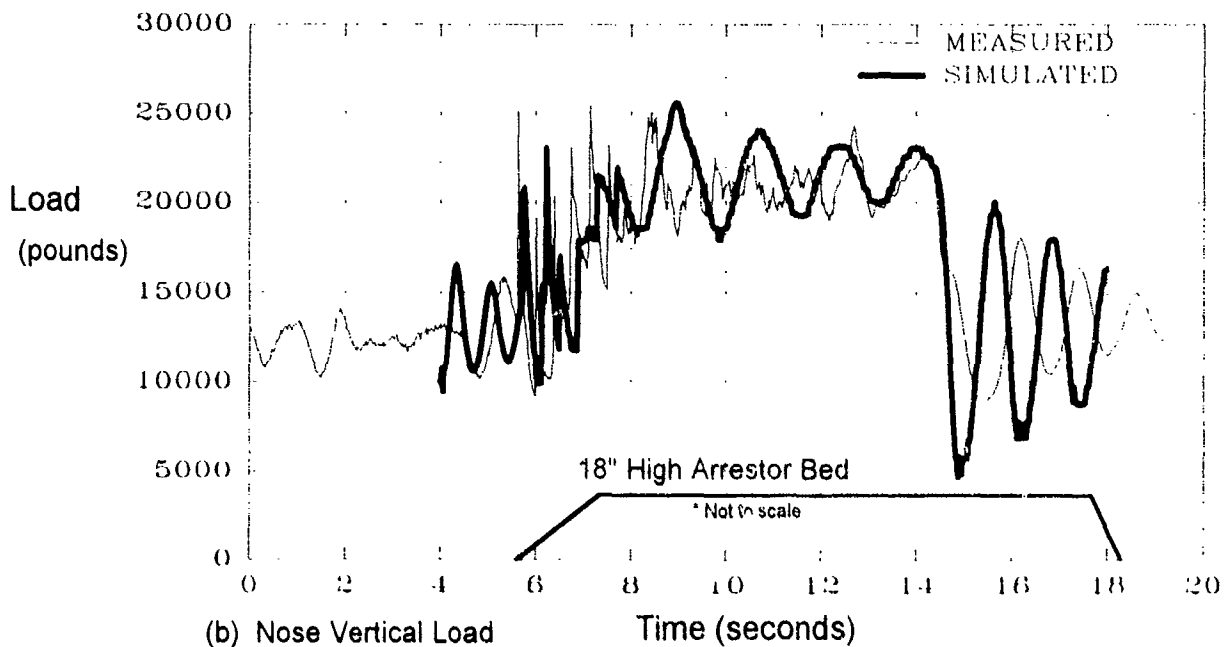
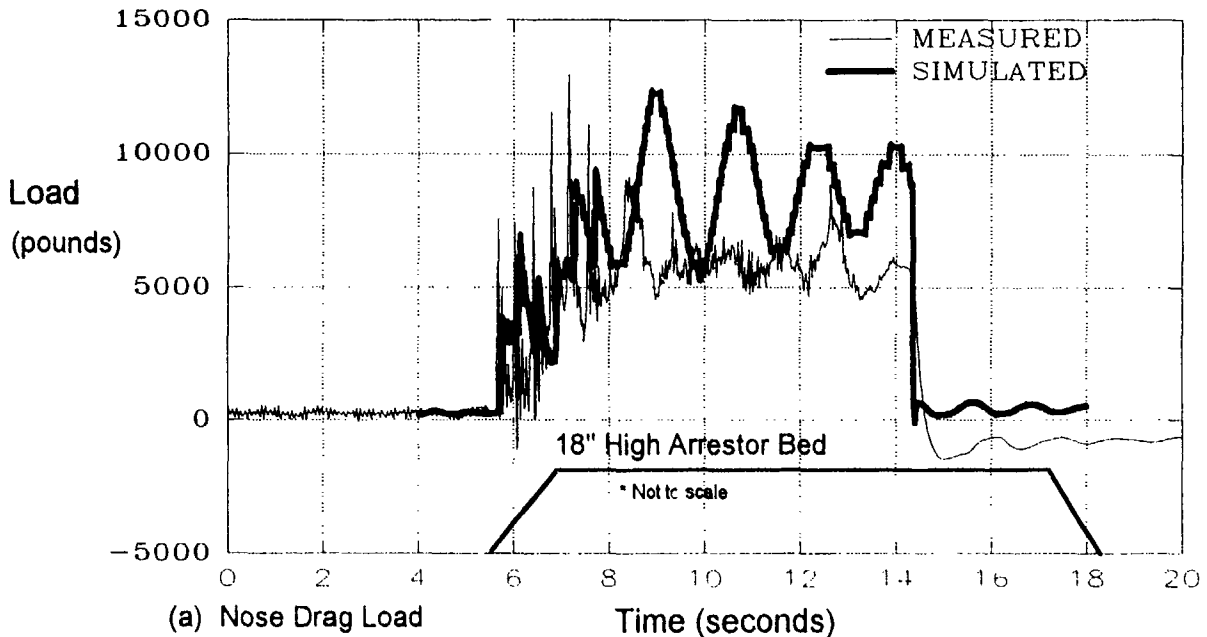


FIGURE B-1. Nose Gear Loads in Foam Arrestor

Figures B-2(a) and B-2(b) compare the simulated and measured drag and vertical loads on the left main gear of the aircraft during the 50-knot simulation and demonstration. The measured vertical load is very noisy but the magnitude averages about 70,000 pounds. This figure is too high because the actual aircraft weight was only 135,000 pounds and approximately 13,000 pounds is on the nose gear (figure B-1(b)). Each main gear vertical load should read about 61,000 pounds prior to entry into the arrestor bed. The simulated and measured vertical loads decrease after the main gear enters the bed.

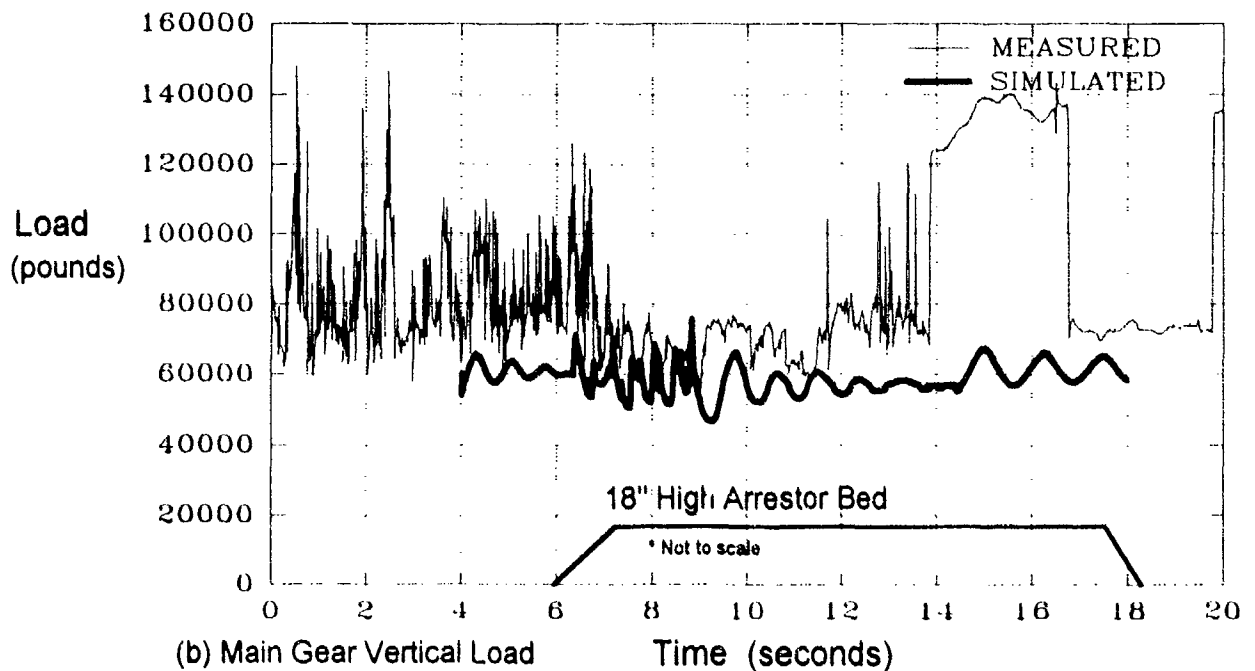
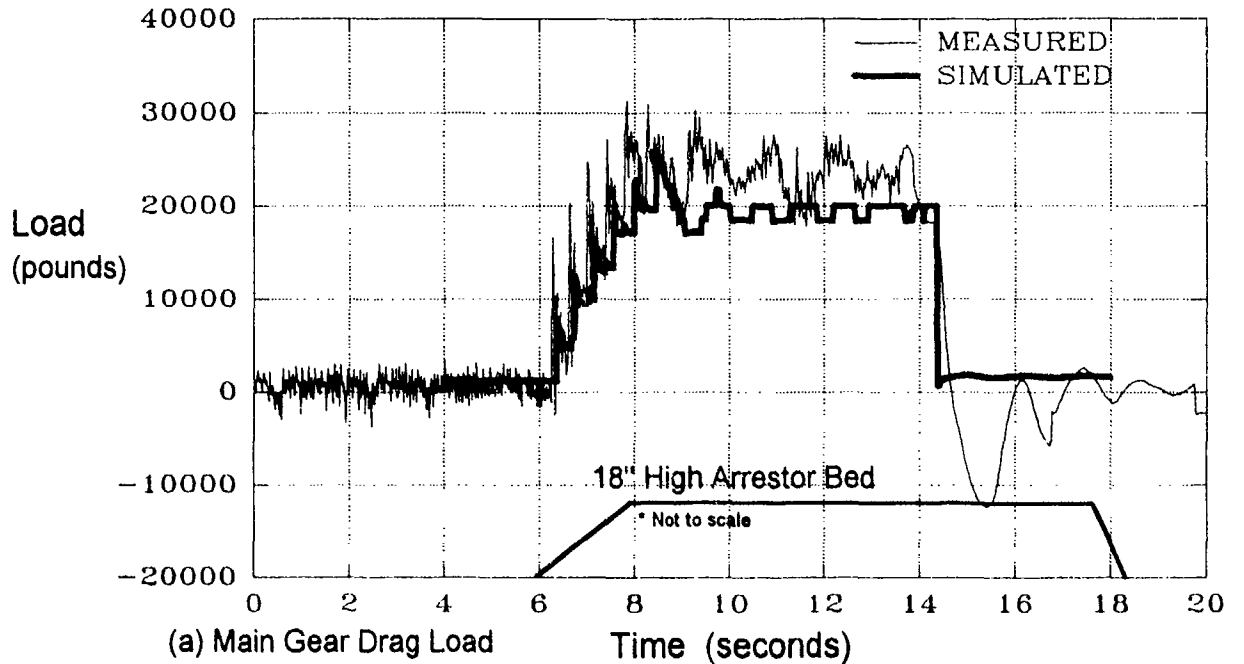


FIGURE B-2. Main Gear Loads in Foam Arrestor (50 Knots)

As the drag on the aircraft increases, the aircraft decelerates and a higher proportion of the aircraft weight is shifted to the nose gear (as can be seen on figure B-1b). This reduces the main gear vertical load a proportionate amount. The graphs for simulated and measured main gear drag load are similar.

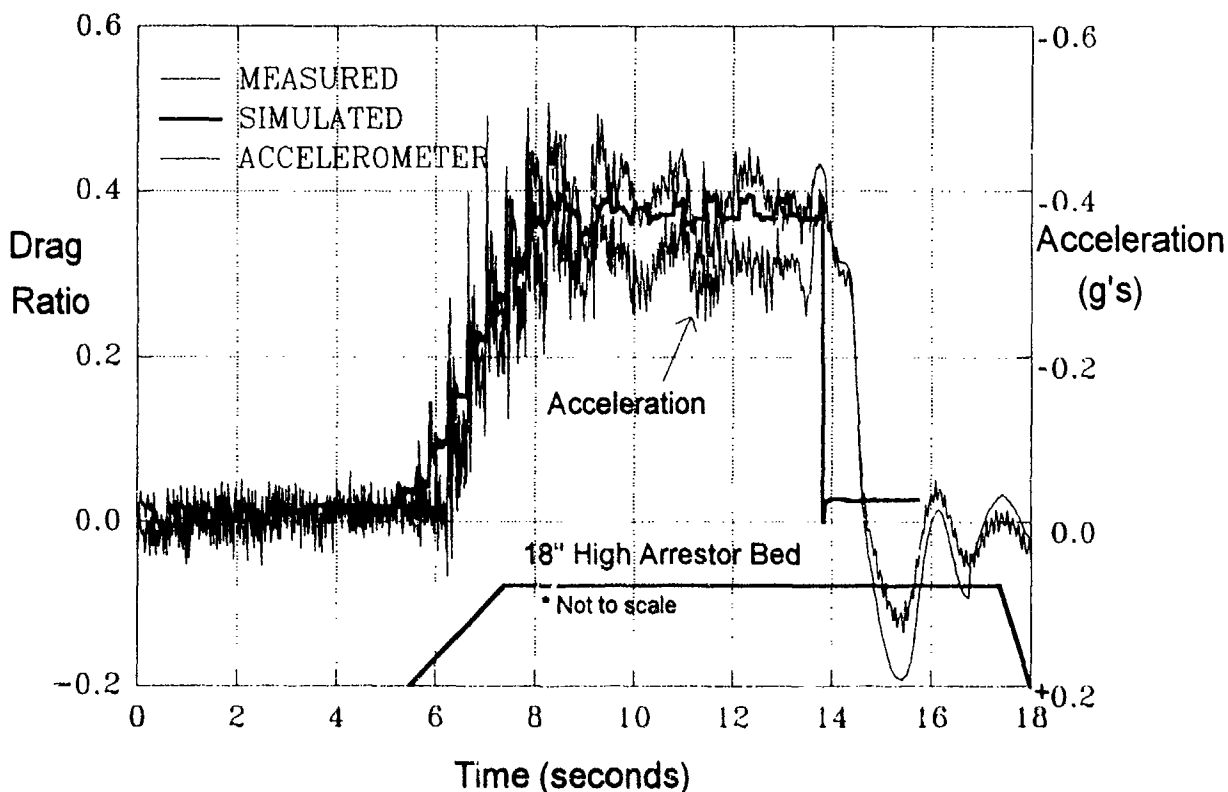


FIGURE B-3. Drag Ratio in Arrestor

The drag ratio was calculated by summing the nose gear and main gear drag loads (for both simulated and measured conditions) and dividing it by the known aircraft weight of 135,000 pounds (figure B-3). (The 2,000 pound discrepancy between the simulated and measured nose gear drag load contributes only about a 2 percent error in this calculation.) The longitudinal deceleration of the aircraft (measured in g's) as it travels through the bed is also shown. Since all three curve values are in reasonable agreement the general performance of the arrestor can be rated to give an effective braking equivalent to a runway surface coefficient of friction of approximately 0.4. The drag ratio can be increased by increasing arrestor thickness and lowering the rebound strength of the foam.

A photograph of the arrested Boeing 727 aircraft is shown in figure B-4. This picture was taken following the 50-knot demonstration.



FIGURE B-4. Picture of Arrested Aircraft



## 2. DATA ANALYSIS FOR 60 KNOT DEMONSTRATION.

Aircraft arrestment with a 60-knot entry speed was simulated on the mathematical model. The nose gear drag and vertical loads for this simulation are plotted against time in figures B-5(a) and B-5(b). The actual loads as measured during the 60-knot demonstration are also shown in these figures. The average simulated and vertical nose gear loads are similar. The simulated nose gear drag loads are approximately 2000 pounds higher than the measured loads.

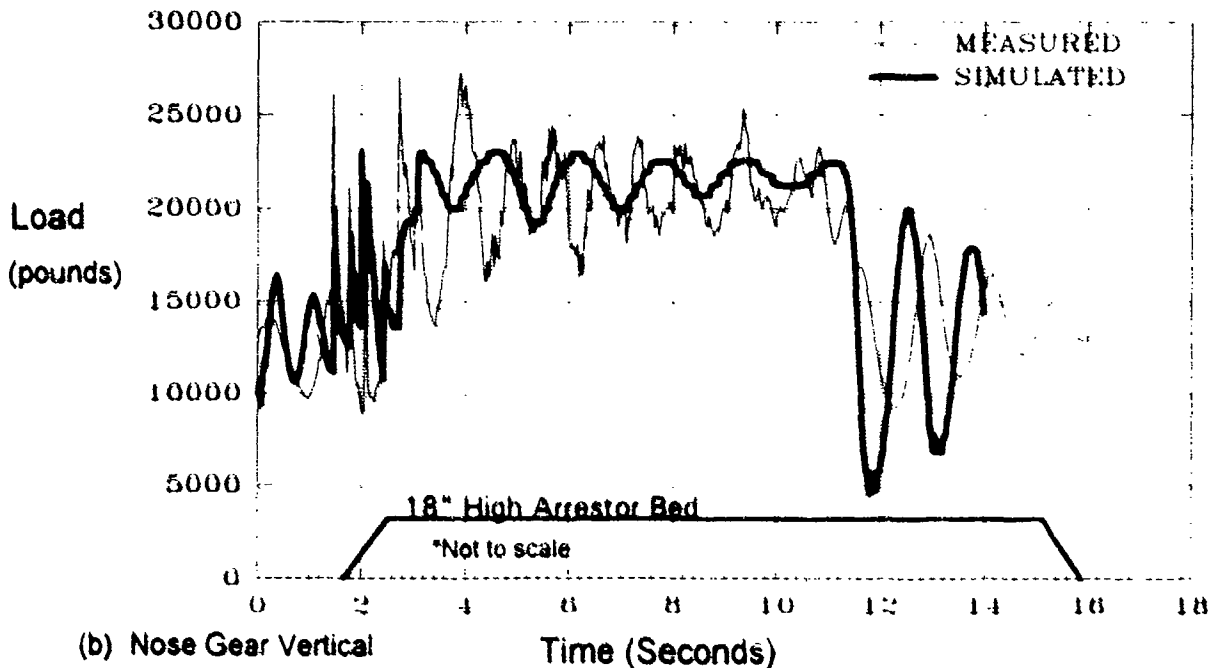
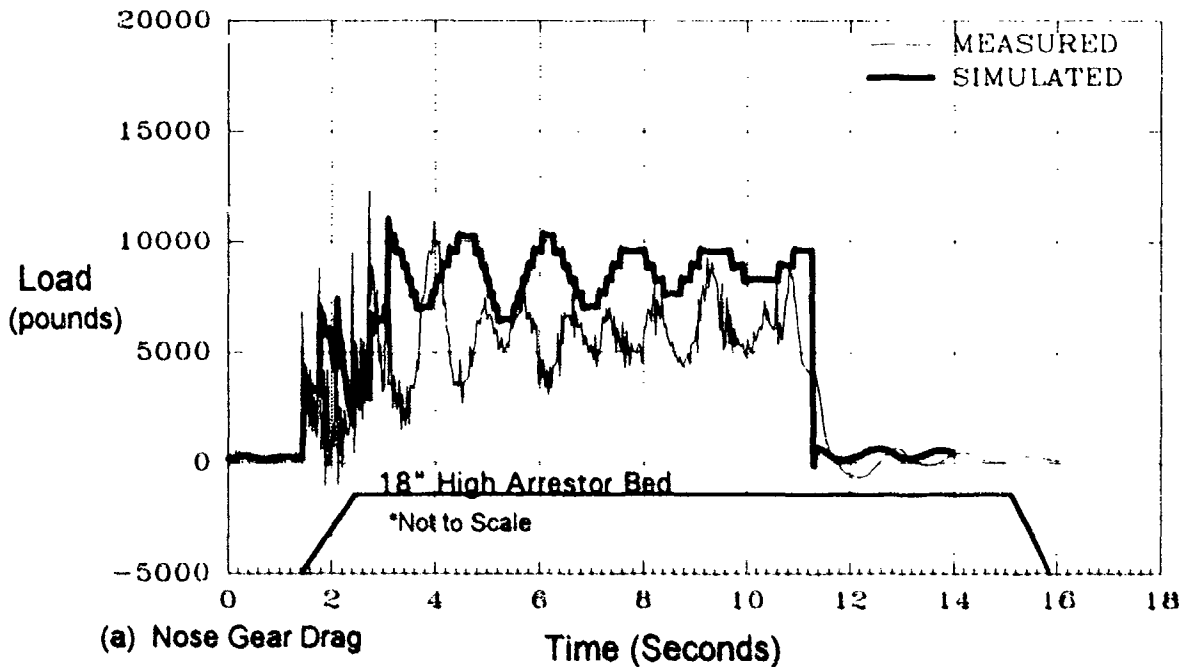


FIGURE B-5. Nose Gear Load Comparison (60 Knots)

Figures B-6(a) and B-6(b) compare the simulated and measured drag and vertical loads on the left main gear of the aircraft during the 60-knot simulation and demonstration. The measured vertical load averages approximately 70,000 pounds which is considered too high for the same reasons as mentioned in the previous section. As the aircraft travels through the arrestor bed, drag on the aircraft increases and some of the vertical load is shifted from the main gear to the nose gear (figures B-5(b) and B-6(b)).

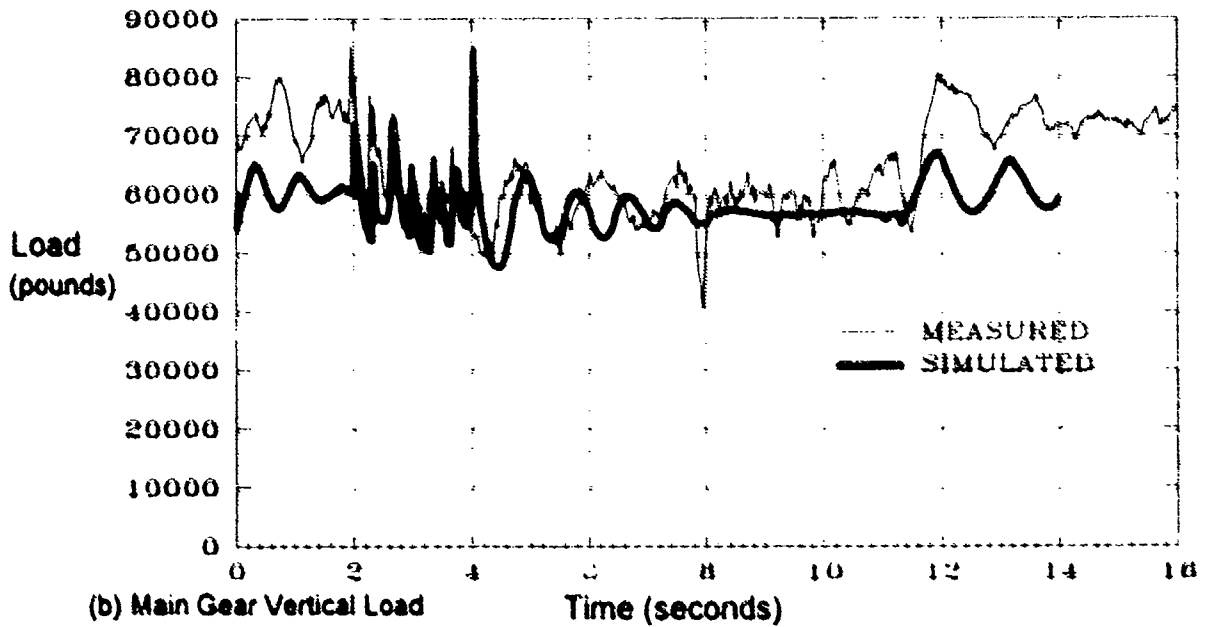
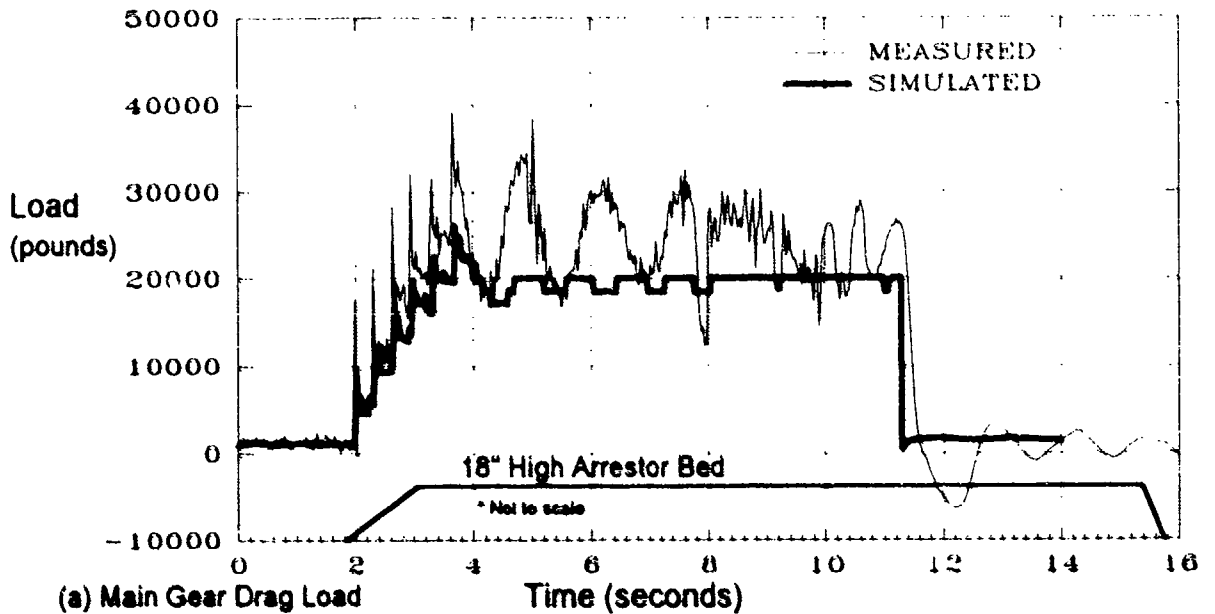


FIGURE B-6. Main Gear Load Comparison (60 Knots)

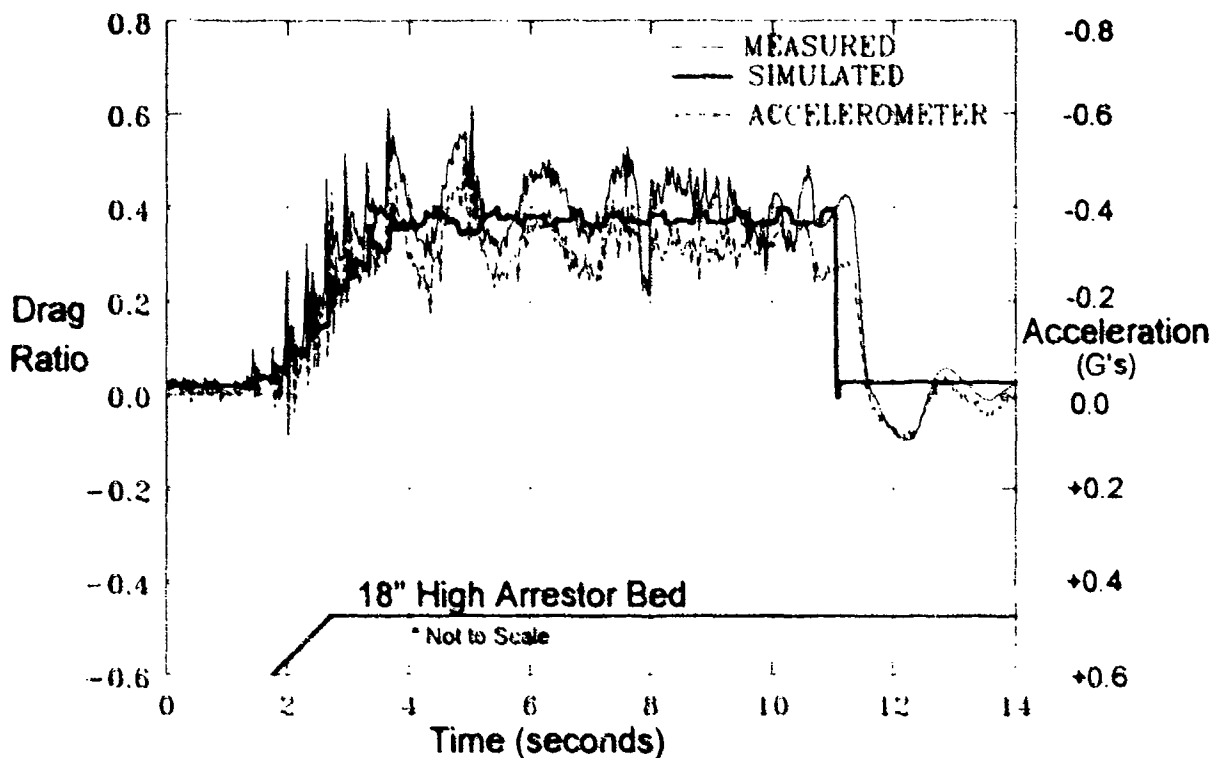


FIGURE B-7. Aircraft Drag Ratio for 60-Knot Demonstration

Figure B-7 shows the simulated and measured drag ratios and the measured aircraft acceleration during the 60-knot arrestment. The reasonable agreement of the three curves can be rated to give an effective braking equivalent to a runway surface coefficient of friction of approximately 0.4. Figure B-8 shows the aircraft traveling through the arrestor bed.



FIGURE B-8 Boeing 727 Traveling in Arrestor Bed

**APPENDIX C**

**COMPUTER INPUTS FOR MATHEMATICAL MODEL**

**Description of Model Inputs**

The computer program used to simulate the performance of the foam arrestor requires many inputs. It simulates aircraft structural dynamic response including structural flexibility, the nonlinear gear characteristics, and the tires operating on rough surfaces (bumps or dips). The major inputs are listed as follows:

**WEIGHT AND CG:** Determines the landing gear distribution. Weight and center of gravity (cg) are given parameters.

**AIRCRAFT SPEED:** The speed of the aircraft is controlled by the forces acting on the structure, i.e. wheel drag, aerodynamic drag, and thrust. Thrust and initial aircraft speed are given parameters for the problem at hand.

**AERODYNAMICS:** Determines the aerodynamic lift and drag. Inputs are primarily  $C_L$ ,  $C_D$  and  $C_M$  (aerodynamic coefficient data) along with the wing and tail surface areas and aircraft speed. The coefficients are functions of the trim, flap, and spoiler settings. The coefficients and wing and tail surface areas are unique for the aircraft selected for the simulation. Aerodynamic forces are generally small at the speeds used for arrestor demonstrations.

**LANDING GEAR:** Inputs include the actual pneumatic strut pressure, metering pin damper geometry, and strut friction versus strut gear stroke. The strut forces are computed using the usual thermodynamic relationships for pressure volume devices, flow through orifices, and sliding friction in the strut at different extensions. These data are provided by the aircraft manufacturer as determined from landing gear design. This data is unique for each aircraft.

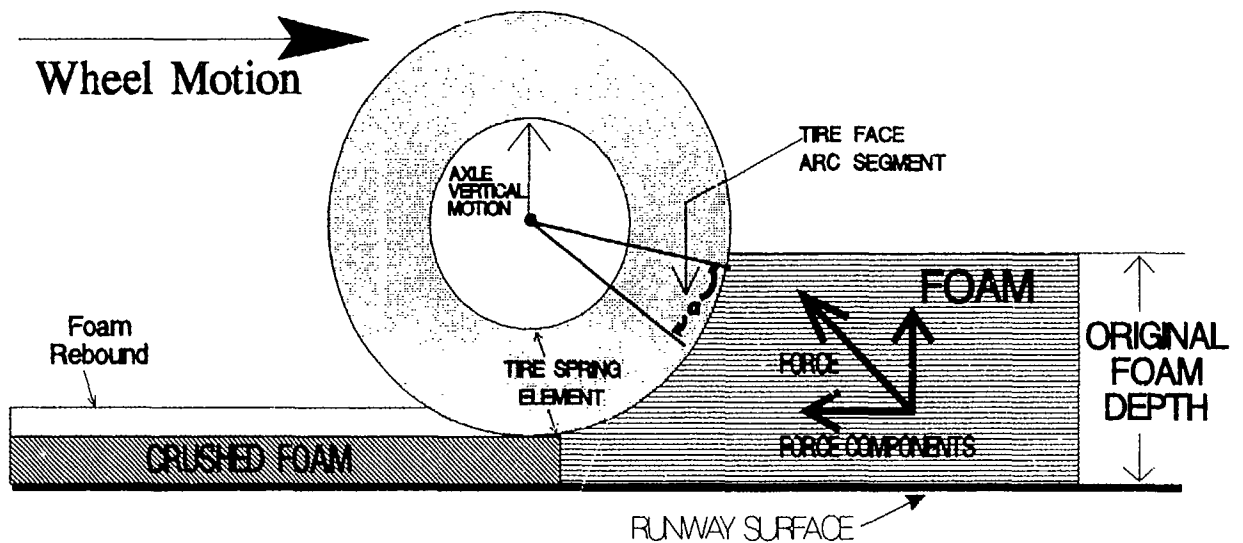
**TIRES:** Tires are represented as a series of radial nonlinear springs spaced 5 degrees apart. Each individual spring deflection is determined from the foam or runway elevation profile. The resulting forces are summed to give the vertical and drag force at the axle. Tire force and deflection characteristics are obtained from the tire manufacturer.

**FOAM:** The compressive strength as well as the rebound strength of the foam are inputs to the model. The compressive stress of the foam is included in the model at the radial elements to determine the vertical and drag loads. (A typical stress-deformation curve is superimposed on the foam depth to show the foam stress at different compressed values.) The tire element depth is determined from the axle position above the bottom of the foam and the corresponding foam stress at that element level is applied to the tire face area for that segment. The vertical and drag components of the force are computed and summed. When the tire element distance is such that the tire pressure and foam pressure are equal the foam is considered rigid and no further foam deformation takes place.

**FOAM REBOUND:** Foam rebound occurs when the load on the crushed foam is released. The foam will expand against the back of the tire surface until it is fully expanded. The expanded height of the foam may be from 5 to 40 percent of the crushed depth, depending on the foam properties and characteristics selected by the manufacturer. Foam rebound can be controlled by the manufacturer and kept at quite low values. Foam rebound is slightly proportional to foam crushing strength.

*The REBOUND stress-deformation is included in the same way as the compressive stress-deformation except it has a much reduced strength and area of contact. The rebound forces act on the back side of the tire thus subtracting from the drag produced on the front of the tire.*

**STOPPING DISTANCE:** Obtained by integrating the computed aircraft acceleration. The aircraft acceleration is a function of all the forces acting on the body.



Wheel/Foam Interface Model

**APPENDIX D**

**AIRCRAFT UNDERSHOOTS INTO PHENOLIC FOAM ARRESTOR BED**

**INSTALLATION AND TESTING ON THE FAA B-727 SIMULATOR**

**OKLAHOMA CITY, OKLAHOMA**

**October 12, 1993, to October 15, 1993.**

## **1. OBJECTIVES.**

In October 1993, a phenolic foam soft ground arrestor was "ins'talled" on the FAA B-727 flight simulator in Oklahoma City, OK. The bed was configured in the simulator to reproduce the foam bed used in the full scale demonstrations at the FAA Technical Center (680 feet long by 48 feet wide by 18 inches high).

The objectives of this effort were: a) to simulate an aircraft landing short of the runway (an undershoot) and touching down inside the phenolic foam arrestor bed, and b) to subjectively evaluate aircraft response and controllability during undershoots.

## **2. TEST PLAN.**

### **2.1. TAXIING TESTS.**

Initial simulator runs would taxi the aircraft into the front of the foam bed at 50, 60, and 70 knots. The aircraft would be allowed to stop without braking. Subsequent runs would be conducted at 60 knots and the aircraft "steered" through the bed at an angle of +/- 10 degrees.

The simulator response would be subjectively evaluated and compared to the response of the instrumented B-727 during the full scale demonstrations. The pilot of the instrumented B-727 was a copilot in the simulator.

### **2.2. UNDERSHOOT TESTS.**

Twenty seven undershoot tests were planned. The aircraft would land short at three different positions in the bed (the front, middle, and back), at three aircraft weights, and with three center of gravity (CG) positions.

Pilots would subjectively evaluate aircraft response and controllability during these landings.

### **2.3. OFF CENTER LANDINGS.**

The simulator would land short into the foam bed with one configuration of weight and CG position and under the following conditions: crosswind with drift angle; touchdown with one main gear in the bed and the other out of the bed; different trim and high sink rates (up to 10 feet per second).

The testing followed the outline of the draft test plan prepared prior to installation of the model. Tests were run in all categories except for the landings with different trim settings and the landings at high sink rates. The number of landings into the bed was also reduced because the aircraft could not be positioned in the bed as accurately as anticipated when the plan was first written.



The bed was clearly visible on the visual display at close range, but could not be accurately tracked during the approach. Three lights were added to the end of the bed away from the runway on the visual display, one at the center and one at each corner. Three lights had also been added along the centerline of the bed at 150 foot spacing as targets for the landing tests. Repeatable landings close to the target lights could not be made into the bed with the approach flown manually and all landings were therefore made using the head-up-display (HUD) which is installed on the simulator. Even using the HUD, it was very difficult to reliably enter the bed within 50 feet of a target light and the test plan was changed to aim for landing either between the front two target lights or between the back two lights. The landings were also made into a head wind of 20 knots to further improve positioning accuracy. All of the tests except for two were performed by Mr. M. Seis because of his experience with the simulator and the HUD. Mr. J.S. Terry (*pilot during full-scale demonstration*) observed and evaluated the tests from the copilot's seat.

### **3. TEST RESULTS.**

The tests run are listed in the attached table. The following variables were stored during the tests and line printer plots made at the conclusion of the testing:

VUG	forward speed in body axes
VTHETA	pitch angle
VEE(1)	position of nose gear extended strut end
FDG(1)	nose gear drag force
FZG(1)	nose gear vertical force
VEE(2)	position of left main gear extended strut end
FDG(2)	left main gear drag force
FZG(2)	left main gear vertical force
VXDLG(1)	position of the nose gear along the runway
VXDLG(2)	position of the left main gear along the runway

Table D-1. Simulator Foam Bed Tests - October 15, 1993.

Test No.	Time	Gross Weight (1,000 lb.)	CG Position (% MAC)	Position of First Contact*	Comments
1	9:40	135	25	-	Taxi, 50 kts
2	9:43	135	25	-	Taxi, 60 kts
3	9:46	135	25	-	Taxi, 70 kts, through bed
4	9:54	135	25	-	Steering, 60 kts, tiller
5	9:56	135	25	-	Steering, 60 kts, pedals
6	10:00	135	25	-	Taxi, right side, not recorded
7	10:02	135	25	-	Taxi, left side, not recorded
8	10:28	135	25	1	Landing
9	10:32	135	25	2	Landing
10	10:39	135	25	3	Landing
11	10:44	135	25	-	Landing, overran
12	10:59	135	18	1	Landing
13	11:04	135	18	1	Landing
14	11:09	135	18	1	Landing
15	11:15	135	35	Zone 2	Landing
16	11:35	135	35	2	Landing
17	11:40	152	25	1	Landing
18	11:44	152	25	3	Landing
19	11:48	152	18	1	Landing
20	11:54	152	18	Zone 2	Landing
21	11:59	152	35	Zone 1	Landing
22	12:02	152	35	Zone 2	Landing, skip
23	12:08	115	25	1	Landing, 2 skips
24	12:27	115	35	Zone 1	Landing, skip
25	12:32	115	35	Zone 2	Landing, large skip
26	14:27	115	35	Zone 2	Landing, firm, no skip
27	14:30	115	18	1	Landing
28	14:37	115	18	2	Landing, skip
29	14:41	115	25	Zone 2	Landing, roll and skip
30	14:45	135	25	2	Landing, 15 knot cross-wind
31	14:52	135	25	-	Landing, left side
32	14:55	115	25	-	Taxi, 60 kts

\* 1, 2, 3, = first, second, third lights  
 Zone 1 = between first and second lights  
 Zone 2 = between second and third lights

#### **4. EVALUATIONS.**

Based on comments made during the testing by the pilots, subjective evaluations were made of aircraft behavior while in the bed. The evaluations are given below.

##### **4.1. TAXI INTO THE BED.**

Preliminary taxi runs into the bed were made at entry speeds of 50, 60, and 70 knots. The program variable IMPFACT was adjusted for the most realistic feel as the aircraft entered the bed. A value of 0.5 gave the best subjective behavior. The 50-knot and 60-knot tests (reproducing the conditions used in the full-scale demonstrations at the FAA Technical Center, Atlantic City International Airport, New Jersey) were judged to realistically reproduce aircraft response for impacts on entry and deceleration during passage through the bed. There was some concern that pitch response was not properly reproduced. The simulated aircraft stopped in 435 ft at 50 knots and 550 ft at 60 knots, compared with 420 ft and 540 ft in the full-scale demonstrations. At 70 knots, the aircraft passed completely through the bed and exited at 10 knots. A full-scale demonstration was not run at 70 knots .

The first steering test was made using the tiller. The aircraft slid sideways after the tiller was moved, but control was easily regained by the pilot. The second steering test was made using the rudder pedals, without moving the tiller wheel. No steering control problems were encountered.

Two tests were run with the aircraft taxiing along the side of the bed. The first was along the right of the bed with the nose gear in the bed and the right main gear outside the bed. The aircraft smoothly turned left until all of the landing gear were in the bed. It then straightened up and came to rest within the bed. (Recordings were not made during these tests, but the heading change was estimated to be approximately ten degrees). The second test was along the left of the bed with the nose gear and left main gear both outside the bed. Aircraft response was the same as in the previous test except that all of the landing gear entered the bed later and the aircraft did not stop in the bed.

##### **4.2. UNDERSHOOTS.**

Landing tests were made with the aircraft configured for the full anticipated range of landing weights and center of gravity positions. No control problems were encountered during the landings. In some cases the sink rate was higher than normal because the aircraft was being aimed to touchdown in a very short length of the runway.

The main difference between landing in the bed and landing on the runway was that the aircraft showed a tendency to "skip" off the bed. This tendency was more pronounced at the lightest weight and the most rearward cg position. The aircraft was also most difficult to position in the bed under these conditions because it tended to

"float" just before touchdown. The skipping did not cause any control problems and the landings were said to be comparable with landings commonly made by student pilots.

#### **4.3. CROSSWIND LANDING.**

A landing was made with a 15-knot crosswind and approximately 5-degree drift angle on approach. The landing was made without straightening the drift at touchdown. The aircraft smoothly straightened up in the bed and then weathervaned slightly while running along the runway after leaving the bed.

#### **4.4. OFF CENTER LANDING.**

A landing was made along the left side of the bed with the right main gear in the bed and the left main gear outside the bed. There was no noticeable difference in aircraft response from the landings made along the center of the bed and with the aircraft in the same configuration.

#### **5. CONCLUSIONS.**

Twenty-four simulated undershoots were conducted on the FAA B-727 flight simulator over a full range of anticipated landing weights and center of gravity positions. The aircraft showed a tendency to "skip" off the bed. The *skipping* did not cause any control problems and the pilots were able to land the aircraft safely.